

# IMPACT OF CLIMATE VARIABILITY AND FOREST MANAGEMENT REGIMES ON WATER AND ENERGY FLUXES IN TEMPERATE FORESTS IN THE GREAT LAKE REGION

## Ву

#### ELIZABETH ARANGO RUDA

#### A Thesis

Submitted to the School of Graduate Studies

In Partial Fulfillment of the Requirements

For the Degree

Doctor of Philosophy

McMaster University

© Copyright by Elizabeth Arango Ruda, September 2024

DOCTOR OF PHILOSOPHY (2024)

(Biogeosciences)

McMaster University School of Earth, Environment and

Society

Hamilton, Ontario, Canada

TITLE: Impact of climate variability and forest management

regimes on water and energy fluxes in temperate forests

in the Great Lake Region

AUTHOR: Elizabeth Arango Ruda

SUPERVISOR: Professor M. Altaf Arain

NUMBER OF PAGES: CLXXX, 180

#### **ABSTRACT**

Forest ecosystems cover about 30% (42 million km²) of the Earth's land surface and 25% of these forests are located in temperate climate zone. Forests play a crucial in global carbon cycle and provide numerous goods and services. Due to warmer temperatures caused by increasing greenhouse gas emissions, forest ecosystems have become an important player in withdrawing carbon dioxide from the atmosphere and providing natural climate solutions. While the role of forests in carbon sequestration is well-recognized, less emphasis has been placed on their role in water and energy exchanges, particularly in the context of climate change and extreme weather events. Understanding these exchanges is crucial for assessing the cooling potential of forests through carbon sequestration and evapotranspiration, which significantly influence the carbon and water cycles, respectively.

This study analyzed long term eddy covariance measurements of water and energy fluxes from 2012 to 2021 at five forest sites in Southern Ontario, Canada, which are part of the Turkey Point Environmental Observatory. These temperate forests, which grow under similar climatic and edaphic conditions, included four conifer forests comprising three white pine plantations of different ages (83, 48, and 20 years old) and an 81-year-old red pine plantation forest that underwent four different variable retention harvesting (VRH) treatments and a >90-year-old naturally regenerated but managed deciduous forest.

The analysis of evapotranspiration (ET) and water use efficiency (WUE) in the deciduous forest revealed impacts of extreme weather events and environmental variables. At daily timescale, ET was primarily controlled by photosynthetically active radiation (PAR) and air temperature (Tair). The mean annual ET was 419 ± 45 mm year<sup>-1</sup> from 2012 to 2020. The highest annual ET of 521 mm occurred in 2020, a year characterized by hot and dry conditions, while the lowest annual ET of 359 mm was recorded in 2014, a wet year with more cloudy conditions. Concurrent hot and dry conditions generally increased ET. On average, ET represented 38% of precipitation (P) for the study period. The highest annual WUE (the ratio of Gross Ecosystem Productivity (GEP) to ET) of 4.4 g C kg H<sub>2</sub>O<sup>-1</sup> was observed in the cool year of 2014, whereas the lowest values of 3.0 and 3.1 g C kg H<sub>2</sub>O<sup>-1</sup> were found in the hot and dry year of 2012 and the dry year of 2020, respectively. WUE

increased from 2012 to 2014, then decreased from 2015 to 2020, where each year (except 2019) experienced extreme weather conditions (e.g., hot, dry, or hot-dry). Dry conditions were defined as periods when the Relative Extractable Water (REW) was below 0.4, while hot conditions were identified when the daily maximum temperature (Tmax) reached or exceeded 27.5°C. This temperature threshold corresponds to the 90th percentile of daily Tmax over the 30-year reference period (1971–2000), based on data from the ECCC weather station in Delhi, Ontario. The results showed the impacts of consecutive and concurrent extreme weather events on the forest water and carbon cycle and the WUE. Overall, WUE was mainly regulated by vapour pressure deficit (VPD).

ET and WUE in the conifer (white pine) forests showed differences among stands due to their ages. The mean annual ET values were  $465 \pm 41$ ,  $466 \pm 32$ , and  $403 \pm 21$  mm yr<sup>-1</sup> in the 83-, 48-, and 20-year-old stands, respectively, from 2008 to 2021. The two oldest forests exhibited higher annual ET values than the youngest forest and the deciduous stand. On average, ET accounted for 43% of total annual precipitation in the two older forests and 38% in the youngest forest, with the ET/P ratio in the latter being similar to that of the deciduous forest. The mean annual WUE values were  $3.4 \pm 0.4$ ,  $3.6 \pm 0.4$ , and  $4.0 \pm 0.8$  g C kg  $H_2O^{-1}$ in the 83-, 48-, and 20-year-old stands, respectively, indicating overall higher WUE compared to the mean annual WUE of  $3.3 \pm 0.4$  g C kg  $H_2O^{-1}$  in the deciduous forest. Similar to the deciduous forest, Tair emerged as the dominant factor controlling ET and WUE across all three conifer stands of varying ages, but specifically at the monthly timescale. The oldest conifer forest exhibited lower sensitivity to drought, suggesting its higher resilience to dry conditions, likely due to its well-established rooting system and more open and diverse species composition in the understory due to management practices. Moreover, a decline in the ET/P ratio was observed in all three conifer stands over three consecutive drought years from 2015 to 2017. WUE during these drought years increased, with the youngest stand generally exhibiting the highest WUE. Such an increase in WUE was also observed in the deciduous forest over the same period.

Lastly, the analysis of sap flow velocity (SV) in the 81-year-old red pine trees was conducted across four different VRH treatments: 33% dispersed basal area retention (33D), 55%

dispersed retention (55D), 33% aggregated retention (33A), and 55% aggregated retention (55A), along with an unharvested control (CN) plot. The results illustrated that the 55D treatment was the most optimal forest management practice to promote forest growth, as indicated by the higher transpiration rates. PAR was identified as the primary driver of daily sap flow across VRH treatments, followed by Tair. However, vapor pressure deficit (VPD) assumed greater importance on hourly timescale.

Overall, studies conducted in this dissertation have enhanced our understanding of water and energy exchange dynamics in temperate conifer and deciduous forests, particularly in response to interannual variability and extreme weather events. The studies have also contributed to valuable insights into the impact of forest management practices on the resilience of the forests to drought events. This work will help to develop strategies for enhancing forest growth, carbon uptake and water use efficiency, which are vital for forest ecosystems adapting to climate change. These findings will aid stakeholders in adopting effective forest management regimes to promote sustainability and resilience to climatic stresses in forest ecosystems.

#### **ACKNOWLEDGEMENTS**

I would like to start by expressing my deepest gratitude to my supervisor, Dr. Altaf Arain, for providing me with the opportunity to pursue my PhD studies within his research group at McMaster University. His unwavering support and guidance in both academic and personal matters have been invaluable throughout these years.

I extend my sincere thanks to the members of my PhD committee: Dr. Sean Carey, Dr. Mike Waddington, and Dr. Alemu Gonsamo. Their valuable feedback and guidance have been instrumental in completing my research.

I am also grateful to the McMaster Hydrometeorology and Climatology Research Group members. Specifically, I would like to thank Alana Bodo, Farbod Tabaei, Lejla Latifovic, Noah Stegman, and Nur Hussain for their assistance with fieldwork and data collection at Turkey Point Observatory. Additionally, I appreciate the valuable guidance of Daniel Mutton, Oliver Champagne, Shawn McKenzie, and Tariq Deen, who helped me navigate academic matters at McMaster.

Special thanks go to my friends, particularly the McMaster graduate students from the Department of Mathematics, many of whom are Latinos and/or international students. Their support was crucial in helping me adapt to a new culture, city, and university, making the transition much more manageable—special thanks to Elkin, Jie, and Lorena for their support.

I am also thankful to the Latin America Network at McMaster University (LANMU) for allowing me to experience the warmth of my homeland in this new country and get involved in activities to advocate for Diversity, Equity, and Inclusion.

I thank for the people who have been a part of my life, even if only for a short time, as they have taught me valuable lessons. I am especially grateful to Dr. Johana Marines Villa from UQAM. Thanks to her help and support, I was able to come to Canada for the first time and access amazing opportunities.

Lastly, but most importantly, I want to express my heartfelt gratitude to my parents. Their life decisions and lessons in perseverance, hard work, and sacrifice have guided my sister and me to where we are today. I am also deeply thankful to my closest friends and family in Colombia, who, despite the distance, have provided constant encouragement and support, constantly reminding me of the significance of this journey.

## TABLE OF CONTENTS

TITLE PAGE	i
DESCRIPTIVE NOTE	ii
ABSTRACT	
ACKNOWLEDGEMENTS	vi
TABLE OF CONTENTS	vii
LIST OF FIGURES	X
LIST OF TABLES	xiv
PREFACE	xvi
CHAPTER 1: INTRODUCTION	18
1.1 Climate Variability and Climate Change	18
1.2 Temperate Forests	
1.3 Forest Water Flux	21
1.4 Significance of the Study	
1.5 Study Sites	
1.6 Summary of the Methodology	
1.7 Study Objectives	
1.8 References	29
<b>CHAPTER 2:</b> IMPACTS OF HEAT AND DROUGHT ON THE DYNAMICS WATER FLUXES IN A TEMPERATE DECIDUOUS FOREST FROM 2012	
TO 2020	
2.1 Abstract	
2.2 Introduction	
2.3 Materials and Methods	
2.3.1 Study Site	
2.3.2 Eddy Covariance (EC) Flux and Meteorological Measurements	
2.3.3 Data Processing and Data Quality Control	
2.3.4 Forest Water Balance and Drought Indicators	
2.3.6 Statistical Analysis	
2.4 Results	
2.4 1 Environmental Conditions	
2.4.2 Dynamics of Evapotranspiration (ET)	
2.4.3 Dynamics of Water Use Efficiency (WUE)	
2.4.4 Variations in the Water Budget	
2.4.5 Environmental Controls on ET and WUE	51
2.5 Discussion	
2.5.1 Dynamics of ET	
2.5.2 Dynamics of WUE	
2.5.3 Variations in Water Budget	

2.6 Conclusions	59
2.7 Acknowledgements	60
2.8 References	61
<b>CHAPTER 3:</b> DROUGHT IMPACTS ON WATER FLUXES AND WATER-U	SE
EFFICIENCY IN AN AGE-SEQUENCE OF TEMPERATE	
CONIFER FORESTS	81
3.1 Abstract	81
3.2 Introduction	82
3.3 Material and Methods	85
3.3.1 Study Site	85
3.3.2 Eddy Covariance Flux and Meteorological Measurements	88
3.3.3 Data Processing and Data Quality Control	89
3.3.4 Leaf Area Index	
3.3.5 Water Availability and Drought Characterization	91
3.3.6 Statistical Analysis	
3.4 Results	94
3.4.1 Environmental Conditions	94
3.4.2 Forest Age and Water Dynamics	
3.4.3 Evapotranspiration and Environmental Controls	
3.4.4 Water Use Efficiency (WUE)	
3.5 Discussion	
3.5.1 Forest Age and Water Dynamics	99
3.5.2 Water Use Efficiency (WUE)	
3.5.3 Evapotranspiration and Environmental Controls	
3.6 Conclusions	
3.7 Acknowledgements	
3.8 References	
	v ,
<b>CHAPTER 4:</b> EVALUATING HYSTERESIS PATTERNS IN SAP FLOW OF A	RED
PINE FOREST SUBJECTED TO DIFFERENT VARIABLE RETENTION	
HARVESTING TREATMENTS	134
4.1 Abstract	134
4.2 Introduction	_
4.3 Methods	
4.3.1 Study Site	
4.3.2 Sap Flow Measurements	
4.3.3 Meteorological Measurements	
4.3.4 Statistical Analysis	
4.4 Results	
4.4.1 Variations in Environmental Conditions	
4.4.2 Dynamic of Sap Flow Velocity	
4.4.3 Hysteresis between Sap Flow and Meteorological Variables across VRH	173
Treatments	145
4.4.4 Relationship between Sap Flow Velocity and Environmental Conditions	-
1 I Lie to	

## Ph.D. Thesis – E. Arango Ruda McMaster – School of Earth, Environment & Society

4.5 Discussion	147
4.5.1 Response of Sap Flow to Environmental Variables	147
4.5.2 Hysteresis Patterns of Sap Flow	
4.5.3 Effects of VRH on Sap Flow of Red Pines	
4.6 Conclusions	
4.7 Acknowledgements	153
4.8 References	154
CHAPTER 5: SUMMARY AND CONCLUSIONS	174
5.1 Summary of Results	174
5.2 Significance and Relevance of the Study Results	176
5.3 Suggestions for Future Research	178
5.4 References	180

#### LIST OF FIGURES

<b>Figure 1.1:</b> (a) Location map of provinces of Canada, (b) Ontario map, and (c) aerial view of the location of the TPEO sites including TP39, TP74, TP02, TPD, and VDT25
<b>Figure 2.1:</b> The interannual course of meteorological conditions from January 2012 to December 2020. (a) daily mean downward photosynthetic active radiation, PAR; (b) daily mean air Temperature, Ta, soil temperature in upper 2 cm (Ts <sub>5</sub> ) and 100 cm (Ts <sub>100</sub> ) layer; (c) daily mean vapor pressure deficit, VPD; and (d) daily mean volumetric water content in the 30 cm soil layer, $\theta_{0\text{-}30\text{cm}}$ . The dotted line in panel (e) represents episodes of elevated precipitation. Characterization of years include hot year (2018), dry year (2015, 2017, 2020), hot and dry years (2012, 2016) and normal year (2013, 2014, 2019)
<b>Figure 2.2:</b> (a) Hysteresis of ET to environmental controls. Ensemble half hourly diurnal relationships over the study period between evapotranspiration (ET) and air temperature, Ta (a) ET and vapor pressure deficit, VPD (b) and photosynthetically active radiation, PAR (c) for dry (yellow), hot (orange), concurrent hot and dry (red) and normal (grey) for days when Tair $\geq$ 15 °C, PAR $\geq$ 500 $\mu$ mol m <sup>-2</sup> and VDP $\geq$ 0.5 kPa from 2012 to 2021. Error bars indicating standard deviation. ET-Tair and ET-VPD relationship show clockwise-loops
<b>Figure 2.3:</b> Response of evapotranspiration (ET), gross ecosystem productivity (GEP) and water use efficiency (WUE) to hot, dry, hot and dry and normal conditions. Daily box plots of (a) ET (b) GEP, and (c) WUE for Dry (D) when REW $\leq$ 0.4, Hot (H) when Tmax $\geq$ 27.5, Concurrent Hot and Dry (HD) when both Tmax $\geq$ 27.5 and REW $\leq$ 0.4, and Normal (N) conditions for days when Tair $\geq$ 15 °C, PAR $\geq$ 500 $\mu$ mol m <sup>-2</sup> and VDP $\geq$ 0.5 kPa from 2012 to 2021. Results from the Wilcoxon Rank-Sum test indicated significant differences were observed in ET between HD and N conditions, as well as D and N conditions. Significant differences were identified in WUE between H and HD, D, and N conditions, as well as HD and D, N conditions (see Table 2.3)
<b>Figure 2.4:</b> Cumulative water fluxes from 2012 to 2020. (a) Cumulative daily evapotranspiration (ET); (b) daily precipitation (P); and (c) surplus water (P-ET) for the period 2012-2020. Characterization of years include hot years (2018), dry year (2015, 2017, 2020), hot and dry years (2012, 2016) and Normal year (2013, 2014, 2019)
<b>Figure 2.5:</b> Water budget of the forest. Cumulative daily values of precipitation (P) (blue line), evapotranspiration (ET) (brown line), and P-ET (green line) from 2012 to 2020. A notable difference between years is evident: 2018 (hot year) exhibits higher P-ET, 2016 (hot and dry year) shows lower P-ET, 2014 (normal year with lower temperature) displays lower ET, 2015 (dry conditions) reflects lower ET, and 2020 demonstrates higher ET. Additionally, the inset includes bars representing monthly total P and ET in mm, along with the mean

<b>Figure 2.6:</b> Principal Component Analysis (PCA) applied to daily profiles of various variables across the growing season. These variables include photosynthetically active radiation (PAR), air temperature (Tair), vapor pressure deficit (VPD), relative extractable water (REW) for the 0 to 30 cm soil layer, gross ecosystem productivity (GEP), evapotranspiration (ET), and water use efficiency (WUE). The first two principal components, PC1 and PC2, accounted for 30.9% and 27.2% of the total variance, respectively. To gain a clearer insight into the influence of available water, we filtered out days when meteorological drivers, such as radiation, held greater sway over fluxes (Tair > 15°C, PAR > 500, VPD > 0.5 kPa). This approach enables a more focused examination of the water-related effects on the variables under consideration
<b>Figure 2.7:</b> Daily relative extractable water (REW) expressing soil moisture relative to field capacity and wilting point for 0 to 30 cm and 50 to 100 cm soil layer
<b>Figure 3.1:</b> Inter-annual variability (2008–2021) of monthly averages of net radiation (Rn), air temperature (Tair), vapor pressure deficit (VPD), relative extractable water (REW) and monthly total precipitation (P)
<b>Figure 3.2:</b> Cumulative daily values of evapotranspiration (ET), runoff plus infiltration (P-ET) and monthly total ET in mm for the 84-Year Conifer (a-c), 49-Year Conifer (d-f) and 21-Year Conifer (g-i) from 2008 to 2021
<b>Figure 3.3:</b> Comparison of (a) daily evapotranspiration (ET), (b) gross ecosystem productivity (GEP) and (c) water use efficiency (WUE) under Wet (REW <sub>0-30</sub> > 0.4) and Dry (REW <sub>0-30</sub> $\le$ 0.4) conditions for the 21-Year Conifer, 49-Year Conifer and 84-Year Conifer when Tair $\ge$ 15°C, PAR>500 $\mu$ mmol and VPD>0.5 kPa for gap-filled values. The Wilcoxon signed-rank test indicated significant difference in ET, GEP, and WUE for dry and wet conditions at all the sites. (d) The coupling between GEP and ET, WUE, is better explained by ET rather than GEP at the three sites (ET <sub>lmg84</sub> = 0.8, ET <sub>lmg49</sub> = 0.8, ET <sub>lmg21</sub> = 0.6)
<b>Figure 3.4:</b> Sensitivity of ET to environmental variables. Correlations between standardized monthly evapotranspiration (ET) and (a) monthly standardized net radiation (Rn), (b) monthly standardized air temperature (Tair), (c) monthly standardized vapor pressure deficit (VPD), and (d) monthly standardized relative extractable water (REW) in spring (AM), summer (JJAS) and autumn (ON) in the 83-, 48-, and 20-Year Conifer using gap ET and gap GEP
<b>Figure 3.5:</b> Daily sensitivities of evapotranspiration to air temperature (a), net radiation (b), vapor pressure deficit (c) and relative extractable water (d) in the 83-, 48-, and 20-Year Conifer using gap filled ET (using day and night values). Curves show the mean sensitivity in the 15 day moving windows. Data were standardized to remove forest growth and long-term climate variability impacts. When the flux vs climate variable correlation for 15 day moving averages was significant ( $p < 0.05$ ), the slope of the regression showed the effect of climate constraints on the water use of the forests. (following Schwalm et al. 2010; Wu and Chen 2013). The response in GEP can be found at Arain et al., 2022

<b>Figure 3.6:</b> Forest evapotranspiration (ET) sensitivity to drought as a function of age. (a-b) Drought coupling is expressed as the percentage of explained variation (R <sup>2</sup> ). (c-d) Drought sensitivity is expressed as the summed absolute values of standardized coefficients of drought variables regressed against evapotranspiration (ET) as a function of daily VPD, soil moisture (SM) and their interaction. The drought coupling and sensitivity were both obtained for each year
<b>Figure S3.1:</b> Meteorological and soil drought indicators. (a) Daily REW0-30 at the 83-Year, 48-Year, and 20-Year stand; (b) Bars represent the number of days per year when REW <sub>0-30</sub> lower than 0.4; (c) Monthly ratio of ET to P calculated from 2008 to 2021
<b>Figure S3.2:</b> Volumetric Water Content across Depths and Forests. A comparison of Volumetric Water Content (VWC) at three soil depths (20 cm, 50 cm, and 100 cm) for the (a) 83-year-old coniferous forest, (b) 48-year-old coniferous forest, and (c) 20-year-old coniferous forest.
<b>Figure S3.3:</b> Trend in evapotranspiration over the years. (a) Trend of standardized monthly evapotranspiration (ET) across a choronosequence of white pine coniferous forest for the 2008 to 2020 period; (b) Trend in standardized yearly evapotranspiration (ET) across a choronosequence of white pine coniferous forest for the 2008 to 2020 period
<b>Figure S3.4:</b> Physiological process on three temperate forests of different age. (a) Relationship between daytime mean (9:00 to 16:00, PPFD > 200 $\mu$ mol m <sup>2</sup> s <sup>-1</sup> ) values of bulk surface conductance Gs and VPD for rain-free and REW $\leq$ 0.4 periods using data from 2008 to 2021. (b) Daily mean gross ecosystem productivity (GEP) vs evapotranspiration (ET) for 2008 to 2021 period when REW $<$ 0.4
<b>Figure 4.1:</b> Aerial photograph of CA-TP39 and CA-TP31 study area obtained from Google Earth 2016 showing the various 1-ha variable retention harvesting (VRH) treatments 164
<b>Figure 4.2:</b> Meteorological and soil moisture conditions. Daily averages of photosynthetic active radiation (PAR), air temperature (Tair), vapor pressure deficit (VPD), relative extractable water at 20 cm depth (REW <sub>0-20</sub> ) and daily sums of precipitation (P)
<b>Figure 4.3:</b> Diurnal patterns of sap flow velocity for different VRH treatments. (a-e) Mean diurnal pattern of sap flow velocity (SV) for all treatments for spring, summer, and fall of 2023; (f-j) Mean diurnal pattern of sap flow velocity (SV) per month per VRH treatment for the growing Season (April-November) of 2023.
Figure 4.4: Hysteresis responses of sap flow velocity (SV) to environmental controls in each VRH treatment and control plot to (a-e) photosynthetic active radiation (PAR); (f-j) air temperature (Tair); and (k-o) vapor pressure deficit (VPD). Data points are hourly values averaged per season including fall (yellow lines), spring (magenta lines), and summer (red lines). The solid blue arrows indicate the direction of the response in the morning and the yellow one indicates the direction of response in the afternoon. The area enclosed by the SV trajectories indicate the strength of the hysteresis loop

<b>Figure 4.5:</b> Hysteresis response of sap flow velocity to environmental controls over the growing season from April to November. (a-e) photosynthetic active radiation (PAR); (f-jair temperature (Tair); and (k-o) vapor pressure deficit (VPD). Data points are hourly value averaged per season. The solid blue arrows indicate the direction of the response in the morning and the yellow one indicates the direction of response in the afternoon. The are enclosed by the SV trajectories indicates the strength of the hysteresis loop
<b>Figure 4.6:</b> Response of sap flow velocity (SV) to meteorological variables and soil water stress (a) Principal Component Analysis (PCA) applied to daily SV values in 2023. The first two principal components, PC1 and PC2, accounted for 79.3% and 8.1% of the total variance respectively. Correlations between bin-average SV values and (b) photosynthetic active radiation (bin of 60 umol m <sup>-2</sup> h <sup>-1</sup> ); (c) air temperature (bin of 0.5 °C); (d) vapor pressure deficit (bin of 0.05 kPa); and (e) relative extractable water (bin of 0.02) for five variable retention harvestin (VRH) treatments (i.e. 33A, 33D, 55A, 55D, CN)
<b>Figure S4.1:</b> Diurnal response of sap flow velocity to contrasting environmental conditions (a-c) the diurnal cycle of sap flow velocity on August 29th (a), September 7th (b), an September 9th (c); (d-f) the diurnal cycle of photosynthetic active radiation (PAR) and at temperature (Tair) on August 29th (d), September 7th (e), and September 9th (f); and (g-the diurnal cycle of vapor pressure deficit (VPD) and relative extractable water (REW) of August 29th (g), September 7th (h), and September 9th (i). Dashed vertical lines indicated noon time
<b>Figure S4.2:</b> Hysteresis responses of sap flow velocity (SV) against environmental variable including (a-c) photosynthetic active radiation (PAR), (d-f) air temperature (Tair) and (g-radiation (VPD)) on August 29th, September 7th, and September 9th in

## LIST OF TABLES

Table 2.1: Characteristics of the deciduous forest site    69
<b>Table 2.2:</b> Mean annual values of meteorological variables (air temperature, Tair; vapor pressure deficit, VPD; photosynthetic active radiation, PAR; soil temperature, Ts at the 5 cm and 100 cm depths and soil moisture, SM for 0-30 soil layer and relative extractable water, REW). Growing season values are given in parenthesis. Characterization of years include hot years (2018), dry year (2015, 2017, 2020), hot and dry years (2012, 2016) and normal year (2013, 2014, 2019)
<b>Table 2.3:</b> Annual and growing season water fluxes from 2012 to 2020: Numbers in parenthesis indicate values in growing season, which is time period when GEP > 0. Characterization of years include hot year (2018), dry year (2015, 2017, 2020), hot and dry years (2012, 2016) and normal year (2013, 2014, 2019)
<b>Table 2.4:</b> Multiple linear regression analysis of standardized daily water uses efficiency (WUE) across different dry-hot conditions (2012-2020) regressed against standardized explanatory variables, including vapor pressure deficit (VPD), air temperature (Tair), photosynthetic active radiation (PAR), and relative extractable water (REW). The analysis aims to identify the variables that best explain the model's performance under varying dry and hot conditions. Significance levels are indicated as follows: [0-0.001] = '***'; (0.01-0.05] = '*'; (0.05-0.1] = '.'; (0.1-1] = '
<b>Table 2.5:</b> Relative importance analysis results for multivariate regression of standardized daily evapotranspiration (ET), gross ecosystem productivity (GEP), and water use efficiency (WUE) against standardized explanatory variables (VPD, Tair, PAR, and REW) across various dry-hot conditions
Table 3.1: Site characteristics of the 84-year-old, 49-year-old, and 21-year-old forests of the Turkey Point Observatory         115
<b>Table 3.2:</b> Annual and seasonal water balance at three white pine stands of different age. Precipitation (P), the ratio of ET to P (ET/P), and runoff plus infiltration (P-ET). YR, SPR, SUM and FAL represent yearly, spring, summer and fall totals
<b>Table 3.3:</b> Annual and seasonal water use efficiency in three white pine stands of different age. Evapotranspiration (ET), gross ecosystem productivity (GEP) and water use efficiency (WUE) calculated as a ratio of gross ecosystem productivity (GEP) to ET. YR, GS, SPR, SUM and FAL represent yearly, growing seasons, spring, summer and fall totals. Leaf area index (LAI) values are also given
<b>Table 3.4:</b> Multiple linear regression analysis regressing monthly average evapotranspiration (ET) against the explanatory variables, including vapor pressure deficit

area index (LAI) from 2008 to 2021. Significance code are: [0-0.001] = '***'; (0.001-0.01] = '**';
(0.01-0.05] = '*'; (0.05-0.1] = '.'; (0.1-1] = '.'
<b>Table S3.1:</b> Contribution of ET and GEP to WUE. Multivariate regression analysis regressing daily standardized WUE against the explanatory variables, including daily standardized ET and daily standardized GEP. Significance code are: [0-0.001] = '***'; (0.01-0.01] = '**'; (0.01-0.05] = '*'; (0.05-0.1] = '.'; (0.1-1] = '.' The relative importance (lmg) of each predictor variable in explaining the variability in WUE is also shown
<b>Table S3.2:</b> ET, GEP and WUE show significant differences during dry and wet conditions. Results for the non-parametric Wilcoxon signed-rank test to test for difference in ET, GEP, and WUE between dry and wet conditions
Table 4.1: Variable Retention Harvesting treatments at CA-TP31 site.         Biometrics were conducted in 2014
<b>Table 4.2:</b> Mean annual values of meteorological variables (air temperature, Tair; vapor pressure deficit, VPD; photosynthetic active radiation, PAR), soil moisture for the 0-20 cm soil layer, SM0-20, relative extractable water for 0-20 cm soil layer, REW <sub>0-20</sub> , and annual total precipitation, P
<b>Table 4.3:</b> Multiple linear regression analysis of standardized daily sap flow velocity (SV) across five variable retention harvesting (VRH) treatments (33A, 33D, 55A, 55D, CN) regressed against standardized explanatory variables, including vapor pressure deficit (VPD), air temperature (Tair), photosynthetic active radiation (PAR), relative extractable water (REW). Significance levels are indicated as follows: [0-0.001] = '***'; (0.01-0.05] = '*'; (0.05-0.1] = '.'; (0.1-1] = '.'
<b>Table S4.1:</b> Total values of transpiration (T) and precipitation (P) in mm, monthly ratios of transpiration to precipitation (T/P) and mean sap flow velocity values (cm h <sup>-1</sup> ) for different Variable Retention Harvesting (VRH) treatments
<b>Table S4.2:</b> Multiple linear regression analysis of standardized hourly sap flow velocity (SV) across five variable retention harvesting (VRH) treatments (33A, 33D, 55A, 55D, CN) regressed against standardized explanatory variables, including vapor pressure deficit (VPD), air temperature (Tair), photosynthetic active radiation (PAR), relative extractable water (REW). Significance levels are indicated as follows: [0-0.001] = '***; (0.01-0.01] = '**; (0.01-0.05] = '*; (0.05-0.1] = '.'; (0.1-1] = '.'

#### **PREFACE**

This dissertation comprises three manuscripts that have been either published or in review in major peer-reviewed journals. For these papers or manuscripts the candidate's contributions included conducting literature reviews, helping in the collection and cleaning of eddy covariance and meteorological data of the Turkey Point Environmental Observatory sites, building sap flow sensors and installing them at three forest sites (i.e. 83-, 48, and 81-year old stands) to measure sap flow (transpiration) and conducting biometric measurements in all forest sites. The candidate led the data analysis and wrote the first drafts of all three manuscripts. The supervisor helped in the field work and data analysis. He edited manuscripts and provided comments for improvements. Finally, the successful completion of this work was made possible by the input and feedback from the members of the supervisory committee and the support from members of the research group in the field work. A brief summary of the status of each chapter or paper/manuscript is given below.

#### Chapter 2

*Title:* Impacts of heat and drought on the dynamics of water fluxes in a temperate deciduous forest from 2012 to 2020

Authors: Elizabeth Arango Ruda & M. Altaf Arain

Status: Published

Full reference: Arango Ruda, E., & Arain, M. A. (2024). Impacts of heat and drought on the dynamics of water fluxes in a temperate deciduous forest from 2012 to 2020. Agricultural and Forest Meteorology, 344, 109791. https://doi.org/10.1016/J.AGRFORMET.2023.109791

#### Chapter 3

*Title:* Drought impacts on water fluxes and water use efficiency in an age-sequence of temperate conifer forests

Authors: Elizabeth Arango Ruda & M. Altaf Arain

Status: In review in Hydrological Processes (Submitted on April 27, 2024. Accepted with major changes).

## **Chapter 4**

*Title:* Hysteresis patterns in sap flow of a red pine forest subjected to different variable retention harvesting treatments

Authors: Elizabeth Arango Ruda & M. Altaf Arain

Status: In Revie in Journal of Geophysical Research Biogeosciences (Submitted on 11 July 2024).

#### **CHAPTER 1:**

#### INTRODUCTION

#### 1.1 Climate variability and climate change

The climate is renowned for its inherent variability, a phenomenon characterized by the World Meteorological Organization (WMO) as the oscillations in the average state of the climate across various spatial and temporal scales, distinctly separate from singular weather events (McMichael, 2003). Key contributors to this variability from year to year are the decadal climate oscillations, exemplified by phenomena like El Niño/Southern Oscillation (ENSO), North Atlantic Oscillation (NAO), and Arctic Oscillation (AO) (Bonan, 2015, Munn, 2002). In addition to climate variability, Earth's climate has experienced a warming trend since the industrial revolution in the 1750s.

The Intergovernmental Panel on Climate Change (IPCC) defines climate change as a statistically discernible alteration in the average state of the climate or its variability, enduring over an extended timeframe, typically spanning decades or more such as the 30-year time frame for climate (IPCC, 2018). One prominent mechanism driving climate change is the accumulation of greenhouse gases, particularly water vapor (H<sub>2</sub>O) and carbon dioxide (CO<sub>2</sub>), within the atmosphere (Jones et al., 2023). The recent increase in CO<sub>2</sub> emissions due to anthropogenic activities, including the burning of fossil fuels and changes in land- cover and use (e.g., deforestation), has contributed to the increase in global mean temperatures, within the range of 0.95 to 1.20°C between 2011 and 2020 (IPCC, 2023). Projections suggest a further rise of 1.5°C in the near term (IPCC, 2023). Climate change exacerbates the likelihood of various extreme weather events, including droughts, heavy precipitation,

windstorms and heatwaves (van der Wiel & Bintanja, 2021), thus causing significant impacts on the environment, ecosystems and the economy.

IPCC (2021, 2023) have highlighted the repercussions of climate change for terrestrial ecosystems in detail. Nonetheless, strategic environmental and ecosystem management approaches offer avenues to reduce, avoid, or mitigate CO<sub>2</sub> emissions into the atmosphere (Anderson et al., 2011). Central to this endeavor is natural climate solutions, which encompass a suite of conservation, restoration, and land management actions aimed at increasing carbon sequestration in forests and other ecosystems and/or avoiding greenhouse gas emissions within global forest ecosystems (Drever et al., 2021; Griscom et al., 2017; Sowińska-Świerkosz & García, 2022). The above require a complete understanding of how climate-forest interactions and feedback work and how they might be impacted by climate change. Such knowledge is essential for developing more effective forest management strategies to mitigate climate change and enhance the sustainability and resilience of forest ecosystems (Novick et al., 2022, 2024).

#### 1.2 Temperate forest

Temperate forests cover approximately 665.8 million ha of the world forest (FAO, 2020) and play a pivotal role in regional and global climate regulation through physical, chemical, and biological processes (Bonan, 2015). Temperate deciduous forests are important carbon sinks and contribute to the water balance through transpiration (Jasechko et al., 2013; Schlesinger & Jasechko, 2014). Beyond their ecological significance, these forests provide communities with an array of goods, services, and economic values. Hence, protecting and restoring forests is critical for mitigating climate change impacts and advancing sustainable

development agendas of the United Nations (Ellison et al., 2017).

Much of the temperate forests in North America were cleared for agriculture in the 18<sup>th</sup> and 19<sup>th</sup> centuries, resulting in a decline in biodiversity and increased carbon emissions, which have exacerbated climate change (Bonan, 2008). To restore degraded agricultural lands that were once forests, the establishment of monoculture plantation forests has become a common practice in North America (Bonan, 2015). Other restoration strategies have also been implemented, including afforestation, reforestation, and natural regeneration (IPCC, 2019).

As these newly planted forests grow, they experience various natural and human disturbances, such as extreme climate events, wildfires, windstorms, insect infestations, thinning treatments, and timber harvests (Franklin et al., 2002; Kulakowski et al., 2011). During their initial growth stages, monoculture forests may be more vulnerable to extreme climate events, including drought, wind, snow, ice, and floods (Bauhus et al., 2010; Messier et al., 2022). Over time, as these forests mature and forest management practices like selective or partial thinning are implemented, a more diverse vegetation community can develop. This diversity enhances the forest's resilience to climate events (Bauhus et al., 2010; Curry & Huybers, 2006; Jactel et al., 2020).

The IPCC (2023) recommends various agricultural, forestry, and other land use (AFOLU) strategies, including sustainable forest management (SFM) and conservation, to protect forests and mitigate climate change impacts. However, forest mitigation strategies assessed within the SFM framework must consider the climate impacts of changes to other processes, such as albedo and the hydrological cycle (Anderson et al., 2011; Marland et al., 2003). Effective forest management practices, such as variable retention harvesting (Franklin &

Donato, 2020) and continuous cover management, can create conditions that alleviate the effects of climatic stresses on trees. These strategies can also optimize ecosystem and environmental services, including biodiversity conservation, carbon sequestration, watershed protection, and nature-based tourism (Bhardwaj, 2019).

#### 1.3 Forest water fluxes

Forest evapotranspiration (ET) plays a pivotal role in the water cycle within terrestrial ecosystems, influencing both local and regional climates (Bonan, 2023). ET is a crucial mechanism connecting the Earth's surface with the atmosphere, linking water and energy exchanges through latent heat that significantly impact climate patterns (Katul et al., 2012; Restrepo-Coupe et al., 2021; Zhao et al., 2021). This linkage is instrumental in shaping the forest environments and their growth.

ET includes evaporation from the soil surface, wet canopy, and biological transpiration, where plants uptake water through their roots and release it as vapor through stomata during photosynthesis (Schlesinger & Jasechko, 2014; Allen et al., 1989). Transpiration constitutes approximately 39% of global precipitation and accounts for 60-80% of ET on land, underscoring its importance in the water cycle (Schlesinger & Jasechko, 2014). In temperate forests, transpiration can account for up to 47% of evapotranspiration in white pine stands in Southern Ontario, featuring its significant role in these ecosystems (McLaren et al., 2008).

Partitioning ET into transpiration and evaporation can be challenging. Various methods are employed to measure evaporation (E) and transpiration (T), including lysimeters, leaf-level gas exchange measurements, and sap flow techniques (Kool et al., 2014). At the ecosystem

level, eddy covariance methods are used to assess ET. Other techniques, based on flux-variance similarity theory, make possible to partitioning ET into E and T (Nelson et al., 2020; Scanlon & Kustas, 2012). At the same time, transpiration can be estimated from sap flow measurements in trees and then scaled up to the stand level. Despite uncertainties, such as the lack of species-specific calibration, these techniques offer valuable approximations of transpiration and evaporation in forest ecosystems (Davis et al., 2012).

At the ecosystem level, the interaction between carbon uptake through photosynthesis (known as gross ecosystem productivity, GEP) and water evaporation in forests is quantified by the ratio of GEP to ET, also known as water use efficiency (WUE) (Giles-Hansen et al., 2021). WUE helps understand the carbon-water relationship in a range of ecosystems. Research indicates climate and land use/cover changes influence the water cycle by altering ET (Shveytser et al., 2023). These changes also impact the WUE of forests due to increased ET relative to GEP (Casson et al., 2019). These ET patterns have significant implications for ecosystem functioning and the global carbon and water cycles, highlighting the importance of understanding how water fluxes in temperate forests interact with the changing climate.

## 1.4 Significance of the study

Temperate forests are the dominant forest type in North America, and they are recognized for their significant contributions as carbon sinks and other ecosystem services (Millar & Stephenson, 2015). Forest management practices are strategically used to restore the original forest cover (Johnston et al., 2009). However, management practices impact the water and carbon balance and their response to changing climate, calling for understanding how these managed forests may respond to variations in environmental conditions. For over 20 years,

the Turkey Point Environmental Observatory has collected data to understand carbon and water exchanges in different ages and species of managed forests in the Great Lakes region. These long-term observations offer a unique opportunity to analyze trends in carbon and water fluxes and their response to environmental variability and extreme weather events. By analyzing the impacts of heatwaves and droughts on the water fluxes of these forests, this work provides researchers with a better understanding of forest-atmosphere interactions in this geographically unique study area.

Most importantly, this study quantifies ET, T, and WUE in deciduous and coniferous forests at temporal scales, ranging from diurnal to annual, examining their responses to environmental variables considering specific forest management practices, age, species composition, and structure. This information is crucial for developing strategies to enhance forest growth, carbon uptake, water use efficiency and water yield, aiding forest ecosystems in adapting to climate change (Siry et al., 2018). Consequently, this information can be used for forest management planning, watershed management, water resource management, and other applications to promote sustainability and resilience to changing climates in forest ecosystems.

#### 1.5 Study sites

The Turkey Point Environmental Observatory (TPEO) was established in 2002 by Dr. M. Altaf Arain's Hydrometeorology and Climatology Lab at McMaster University (Arain & Restrepo-Coupe, 2005; Arain et al., 2022). Located near St. Williams Conservation Reserve (42°42'24.86" N, 80°21'30.24" W), north of Lake Erie in southern Ontario, Canada, the TPEO encompasses three different ages of conifer forests (eastern white pine stands planted

in 1939, 1974, and 2002, respectively), a deciduous forest (>90-year old) and a 21-hectare experimental setup in a mature conifer forest (red pine stand, planted in 1931) where different proportion and compositions of variable retention harvesting has been applied to explore their effectiveness to enhance forest growth and carbon sequestration (Fig. 1.1). Therefore, as of 2021, the white pine stands were 83-, 48-, and 20-year old, while red pine forest was 91-year old and the deciduous forest was >90 years old. These stands are situated within a 20 km radius at approximately the same elevation (232 m).

TPEO is associated with various networks, including the Global Water Futures Observatory (GWFO) program, the former FLUXNET-Canada/Canadian Carbon Program, US-Canada Global Centre for Climate Change and Transboundary Waters, AmeriFlux, and global FLUXNET. Within these networks, the white pine plantations are referred to as CA-TP1 (Arain, 2023), CA-TP3 (Arain, 2022), and CA-TP4 (Arain, 2018a). The deciduous forest is designated as CA-TPD (Arain, 2018b). In some studies, the white pine plantations have also been identified as TP02, TP74, and TP39, and the red pine plantation as TP31, corresponding to the years they were established, i.e. 2002, 1974, 1939, and 1931, respectively. The deciduous forest is also referred to as TPD.

The 83- and 48-year conifer stands were planted in areas that were previously oak-dominated Carolinian forest, which had been cleared. The 20-year old forest, however, was established on land previously used for agriculture and left fallow for several years before tree planting. The 83- forest undergone partial thinning in 1983 and 2012, where 13% of basal area was removed (Arain et al., 2022). A similar partial thinning treatment was applied in 48-year old stand in 2021. The 81-year old red pine plantation was also partially thinned in 2014 to

establish variable retention harvesting (VRH) treatments, which included three replicates of four different treatments: an unharvested control (CN) plot, 33% dispersed crown retention (33D), 55% dispersed crown retention (55D), 33% aggregated crown retention (33A), and 55% aggregated crown retention (55A) (Bodo & Arain, 2022; Zugic et al., 2021). The deciduous forest naturally regrew but was subjected to partial thinning in 1986 and 1994 (Latifovic & Arain, 2024). This thesis utilized data collected from all these forests.

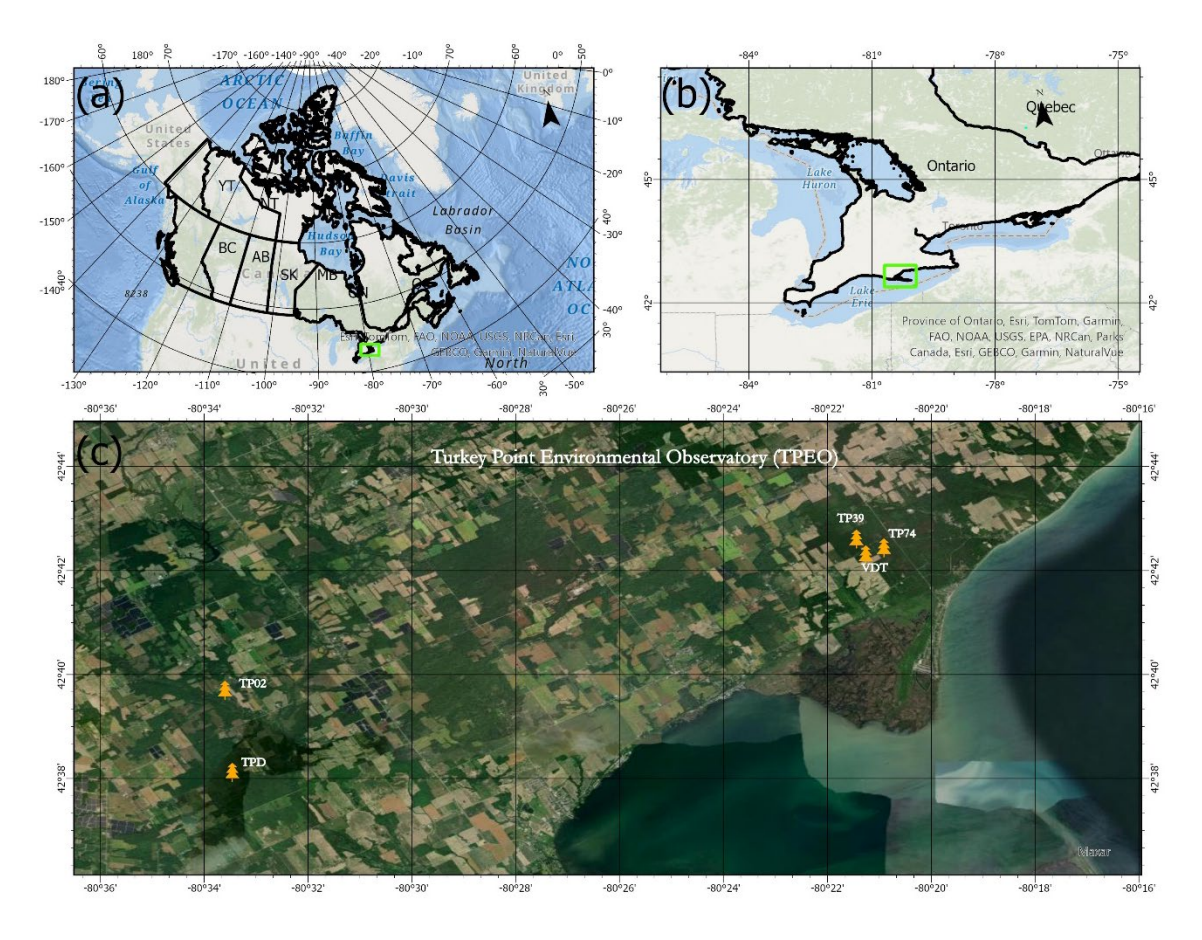


**Figure 1.1**: (a) Location map of provinces of Canada, (b) Ontario map, and (c) aerial view of the location of the TPEO sites including TP39, TP74, TP02, TPD, and VDT.

### 1.6 Summary of the methodology

The water, carbon and energy flux data for this research was collected using eddy covariance (EC), a widely used method for biometeorology and ecosystem studies (Baldocchi, 2019).

The eddy covariance technique relies on the physical principle of boundary layer turbulence, quantifying the vertical turbulent transport of gases between the surface and the atmosphere (Burba & Anderson, 2008). The statistical assumptions for eddy covariance measurements include stationarity, where turbulence statistics remain constant over time, and homogeneity, where these statistics remain constant over space (Blanken et al., 1997).

The EC systems at TPEO sites include an infrared gas analyzer (IRGA, models Li-72000 and LI-7200, Li-COR Inc.) and a three-dimensional sonic anemometer (model CSAT, Campbell Scientific Inc.). Positioned above the forest canopy, these systems measure fluxes at a high frequency (20 Hz) which are then processed following standardized community practices and saved at half-hourly intervals (Brodeur, 2014). The latent heat flux (LE) measured using this technique was converted to ET by dividing by the latent heat of vaporization and multiplying by 1800 to adjust for the 30-minute measurement period (Moorhead et al., 2019). Carbon flux was used to estimate GEP following Brodeur (2014).

Soil and meteorological variables were measured at half-hourly intervals for each site. These variables included air temperature, relative humidity, wind speed and direction, photosynthetically active radiation, all four components and/or net radiation, and precipitation. Additionally, soil moisture, soil temperature, and soil heat flux were measured at several soil depths (2, 5, 10, 20, 50 and 100 cm) at two locations at each flux tower site.

Sap flow measurements were conducted using the thermal dissipation probe (TDP) method developed by Granier (1985). Thermal dissipation probes (TDP) obtained from Dynamix Inc were installed at the 83- and 48-year old forest while TDP probes deployed at the VRH experimental treatment site were home-made in the lab. Axially aligned probes were inserted

into the sapwood to determine the temperature difference between a continuously heated probe and a non-heated reference (expressed as  $\Delta T$  (°C)). Xylem sap flow was used to estimate tree transpiration by scaling point measurements of sap flow velocity to represent the entire stem (Granier et al., 2000). These measurements allowed us to accurately estimate stand-level transpiration.

#### 1.7 Study objectives

The primary objective of this doctoral thesis is to investigate the impact of year-to-year climate variability and extreme weather events on water and energy fluxes in different ages and different species of managed coniferous and deciduous forests the Great Lakes region in Southern Ontario, Canada and explore methodologies that can be deployed for the sustainable growth of these forest in changing climate. The specific study objectives, where each one of them constituted a peer-reviewed paper or a manuscript are to:

- (1) Examine the seasonal and year-to-year variations in water cycle in the deciduous forest and assess the potential impact of heat and drought events on evapotranspiration and water use efficiency.
- (2) Determine the influence of environmental conditions, such as drought, and management practices, like partial thinning, on the water flux dynamics of three different age conifer plantation forests (i.e. 83-, 48-, and 20-year old as of 2021).
- (3) Explore the seasonal dynamics of transpiration and its major environmental controls in different variable retention harvesting treatments in the red pine forest by examining the hysteresis patterns in sap flow and determine which variable retention

Ph.D. Thesis – E. Arango Ruda McMaster – School of Earth, Environment & Society

harvesting treatment may be the most effective in sustaining evaporative demand and hence forest growth under environmental stresses.

The data and analysis presented in this dissertation is relevant to the biometeorology, ecohydrology and forest management and land restoration research communities and those studying the impact of managed forests on the water cycle and water security in the context of climate change.

#### 1.8 References

- Allen, R. G., Jensen, M. E., Wright, J. L., & Burman, R. D. (1989). Operational Estimates of Reference Evapotranspiration. Agronomy Journal, 81, 650–662.
- Anderson, R. G., Canadell, J. G., Randerson, J. T., Jackson, R. B., Hungate, B. A., Baldocchi,
  D. D., Ban-Weiss, G. A., Bonan, G. B., Caldeira, K., Cao, L., Diffenbaugh, N. S.,
  Gurney, K. R., Kueppers, L. M., Law, B. E., Luyssaert, S., & O'Halloran, T. L.
  (2011). Biophysical considerations in forestry for climate protection. In Frontiers in
  Ecology and the Environment (Vol. 9, Issue 3, pp. 174–182).
  https://doi.org/10.1890/090179
- Arain, A. (2018a). AmeriFlux BASE CA-TP4 Ontario Turkey Point 1939 Plantation White Pine, Ver. 4-5, AmeriFlux AMP, (Dataset).
- Arain, A. (2018b). AmeriFlux BASE CA-TPD Ontario Turkey Point Mature Deciduous, Ver. 2-5, AmeriFlux AMP, (Dataset).
- Arain, A. (2022). AmeriFlux FLUXNET-1F CA-TP3 Ontario Turkey Point 1974 Plantation White Pine, Ver. 3-5, AmeriFlux AMP, (Dataset).
- Arain, A. (2023). AmeriFlux FLUXNET-1F CA-TP1 Ontario Turkey Point 2002 Plantation White Pine, Ver. 3-5, AmeriFlux AMP, (Dataset).
- Arain, A., Xu, B., Brodeur, J. J., Khomik, M., Peichl, M., Beamesderfer, E., Restrepo-Couple, N., & Thorne, R. (2022). Heat and drought impact on carbon exchange in an age-sequence of temperate pine forests. Ecological Processes, 11(1). https://doi.org/10.1186/s13717-021-00349-7
- Arain, M. A., & Restrepo-Coupe, N. (2005). Net ecosystem production in a temperate pine plantation in southeastern Canada. Agricultural and Forest Meteorology, 128(3–4), 223–241. https://doi.org/10.1016/j.agrformet.2004.10.003
- Baldocchi, D. (2019). How eddy covariance flux measurements have contributed to our understanding of Global Change Biology. Global Change Biology, 26(1), 242–260. https://doi.org/10.1111/gcb.14807
- Bauhus, J., van der Meer, P. J., & Kanninen, M. (2010). Ecosystem goods and services from plantation forests. In Earthscan.
- Brodeur, J. (2014). Data-driven approaches for sustainable operation and defensible results in a long-term, multi-site ecosystem flux measurement program. McMaster University.
- Blanken, P. D., Black, T. A., Yang, P. C., Neumann, H. H., Nesic, Z., Staebler, R., Den

- Hartog, G., Novak, M. D., & Lee, X. (1997). Energy balance and canopy conductance of a boreal aspen forest: Partitioning overstory and understory components. Journal of Geophysical Research Atmospheres, 102(24), 28915–28927. https://doi.org/10.1029/97jd00193
- Bodo, A. V., & Arain, M. A. (2022). Effects of variable retention harvesting on canopy transpiration in a red pine plantation forest. Ecological Processes, 11(1). https://doi.org/10.1186/S13717-022-00366-0
- Bonan, G. (2023). Water Yield. In Seeing the Forest for the Trees (pp. 149–156). Cambridge University Press. https://doi.org/10.1017/9781108601559.013
- Bonan, G. B. (2008). Forests and Climate Change: Forcings, Feedbacks, and the Climate Benefits of Forests. Science, 320(5882), 1444–1449. https://doi.org/10.1126/science.1155121
- Bonan, G. B. (2015). Ecological Climatology: Concepts and Applications (3rd ed.). Cambridge University Press. https://doi.org/10.1017/CBO9781107339200
- Burba, G., & Anderson, D. (2008). A Brief Practical Guide to Eddy covariance CO2 flux measurements. Ecological Applications: A Publication of the Ecological Society of America, 18(6), 1368–1378. http://www.ncbi.nlm.nih.gov/pubmed/18767616
- Casson, S. A., Cushman, J. C., Yoo, C. Y., Hatfield, J. L., & Dold, C. (2019). Water-Use Efficiency: Advances and Challenges in a Changing Climate. https://doi.org/10.3389/fpls.2019.00103
- Curry, W., & Huybers, P. (2006). Links between annual, Milankovitch and continuum temperature variability [Article]. Nature, 441(7091), 329–332. https://doi.org/10.1038/nature04745
- Davis, T. W., Kuo, C. M., Liang, X., & Yu, P. S. (2012). Sap flow sensors: Construction, quality control and comparison. Sensors, 12(1), 954–971. https://doi.org/10.3390/s120100954
- Drever, C. R., Cook-Patton, S. C., Akhter, F., Badiou, P. H., Chmura, G. L., Davidson, S. J., Desjardins, R. L., Dyk, A., Fargione, J. E., Fellows, M., Filewod, B., Hessing-Lewis, M., Jayasundara, S., Keeton, W. S., Kroeger, T., Lark, T. J., Le, E., Leavitt, S. M., Leclerc, M.-E., ... Kurz, W. A. (2021). A P P L I E D E C O L O G Y Natural climate solutions for Canada. In Sci. Adv (Vol. 7). https://www.science.org
- Ellison, D., Morris, C. E., Locatelli, B., Sheil, D., Cohen, J., Murdiyarso, D., Gutierrez, V., Noordwijk, M. van, Creed, I. F., Pokorny, J., Gaveau, D., Spracklen, D. V., Tobella, A. B., Ilstedt, U., Teuling, A. J., Gebrehiwot, S. G., Sands, D. C., Muys, B., Verbist, B., ... Sullivan, C. A. (2017). Trees, forests and water: Cool insights for a hot world. Global Environmental Change, 43, 51–61.

- https://doi.org/10.1016/j.gloenvcha.2017.01.002
- Franklin, J. F., & Donato, D. C. (2020). Variable retention harvesting in the Douglas-fir region. Ecological Processes, 9(1). https://doi.org/10.1186/s13717-019-0205-5
- Franklin, J. F., Spies, T. A., Pelt, R. Van, Carey, A. B., Thornburgh, D. A., Berg, D. R., Lindenmayer, D. B., Harmon, M. E., Keeton, W. S., Shaw, D. C., Bible, K., & Chen, J. (2002). Disturbances and structural development of natural forest ecosystems with silvicultural implications, using Douglas-fir forests as an example. Forest Ecology and Management, 155(1–3), 399–423. https://doi.org/10.1016/S0378-1127(01)00575-8
- Giles-Hansen, K., Wei, X., & Hou, Y. (2021). Dramatic increase in water use efficiency with cumulative forest disturbance at the large forested watershed scale. Carbon Balance and Management, 16(1), 1–15. https://doi.org/10.1186/s13021-021-00169-4
- Granier, A. (1985). Une nouvelle méthode pour la mesure du flux de sève brute dans le tronc des arbres. Ann. Sci. For., 42(2), 81–88. https://doi.org/10.1051/forest:19850204
- Granier, A., Biron, P., & Lemoine, D. (2000). Water balance, transpiration and canopy conductance in two beech stands. Agricultural and Forest Meteorology, 100(4), 291–308. https://doi.org/10.1016/S0168-1923(99)00151-3
- Griscom, B. W., Adams, J., Ellis, P. W., Houghton, R. A., Lomax, G., Miteva, D. A., Schlesinger, W. H., Shoch, D., Siikamäki, J. V., Smith, P., Woodbury, P., Zganjar, C., Blackman, A., Campari, J., Conant, R. T., Delgado, C., Elias, P., Gopalakrishna, T., Hamsik, M. R., ... Fargione, J. (2017). Natural climate solutions. Proceedings of the National Academy of Sciences of the United States of America, 114(44), 11645–11650. https://doi.org/10.1073/pnas.1710465114
- IPCC. (2018). Annex I: Glossary (J.B.R. Matthews, Ed.). In: Global Warming of 1.5°C. An IPCC Special Report on the impacts of global warming of 1.5°C above pre-industrial levels and related global greenhouse gas emission pathways, in the context of strengthening the global response to the threat of climate change, sustainable development, and efforts to eradicate poverty (pp. 541–562). Cambridge University Press. https://doi.org/10.1017/9781009157940.008
- IPCC. (2019). Climate Change and Land: an IPCC special report. Climate Change and Land: An IPCC Special Report on Climate Change, Desertification, Land Degradation, Sustainable Land Management, Food Security, and Greenhouse Gas Fluxes in Terrestrial Ecosystems, 1–864. https://www.ipcc.ch/srccl/
- IPCC. (2021). Climate Change 2021: The Physical Science Basis. Contribution of Working Group I to the Sixth Assessment Report of the Intergovernmental Panel on Climate Change.

- IPCC. (2023). Climate Change 2023: Synthesis Report. Contribution of Working Groups I, II and III to the Sixth Assessment Report of the Intergovernmental Panel on Climate Change [Core Writing Team, H. Lee and J. Romero (eds.)]. IPCC, Geneva, Switzerland. (P. Arias, M. Bustamante, I. Elgizouli, G. Flato, M. Howden, C. Méndez-Vallejo, J. J. Pereira, R. Pichs-Madruga, S. K. Rose, Y. Saheb, R. Sánchez Rodríguez, D. Ürge-Vorsatz, C. Xiao, N. Yassaa, J. Romero, J. Kim, E. F. Haites, Y. Jung, R. Stavins, ... C. Péan, Eds.). https://doi.org/10.59327/IPCC/AR6-9789291691647
- Jactel, H., Moreira, X., & Castagneyrol, B. (2020). Annual Review of Entomology Tree Diversity and Forest Resistance to Insect Pests: Patterns, Mechanisms, and Prospects. Annu. Rev. Entomol. 2021, 66, 277–296. https://doi.org/10.1146/annurev-ento-041720
- Jasechko, S., Sharp, Z. D., Gibson, J. J., Birks, S. J., Yi, Y., & Fawcett, P. J. (2013). Terrestrial water fluxes dominated by transpiration. Nature, 496(7445), 347–350. https://doi.org/10.1038/nature11983
- Johnston, M. H. (Mark H., Campagna, M., Canadian Council of Forest Ministers., & Gibson Library Connections. (2009). Vulnerability of Canada's tree species to climate change and management options for adaptation: an overview for policy makers and practitioners. Canadian Council of Forest Ministers.
- Jones, M. W., Peters, G. P., Gasser, T., Andrew, R. M., Schwingshackl, C., Gütschow, J., Houghton, R. A., Friedlingstein, P., Pongratz, J., & Le Quéré, C. (2023). National contributions to climate change due to historical emissions of carbon dioxide, methane, and nitrous oxide since 1850. Scientific Data, 10(1). https://doi.org/10.1038/s41597-023-02041-1
- Katul, G. G., Oren, R., Manzoni, S., Higgins, C., & Parlange, M. B. (2012). Evapotranspiration: A process driving mass transport and energy exchange in the soil-plant-atmosphere-climate system. In Reviews of Geophysics (Vol. 50, Issue 3). Blackwell Publishing Ltd. https://doi.org/10.1029/2011RG000366
- Kool, D., Agam, N., Lazarovitch, N., Heitman, J. L., Sauer, T. J., & Ben-Gal, A. (2014). A review of approaches for evapotranspiration partitioning. In Agricultural and Forest Meteorology (Vol. 184, pp. 56–70). Elsevier B.V. https://doi.org/10.1016/j.agrformet.2013.09.003
- Kulakowski, D., Bebi, P., & Rixen, C. (2011). interacting effects of land use change, climate change and suppression of natural disturbances on landscape forest structure in the Swiss Alps [Article]. Oikos, 120(2), 216–225. https://doi.org/10.1111/j.1600-0706.2010.18726.x
- Latifovic, L., & Arain, M. A. (2024). The impact of spongy moth (Lymantria dispar dispar) defoliation on carbon balance of a temperate deciduous forest in North America.

- Agricultural and Forest Meteorology, 354. https://doi.org/10.1016/j.agrformet.2024.110076
- Marland, G., Pielke, R. A., Apps, M., Avissar, R., Betts, R. A., Davis, K. J., Frumhoff, P. C., Jackson, S. T., Joyce, L. A., Kauppi, P., Katzenberger, J., MacDicken, K. G., Neilson, R. P., Niles, J. O., Niyogi, D. dutta S., Norby, R. J., Pena, N., Sampson, N., & Xue, Y. (2003). The climatic impacts of land surface change and carbon management, and the implications for climate-change mitigation policy. Climate Policy, 3(2), 149–157. https://doi.org/10.1016/S1469-3062(03)00028-7
- McLaren, J. D., Arain, M. A., Khomik, M., Peichl, M., & Brodeur, J. (2008). Water flux components and soil water-atmospheric controls in a temperate pine forest growing in a well-drained sandy soil. Journal of Geophysical Research: Biogeosciences, 113(4), 1–16. https://doi.org/10.1029/2007JG000653
- McMichael, A. J. (2003). Climate change and human health: risks and responses (A. J. (Anthony J.) McMichael, Ed.) [Book]. World Health Organization.
- Messier, C., Bauhus, J., Sousa-Silva, R., Auge, H., Baeten, L., Barsoum, N., Bruelheide, H., Caldwell, B., Cavender-Bares, J., Dhiedt, E., Eisenhauer, N., Ganade, G., Gravel, D., Guillemot, J., Hall, J. S., Hector, A., Hérault, B., Jactel, H., Koricheva, J., ... Zemp, D. C. (2022). For the sake of resilience and multifunctionality, let's diversify planted forests! Conservation Letters, 15(1), 1–8. https://doi.org/10.1111/conl.12829
- Millar, C. I., & Stephenson, N. L. (2015). Temperate forest health in an era of emerging megadisturbance. https://www.science.org
- Moorhead, J. E., Marek, G. W., Gowda, P. H., Lin, X., Colaizzi, P. D., Evett, S. R., & Kutikoff, S. (2019). Evaluation of evapotranspiration from eddy covariance using large weighing lysimeters. Agronomy, 9(2), 1–17. https://doi.org/10.3390/agronomy9020099
- Munn, R. E. (2002). Encyclopedia of global environmental change. Wiley.
- Nelson, J. A., Sha, O. P., Poyatos, R., Zhang, Y., Blanken, P. D., Gimeno, T. E., Wohlfahrt, G., Black, T. A., Knohl, A., Hörtnagl, L., Magliulo, V., Besnard, S., Weber, U., Carvalhais, N., Migliavacca, M., Reichstein, M., & Jung, M. (2020). Ecosystem transpiration and evaporation: Insights from three water flux partitioning methods across FLUXNET sites. January, 6916–6930. https://doi.org/10.1111/gcb.15314
- Novick, K. A., Keenan, T. F., Anderegg, W. R. L., Normile, C. P., Runkle, B. R. K., Oldfield, E. E., Shrestha, G., Baldocchi, D. D., Evans, M. E. K., Randerson, J. T., Sanderman, J., Torn, M. S., Trugman, A. T., & Williams, C. A. (2024). We need a solid scientific basis for nature-based climate solutions in the United States. In Proceedings of the National Academy of Sciences of the United States of America (Vol. 121, Issue 14). National Academy of Sciences. https://doi.org/10.1073/pnas.2318505121

- Novick, K. A., Metzger, S., Anderegg, W. R. L., Barnes, M., Cala, D. S., Guan, K., Hemes, K. S., Hollinger, D. Y., Kumar, J., Litvak, M., Lombardozzi, D., Normile, C. P., Oikawa, P., Runkle, B. R. K., Torn, M., & Wiesner, S. (2022). Informing Nature-based Climate Solutions for the United States with the best-available science. Global Change Biology, 28(12), 3778–3794. https://doi.org/10.1111/gcb.16156
- Restrepo-Coupe, N., Albert, L. P., Longo, M., Baker, I., Levine, N. M., Mercado, L. M., da Araujo, A. C., Christoffersen, D., Costa, M. H., Fitzjarrald, D. R., Galbraith, D., Imbuzeiro, H., Malhi, Y., von Randow, C., Zeng, X., Moorcroft, P., & Saleska, S. R. (2021). Understanding water and energy fluxes in the Amazonia: Lessons from an observation-model intercomparison. Glob Change Biol, 27, 1802–1819. https://doi.org/10.1111/gcb.15555
- Scanlon, T. M., & Kustas, W. P. (2012). Partitioning Evapotranspiration Using an Eddy Covariance-Based Technique: Improved Assessment of Soil Moisture and Land–Atmosphere Exchange Dynamics. Vadose Zone Journal, 11(3). https://doi.org/10.2136/vzj2012.0025
- Schlesinger, W. H., & Jasechko, S. (2014). Transpiration in the global water cycle. Agricultural and Forest Meteorology, 189–190, 115–117. https://doi.org/10.1016/J.AGRFORMET.2014.01.011
- Siry, J. P., Cubbage, F. W., Potter, K. M., & McGinley, K. (2018). Current Perspectives on Sustainable Forest Management: North America. In Current Forestry Reports (Vol. 4, Issue 3, pp. 138–149). Springer International Publishing. https://doi.org/10.1007/s40725-018-0079-2
- Sowińska-Świerkosz, B., & García, J. (2022). What are Nature-based solutions (NBS)? Setting core ideas for concept clarification. Nature-Based Solutions, 2, 100009. https://doi.org/10.1016/j.nbsj.2022.100009
- van der Wiel, K., & Bintanja, R. (2021). Contribution of climatic changes in mean and variability to monthly temperature and precipitation extremes. Communications Earth and Environment, 2(1). https://doi.org/10.1038/s43247-020-00077-4
- Zhao, J., Feng, H., Xu, T., Xiao, J., Guerrieri, R., Liu, S., Wu, X., He, X., & He, X. (2021). Physiological and environmental control on ecosystem water use efficiency in response to drought across the northern hemisphere. Science of the Total Environment, 758. https://doi.org/10.1016/j.scitotenv.2020.143599
- Zugic, J. I., Pisaric, M. F. J., McKenzie, S. M., Parker, W. C., Elliott, K. A., & Arain, M. A. (2021). The Impact of Variable Retention Harvesting on Growth and Carbon Sequestration of a Red Pine (Pinus resinosa Ait.) Plantation Forest in Southern Ontario, Canada. Frontiers in Forests and Global Change, 4(December), 1–13. https://doi.org/10.3389/ffgc.2021.725890

#### **CHAPTER 2:**

## IMPACTS OF HEAT AND DROUGHT ON THE DYNAMICS OF WATER FLUXES IN A TEMPERATE DECIDUOUS FOREST FROM 2012 TO 2020

#### 2.1 Abstract

Temperate deciduous forests play a significant role in the regional and global water cycles. However, climate change and associated extreme weather events are affecting the growth, water use, and survival of these forests. This study examined nine years of water flux measurements made using the eddy covariance (EC) technique in a temperate deciduous forest in eastern North America from 2012 to 2020 and assessed the impacts of heat and drought events on forest evapotranspiration (ET) and water use efficiency (WUE). The study results showed that the highest annual evapotranspiration (ET) of 521 mm yr<sup>-1</sup> was observed in 2020, while the lowest annual ET of 359 mm yr<sup>-1</sup> was recorded in 2014. At daily timescale excluding winter values, photosynthetically active radiation (PAR, lmg = 0.33) and air temperature (Tair, lmg = 0.33) were the primary drivers of ET, while vapor pressure deficit (VPD, lmg = 0.41) was the primary regulator of WUE. Over the nine-year study period, observed mean annual ET and precipitation (P) values were  $367 \pm 40$  mm yr<sup>-1</sup> and  $1148 \pm$ 262 mm yr<sup>-1</sup>, respectively, while mean annual P-ET value was  $729 \pm 272$  mm yr<sup>-1</sup>. Annual ET accounted for 38% of P over the study period. Mean growing season WUE, which is an indicator of water utilization by the forest for growth and carbon assimilation was  $3.8 \pm 0.4$ g C Kg H<sub>2</sub>O<sup>-1</sup>, with the highest WUE of 4.4 g C Kg H<sub>2</sub>O<sup>-1</sup> observed in 2014 (cool year), and the lowest values of 3.0 and 3.1 g C Kg H<sub>2</sub>O<sup>-1</sup>observed in 2012 (hot-dry year) and 2020 (dry year), respectively. We found an increasing trend in WUE values from 2012 to 2014 and then a decreasing trend from 2015 to 2020, when every year experienced extreme weather conditions (e.g. hot, dry or hot-dry), except 2019. This long-term flux observation study will help to enhance our understanding of water exchanges and water use in temperate deciduous forests in Eastern North America and develop strategies for managing forest water resources and ensuring water security in the region in changing climate.

## 2.2 Introduction

Forests provide essential services to society, such as timber, clean air and water, fertile soils, wildlife habitat, and conservation of biodiversity (Bonan, 2008). Forests also absorb carbon dioxide (CO<sub>2</sub>) from the atmosphere through photosynthesis which is a key mechanism to mitigate climate change (Moomaw et al., 2020). Establishing and conserving forests is considered one of the most promising natural climate solutions that can potentially offset about 25% of anthropogenic CO<sub>2</sub> emissions (Friedlingstein et al., 2010; Griscom et al., 2017).

Recent studies in the literature suggest that forests are being increasingly impacted by climate change and associated extreme weather events, such as more frequent, severe, consecutive and/or concurrent heat and drought events (Arain et al., 2022; Graf et al., 2020; Hammond et al., 2022). Forests utilize their deep rooting system to access lager soil water stores to diminish the impacts of droughts (Lawrence et al., 2022; Lejeune et al., 2018). They also enhance evapotranspiration (ET) during heatwaves to cool their canopy up to a certain point (Seneviratne et al., 2010; Zhao et al., 2022). However, forest structure, canopy composition, large leaf area index (LAI) and high aerodynamic roughness may result in large

ET and hence causing more severe water stress (Farley et al., 2005). Dense forest canopy may also intercept precipitation (P), causing reduction in soil water availability, especially during smaller P events. On the other hand, enhanced ET from forest ecosystems may affect atmospheric humidity and hence cloud formation causing changes in radiation availability and regional precipitation patterns (Gaertner et al., 2019; Oki & Kanae, 2006; Shuttleworth, 2012). Increase in atmospheric CO<sub>2</sub> concentrations due to greenhouse gas emissions is also impacting forest carbon uptake and water use, and thus water use efficiency (WUE) (e.g., He et al., 2022; Keenan et al., 2013; Lemordant et al., 2018). Therefore, there are large uncertainties or gaps in our knowledge about the response of forest ecosystems to climate change and extreme weather events such as heatwaves and droughts (Buras et al., 2020; Teuling et al., 2010).

Temperate deciduous forests are a large sink of atmospheric CO2 and a major player in regulating water exchanges in North America (Beamesderfer et al., 2020a). These forest may specifically be susceptible to climate change and extreme weather events due to their northern location where warming rates are much higher, greater evaporative demand, more frequent and intense droughts and changes in precipitation patterns and growing season length (Beamesderfer et al., 2020a; Ciais et al., 2005; Gaertner et al., 2019; Givnish, 2002). While some of the deciduous forests in eastern North America have shown resilience and adaptability to drought conditions, typically experienced in late summer in the region, these forests may not be well adapted to other climatic changes such as heatwaves. Specifically, there is a lack of studies focusing on the growth, water budget and WUE of deciduous forests in response to concurrent and consecutive heat and drought events which are increasingly becoming common in temperate regions (Beer et al., 2009; Liu et al., 2017; Arain et al.,

2022). As such, long-term water flux observations in temperate deciduous forests may help to improve our understanding of their response to heat and drought stresses and develop strategies to enhance their adoptability and resilience to climate change (Jasechko et al., 2013; Pan et al., 2014).

In this study, we conducted long-term water flux measurements spanning from 2012 to 2020 in a temperate deciduous forest in the Great Lakes region of eastern North America using the eddy covariance technique (Baldocchi, 2019). The specific objectives were to (1) examine the seasonal dynamics and year-to-year variation in forest ET and water budget, (2) determine the major environmental controls on ET and WUE and (3) assess how ET and WUE is impacted by heat, drought and concurrent or consecutive heat and drought. These findings will provide valuables insights to advance our understanding of water dynamics in deciduous forests of eastern North America in the face of climate change. Therefore, our study is well aligned with the objectives of this special issue commemorating the 25th anniversary of AmeriFlux.

#### 2.3 Materials and methods

## 2.3.1 Study Site

The study was conducted in a > 90-year-old temperate deciduous (Carolinian) forest (42.635° N, 80.558° W, 265 m elevation) located north of Lake Erie in Norfolk County, Ontario, Canada. The Long Point Region Conservation Authority (LPRCA) owns and manages the forest. The site is part of the Turkey Point Environmental Observatory (TPEO) and is known as the Canadian Turkey Point Deciduous Forest (CA-TPD) in the AmeriFlux and global FLUXNET (Arain, 2018). It is also part of the Global Water Future (GWF) Program. The forest grows on abandoned sandy and agricultural land and is largely comprised of natural forest with native Carolinian tree species with some patches on in-fill plantations over time (Beamesderfer et al., 2020a).

The dominant species include white oak (*Quercus alba* L.), with secondary hardwood species including red maple (*Acer rubrum* L.), sugar maple (Acer Saccharum Marshall.), black oak (*Quercus velutina* Lam.), red oak (*Quercus Rubra* L.), white ash (*Fraxinus americana* L.), yellow birch (*Betula alleghaniensis* Britton.), and American beech (*Fagus Grandifolia* Ehrh.). Conifer species such as white pine (*Pinus strobus* L.) conform to approximately 5% of the total tree population. The understory is almost exclusively composed of young deciduous trees as well as Canada mayflower (*Maianthemum canadense* Desf.), putty root (*Aplectrum hyemale* Nutt.), yellow mandarin (*Disporum lanuginosum* Britton.), red trillium (*Trillium erectum* L.), and horsetail (*Esquistum*). The stand has been managed several times in recent decades. The last harvestings occurred in 1984 and 1986, during which 440 and 39.87 m<sup>3</sup> of wood were removed, respectively (Beamesderfer et al.,

2020a). From 1989 to 1994, specific harvesting of white pine (106 m³), red pine (*Pinus resinosa* Aiton.; 71.42 m³), poplar (*Populus* L.; 48.22 m³), and dead oak (61.53 m³) also occurred as per Long Point Region Conservation Authority records (LPRCA, 2023). Based on measurements conducted in the winter of 2020 to 2021 period, the average tree height is 25.7 m, the average tree diameter at breast height is 25.4 cm and the stand density is  $504 \pm 181$  trees ha<sup>-1</sup> (Table 2.1). See Beamesderfer et al. (2020a, b) for further details.

The soils are predominantly sandy (Brunisolic Gray Brown Luvisol) with 5-10 cm litter layer on the top and an organic-rich loamy-sand layer (18% organic matter). Soil water holding capacity is low to moderate, resulting in rapid water draining. The root system reaches down to at least a 1m depth with the bulks of the roots (~3.46 t ha<sup>-1</sup>) reside in the top 0-30 cm soil layer, but some roots reach 1 m depth or more (Khalid, 2016).

The region's climate is humid continental, with humid and warm summers and cold winters (Köppen climate classification). The 30-year (1981-2010) mean annual temperature is 8.0 °C, with 145 days frost-free weather. The mean total precipitation is 997 mm, with approximately 13% falling as snow as per records at the weather station in Delhi, Ontario, which is located about 25 km north-northwest of the site (Environment and Climate Change Canada (ECCC), 2023).study site (42°38′ 7″N, 80° 33′ 28″W; elevation 265 m) is located north of Lake Erie near Long Point Provincial Park, roughly 5 km southwest of Walsingham in Norfolk County, Ontario, Canada (Table 2.1). The study site is part of the Turkey Point Observatory and Global Water Futures Program. The Turkey Point Observatory is comprised of an age-sequence of three planted and managed white pine conifer forests (Peichl et al., 2010a), and this 70-110-year-old, naturally regenerated, deciduous forest. The forest grows

on abandoned agricultural land, with nearby forest tracts subject to periodic timber extraction. The site is owned by the Ontario Ministry of Natural Resources and Forestry (OMNRF) and managed by the Long Point Region Conservation Authority (LPRCA) (Parsaud, 2013). Some key site characteristics are listed in Table 2.1 and described further below.

### 2.3.2 Eddy Covariance (EC) Flux and Meteorological Measurements

Energy, water, and carbon fluxes were measured using the closed-path eddy covariance (EC) system starting in January 2012 and have been continuously measured since then. The EC system consists of a three-dimensional sonic anemometer (model CSAT3, Campbell Scientific Inc.) and a closed-path infrared gas analyzer (IRGA, model LI-7200 LI-COR Inc.), with an analyzer interface unit (LI-7550, LI-COR Inc.) and a flow module pump (7200-101, LI-COR Inc.). The air was sampled at 15 liters min<sup>-1</sup> through the 1 m long insulated intake tube. The EC sensors are installed at 36 m height on top of a walk-up scaffolding tower. The EC setup followed protocols developed by the Fluxnet-Canada Research Network (FCRN). IRGA was calibrated approximately once a month or as needed using high-purity N<sub>2</sub> gas for the zero offsets and CO<sub>2</sub> gas (360 μmol mol<sup>-1</sup> CO<sub>2</sub>, following WMO standards) for the CO<sub>2</sub> span check.

Meteorological variables were continuously measured using sensors installed at the top of the tower. Air temperature (Tair) and relative humidity (RH) were measured by a probe, which contains a platinum resistance temperature detector and a Vaisal humicap capacitive relative humidity sensor (model HMP155A, CSI). The four components of net radiation were measured using the four-dome radiometer (model CNR4, Kipp & Zonen Ltd.).

Photosynthetically active radiation (PAR) was measured using two quantum sensors facing opposite directions upwards and downward (model PQSI, LI-COR Inc./Kipp & Zonen Ltd.) on top of the tower, and a third PAR sensor was used to measure below canopy PAR at 2 m height. Wind speed and direction (model 05013-10RE, R.M. Young Co.), and atmospheric pressure (model 61,205 V, R.M. Young Co.) were also measured. Precipitation (P) was measured in an open area approximately 400 m southwest of the flux tower using an all-season heated tipping-bucket rain gauge installed at 2 m in cleared forest area (model CS700H, CSI). The rain gauge is protected by a windshield (model 260-953, Alter Wind Screen, CSI). Precipitation data were cross-checked, and gap filled as required using precipitation measurements from an accumulation rain gauge (model T-200B, Geonor Inc.), installed 20 km east at the TPEO conifer forest (CA-TP4 or TP39) site as well as the ECCC weather station at Delhi, Ontario.

Soil temperature (Ts) (model 197B, CSI) and water content ( $\theta$ ) (model CS650, CSI) are also measured at 2, 5, 10, 20, 50, and 100 cm depths in two locations. In addition, the soil water potential ( $\Psi$ ) was monitored using Soil Moisture Bloc Watermark (model 253-L, CSI) at the same depths at two locations.  $\theta$  for the rooting zone (0-30 cm) was calculated using depth-weighted averages. Soil moisture wilting point was considered at  $\theta = 0.01$  m<sup>3</sup> m<sup>-3</sup>, and field capacity was achieved when  $\theta = 0.16$  m<sup>3</sup> m<sup>-3</sup>, corresponding to  $\Psi = -1500$  kPa and  $\Psi = -33$  kPa, respectively following Peichl et al. (2010). Fluxes were measured at 20 Hz, and meteorological variables were sampled at 5 second intervals. Subsequently these data were averaged to half-hourly time scales. Further details of the instrumentation and data acquisition systems are presented in Beamesderfer et al. (2020a, b).

### 2.3.3 Data Processing and Data Quality Control

The quality control of meteorological and flux data was performed following the Fluxnet Canada Research Network (FCRN) guidelines as described in Brodeur (2014) and following Papale et al. (2006). Flux and meteorological data cleaning consisted of removing values above or below predefined upper and lower thresholds and removing erroneous values due to instrument malfunction, power failure, instrument calibrations, and data quality control. A friction velocity (u\*) threshold of 0.5 was applied to daytime and nighttime flux data to remove erroneous flux values during low turbulence periods (Arain et al., 2022; Peichl et al., 2010). A three-dimensional Lagrangian footprint model was used to calculate flux footprints for each half-hourly measurement (Kljun et al., 2003). Fluxes were retained within 80% of the cumulative flux threshold. Subsequently, data filling was performed through linear interpolation for smaller gaps (a few hours) and data from other TPEO EC flux sites and the ECCC weather station in Delhi, Ontario.

The mean energy balance closure for daily data from 2012 to 2020 was  $0.74 \pm 0.03$  ( $R^2 = 0.87$ ). The best energy balance closure was observed in the spring of 2019 (slope = 0.89,  $R^2 = 0.78$ ), while the best GS energy balance closure was observed in 2012 (slope = 0.81).

# 2.3.4 Forest Water Balance and Drought Indicators

The water balance of a forest is typically expressed as follows:

$$P = ET + D + \Delta S \tag{1}$$

where P is precipitation, ET is evapotranspiration (sum of transpiration, soil evaporation,

and evaporation of water intercepted by the canopy), D is vertical drainage, and  $\Delta S$  is changed in water storage in the soil layer from 0 to 30 cm depth. All the water balance terms are expressed in mm. In this study, the term P-ET reflects the D+ $\Delta S$  in the forest.

We also calculated the evaporative index (ET/P) which is an index that encapsulates the dynamic interaction between water availability to stand through precipitation and evaporative losses, providing insights into the efficiency of the ecosystem to utilize water resources (Diao et al., 2021). We used the relative extractable water (REW) as an ecophysiological drought indicator for our forest site. REW expresses the amount of soil water available to plants as a proportion of the maximum possible extractable water. REW was calculated as follows (Black, 1979; Arain et al., 2022):

$$REW = \frac{\theta - \theta_{wp}}{\theta_{fc} - \theta_{wp}} \tag{2}$$

Where  $\theta$  is the measured soil water content in m<sup>3</sup> m<sup>-3</sup> for the 0-30 cm soil layer,  $\theta_{wp}$  is the soil volumetric soil water content at wilting plant point (0.01 m<sup>3</sup> m<sup>-3</sup>), and  $\theta_{fc}$  is the volumetric soil water content at field capacity (0.16 m<sup>3</sup> m<sup>-3</sup>). The expression  $\theta_{fc}$  -  $\theta_{wp}$  is the difference between the soil water reserve at field capacity and the permanent wilting point.

We estimated water use efficiency (WUE, g C  $m^{-2}$  kg  $H_2O^{-1}$ ) as the ratio of observed gross ecosystem productivity (GEP, g C  $m^{-2}$ ) to ET (kg  $H_2O^{-1}$ , where one mm of ET is equal to 1 kg of water loss) as:

$$WUE = \frac{GEP}{ET} \tag{3}$$

Given the dynamic interplay of key process influencing carbon transfer and storage across varying time scales in forests (Li et al., 2023; Yu et al., 2007), the ecophysiological implications of WUE may exhibit changes at different time scales. To capture these relationships, we calculated and analyzed WUE values on daily, growing season and annual time scales. Growing season was defined as days when GEP was greater than zero.

### 2.3.5 Characterization of Extreme Weather Events

Dry and hot conditions were characterized based on REW and daily maximum temperature (Tmax) following Arain et al., (2022). Daily variables were filtered to exclude days when Tair  $\geq 15^{\circ}$ C, PAR  $\geq 500$  umol m<sup>-2</sup>, and VPD  $\geq 0.5$  kPa (Anderegg et al., 2018). This refined selection aimed to pinpoint days with clear sky conditions when soil water held a more pronounced influence on the dynamics of water and carbon fluxes. Subsequently, a dry (D) period or drought was assumed to occurred when REW was ≤ 0.4 following studies in the literature (e.g., Bréda et al., 1995; Granier et al., 2007; Vilhar, 2016). A year was characterized as a drought year when the number of days with REW  $\leq$  0.4 occurred for more than 2 months (62 days) in a given year (Arain et al., 2022). Hot (H) days were characterized as days when the daily maximum temperature (Tmax) was  $\geq 27.5$  °C, corresponding to the 90th percentile of daily Tmax over the 30-year reference period (1971-2000) based on data from the ECCC weather station at Delhi, Ontario (ECCC, 2023). A hot year was categorized as a year that had 30 or more days with daily Tmax  $\geq 27.5$  °C (Arain et al., 2022). Utilizing the criteria outlined above to define extreme weather conditions - hot (H), dry (D), concurrent hot and dry (HD), and normal (N), we analyzed ET and WUE along with key environmental variables i.e., PAR, Tair, VPD and REW. This approach enabled us to identify periods and years when ET displayed unique patterns and divergent patterns in response to changes in environmental conditions.

#### 2.3.6 Statistical Analysis

We categorized the daily values of ET and WUE into four predetermined weather conditions (i.e., H, D, HD, and N). Since the data within these groups did not conform to a normal distribution, we employed the Mann-Whitney test, a non-parametric method, to assess significant differences among the group means. This analysis was carried out using the "wilcox.test" function from the R package "stats".

Furthermore, we investigated the relationship between ET, GEP, and WUE and environmental variables under each characterized extreme weather condition using multivariate regression analysis. Before conducting this analysis, we examined the multicollinearity among predictor variables through Pearson correlation analysis and the variance inflation factor (VIF) in different extreme weather conditions e.g., H, D or H-D (results not shown). This ensured the absence of substantial collinearity among variables. We then performed a stepwise Akaike Information Criterion (AIC) regression using the "leaps" package in (Lumley, 2020). The algorithm evaluated all possible models using a predefined set of variables and identified the best model based on AIC values, departing from the initial model as shown in Equation 4.

$$ET = \beta_0 + \beta_1 PAR + \beta_2 Tair + \beta_3 VPD + \beta_4 REW \tag{4}$$

Once the optimal model was selected, we conducted the multivariate regression analysis using standardized (z-scored) variables for PAR, Tair, VPD and REW. Standardization

allowed for a quantitative comparison of the regression coefficients (Clogg et al., 1995). Furthermore, we assessed each variable's relative significance using the "relaimpo" in R (Groempings, 2021). Partial correlation was employed to gauge the strength of associations between two variables while considering the impacts of other variables within the model. Noteworthy variables were distinguished by exhibiting a p-value ( $\alpha$ ) of less than 0.05.

To capture the intricate patterns and variations within the dataset, we executed a principal component analysis (PCA), which allows visualization and analysis of complex relationships. Each daily value for the explanatory variables (PAR, Tair, VPD, REW) as well as ET, GEP, and WUE was transformed into a vector (eigenvector) paired with an associated value (eigenvalue). These were collectively plotted across the study period. The proximity of the two vectors indicated the degree of influence exerted by environmental variables on ET, GEP, and/or WUE. The PCA analysis was conducted using the prcomp() function, and the resulting visualization plot was created using the "ggbiplot" in R package.

#### 2.4 Results

#### 2.4.1 Environmental Conditions

The time series of meteorological variables measured from 2012 to 2020 is shown in Figure 2.1. PAR exhibited relatively high values in the growing season in years that experienced clear sky conditions, particularly in 2020 (Table 2.2, Fig. 2.1a). Peak Tair consistently occurred in August (Fig. 2.1b), with 2012, 2016, 2018, and 2020 exhibiting high Ta values. Ts followed Ta closely, averaging 9.6 °C (5 cm depth) and 9.4 °C (100 cm depth) (Table 2.2). VPD reached high values during the growing season in 2012 (0.82 kPa) and 2016 (0.61

kPa), with the lowest values observed in 2019 (Fig. 2.1c). Annual P was lowest in 2016 (778 mm) and highest in 2018 (1649 mm) (Table 2.3, Fig. 2.4).  $\theta$  (0-30cm) exhibited peak levels in early spring and decreased to lowest values in the late growing season in July-August in the absence of major rain events (Fig. 2.1d).

Analysis of extreme weather events suggested that 2015, 2017 and 2020 were dry years, 2012, 2016 were concurrent hot and dry years, 2018 was a hot year and 2013, 2014 and 2019 were characterized as normal years (Table 2.2 and 2.3). Consecutive extreme weather conditions were observed in 2015 (dry), 2016 (hot and dry), 2017 (dry), and 2018 (hot) in the growing season - GS (Table 2.2 and 2.3).

## 2.4.2 Dynamics of Evapotranspiration (ET)

Analysis of mean diurnal patterns of ET and its regression with mean Tair and VPD over the growing season showed a very clear clockwise hysteresis loop. It showed that at the same Tair or VPD level, ET was higher in the morning hours as compared to the afternoon (Fig. 2.2b). As Tair and hence VPD increased after the sunrise, ET also increased in response to photosynthesis activity until noon. Then ET declined in the afternoon with decreasing Tair and VPD (Fig. 2.2c). These hysteresis loops were stronger during hot and concurrent hot and dry periods (not shown). Conversely, lower peak ET values were observed on days characterized as normal, which can be attributed to cooler temperatures. In contrast, the diurnal pattern of ET to PAR showed counterclockwise hysteresis loop where PAR attained its peak values at approximately the same time as ET. The association between ET and PAR revealed compelling in-phase hysteresis loops, signifying the robust control of PAR on ET with minimal time lag time in the response (Fig. 2.2a).

The boxplot analysis of daily ET values indicated that the highest mean daily ET values were observed during concurrent hot and dry conditions, while lower mean daily ET values were observed on dry and normal days (Fig 2.3). This was supported by the Wilcoxon Rank-Sum test as well which indicated the large difference between ET during concurrent hot and dry conditions and dry conditions, in comparison to normal conditions (data not shown). Mean daily ET values were  $3.2 \pm 0.8$ ,  $2.9 \pm 0.8$ ,  $2.3 \pm 0.9$  and  $2.2 \pm 0.9$  for hot, hot-dry, dry, and normal days, respectively.

The analysis of seasonal dynamics and interannual fluctuations in ET also revealed a pattern of lower values during dry and normal years (Fig. 2.4). Lower ET during normal years (e.g., 2014) may have been caused by low Tair as well as low PAR, which could be attributed to higher cloudy conditions (Table 2.2, 2.3). Similarly, low levels of ET during dry conditions (e.g., 2015) primarily caused by lower P and hence soil water stress (Fig. 2.4). Higher ET values were observed during concurrent hot and dry periods. For example, in 2016, a hot and dry year, ET values were relatively high during the GS despite very low P (Table 2.3, Fig. 2.4). Higher ET during hot and dry years were largely caused by the clear sky conditions, with high PAR and high Ta.

The highest annual (GS) ET of 521 (456) mm yr<sup>-1</sup> was recorded in 2020 (dry) which experienced warm annual and GS temperatures (i.e. 10.6 and 17.7 °C) and more clear sky conditions in the GS (Table 2.2, 2.3). The lowest annual (GS) ET of 359 (315) and 365 (321) mm yr<sup>-1</sup> was recorded in 2014, which was a (normal or cool year) and 2015 (dry year), respectively. However, consecutive extreme weather events such as 2016 (hot-dry), 2017 (dry) and 2018 (hot) did not show any major reduction in annual or GS ET values (Table

2.2). Mean annual (GS) ET over the study period was  $419 \pm 45 (367 \pm 40)$  mm yr<sup>-1</sup>.

## 2.4.3 Dynamics of Water Use Efficiency (WUE)

The analysis of daily values of WUE (GEP/ET) revealed notable variations in WUE under extreme weather conditions. Mean daily WUE values ranged from 1.8 to 5.9 g C m<sup>-2</sup> kg H2O<sup>-1</sup> during hot days and from 1.7 to 6 g C m<sup>-2</sup> kg H<sub>2</sub>O during hot-dry days, while dry and normal days exhibited slightly higher values as shown by box plots (Fig 2.3). These differences were further highlighted by the Wilcoxon Rank-Sum test where there were significant differences in p-values of WUE during dry and hot-dry conditions as compared to normal conditions (results not shown).

The years 2012 (hot-dry) and 2020 (dry) stood out for exhibiting the lowest mean WUE values, while 2014 (normal or cool) showed the highest WUE (Table 2.3). In 2012, low WUE value of 3.0 g C kg  $\rm H2O^{-1}$  is attributed to reduced GEP (Table 2.3). Although 2020 experienced high GEP levels but simultaneously ET was high during the GS causing a decline in WUE (3.1 g C kg $\rm H2O^{-1}$ ). Overall, our analysis reveals an increasing trend in annual and GS WUE values from 2012 and 2014, followed by a subsequent decline from 2015 to 2020, with the exception of 2019, which experienced a slightly higher WUE value. Mean annual (GS) WUE over the study period was  $3.3 \pm 0.4$  (3.8.  $\pm 0.4$ ) g C kg  $\rm H_2O^{-1}$ .

#### 2.4.4 Variations in the Water Budget

P-ET, which is characterized as water available for runoff and infiltration over the study period showed the lowest annual (GS) values of 446 (179) mm and 350 (11) mm in 2015 (dry) and 2016 (hot-dry), respectively (Table 2.3, Fig. 2.4d, e). P-ET was remarkably low

(11 mm only) in the GS of 2016. The highest annual (GS) P-ET values of 1239 (573) mm and 1070 (275) mm were observed 2018 (hot) and 2014 (cool or normal), respectively (Table 2.3, Fig. 2.4g, c). These high P-ET values were largely driven by high P, while there was not a substantial increase on ET in these years. The only exception was 2020 (dry) when despite being a dry year, annual ET was 24% higher than the mean annual ET of 419  $\pm$  45 mm y<sup>-1</sup> over the study period, due to warm temperatures and more clear sky conditions. Overall, mean annual P-ET over the nine-year study period was 729  $\pm$  258 mm yr<sup>-1</sup> (Table 2.3).

The evaporative index (ET/P) remained below one for all study years. However, instances of elevated GS evaporative index values were typically observed in years that experienced concurrent hot and dry and dry conditions, such as 2016 (0.97) and 2020 (0.76), with the exception on 2018 (0.39), which experienced the highest P over the study period. Conversely, years with normal environmental conditions showed lower GS evaporative index values such as in 2013 (0.52) and 2014 (0.53) (Table 2.3). On average, ET accounted for 38% of the total P over the study period.

#### 2.4.5 Environmental Controls on ET and WUE

Prior to conducting a multiple linear regression analysis (MLR) to determine the influence of environmental control variables such as PAR, Tair, VPD, and REW on ET, GEP, and WUE, we evaluated multicollinearity among environmental variables. This analysis showed correlation between PAR and VPD, as well as between Tair and VPD as expected (data not shown). This correlation pattern was further substantiated by the variance inflation factor (VIF) calculated to assess the multicollinearity among environmental variables (e.g., PAR, Tair, VPD, REW) (data not shown). These correlations and VIF results were with acceptable

ranges, indicating collinearity among the environmental control variables was not a major issue for our study. Furthermore, VPD consistently featured in most of the final models for each variable as determined by the stepwise AIC regression.

Employing four MLR models to pre-defined environmental conditions (i.e., hot, dry, hot-dry, normal) to ascertain their importance in explaining ET, GEP and WUE using the standardized beta coefficient and the relative importance analysis, we found that at the daily timescale PAR (lmg = 0.33) and Tair (lmg = 0.33) were the dominant control on daily ET (Table 2.5). In contrast, Tair proved to be the primary determinant of GEP (Table 2.5). While VPD was the primary control of WUE (Table 2.4). These results were further supported by the relative importance analysis (Table 2.5), where Tair explained ~ 37% and ~ 41% of the variability of ET under hot and dry conditions, respectively, while VPD explained ~37%, ~44%, ~61% and ~79% of the variability of WUE under hot, dry, hot-dry, and normal conditions, respectively. Additionally, REW emerged as a better explainer of WUE under hot or dry conditions, while VPD exhibited greater explanatory power for WUE under normal and concurrent hot and dry conditions. The proportion of the variance explained by the models is shown in Table 2.5.

Furthermore, the principal component analysis performed using daily PAR, Tair, VPD and REW indicated that the first component (PC1) explained 30.9% of the total variance, which means it can encapsulate nearly one-thirds of the information in the dataset. PC1 was positively associated with Tair and ET and GEP. Variables in this cluster belonged to growing season months such as July, August, and September. The second component (PC2) explained 27.2% of the variance. It was positively associated with REW and WUE (Fig. 2.6).

Higher degree to separation between variables in the PCA indicated that variables were uncorrelated such as Tair and WUE (~90° separation). The PCA also showed high degree of correlation between Tair and ET, and Tair and GEP. VPD and REW showed negative correlations with WUE, GEP and ET (>90° separation). These results are consistent with those found from the regression analysis.

#### 2.5 Discussion

### 2.5.1 Dynamics of ET

Our analysis and study results highlighted the temporal dependencies of ET on changes in environmental controls. We found a close synchronization between ET and fluctuations in light levels, while there was a lag between ET and changes in Tair and VPD as shown by hysteresis loops. The immediate response of ET to PAR can be attributed to the role of light in driving the opening and closing of stomata for CO<sub>2</sub> uptake for photosynthesis as discussed by Matthews et al. (2020). However, the hysteresis response of ET is influenced by a range of other factors including plant physiological processes, root water uptake dynamics, and soil water availability. Our findings were aligned with those reported by Zheng et al., (2014), who observed pronounced ET hysteresis loop in response to Tair and VPD and relatively smaller ET hysteresis loop against net radiation in an alpine meadow in Qinghai, China. They discussed the interplay of plant physiology and water status for the observed hysteresis responses of ET.

In our analysis, we found an increase in ET during concurrent hot and dry conditions, which is mainly attributed to high PAR and Tair during these extreme events. However, higher ET

due to elevated PAR and Tair can only be sustained until enough water is available in the soil (Condon et al., 2020). Given the higher values of ET during concurrent hot and dry conditions, we assumed that the forest generally had enough water available to sustain ET rates. Higher ET during these events can also be attributed to the combined effect of high Tair and high VPD, which promotes transpiration when trees can access larger soil water stores through their deeper roots. We observed a reduction in ET during dry conditions that may partly be linked to stomatal closure in response to soil water stress and decrease in evaporation from the understory and ground surface. While, water stress clearly reduced ET, there was a weak dependence of ET on the environmental variables during normal or wet conditions likely due to higher atmospheric humidity and/or cloudy conditions causing lower atmospheric demand (Nalevanková et al., 2020).

We also found that mean annual ET value of  $419 \pm 45$  mm yr<sup>-1</sup> in our deciduous forest was slightly lower than the mean annual ET value of  $442 \pm 33$  mm yr<sup>-1</sup> observed in a mature conifer forest in the area (Beamesderfer et al., 2020b) and much lower than those reported in a oak-dominated temperate deciduous forest in Ohio, USA, where mean annual ET was  $628 \pm 41$  mm (Xie et al., 2016) and in a deciduous broadleaf forest in Indiana, USA where mean annual transpiration was approximately 490 mm yr<sup>-1</sup> plus ~5% below canopy evaporation in the GS (Sulman et al., 2016).

## 2.5.2 Dynamics of WUE

We observed reduced WUE levels during hot and concurrent hot and dry conditions as shown in Figure 2.3. High temperatures have been shown to increase ET levels (Liu et al., 2015), with relatively smaller increase in GEP (Yu et al., 2007). Consequently, this

imbalance between elevated ET and marginal increase in GEP leads to a considerable reduction in WUE as reported by Law et al. (2002) and Xue et al. (2015). The higher ET and hence lower WUE during hot and hot-dry conditions in our forest can be explained by enhanced energy availability for evaporation and higher atmospheric water demand (VPD) during warm temperatures.

In our forest, we found an increasing trend in annual and GS WUE values from 2012 to 2014 and then a consistently decreasing trend from 2015 to 2020, except for 2019 which experienced a slightly higher WUE value. This was in contrast with Keenan et al. (2013), who found a substantial increasing trend in WUE in temperate forests due to increase in atmospheric CO<sub>2</sub> concentrations. Our study results suggested that climate variability and extreme weather events, rather than CO<sub>2</sub> fertilization effects played a dominant role on WUE trends at our site where six out seven recent years experienced extreme weather conditions. It further enhances the significance of long-term observation studies to fully understand the processes driving the declining trends of WUE in rapidly changing climate and extreme events.

Among forest biomes, deciduous forests usually have the larger WUE, such a mean WUE of 2.31 g C m<sup>-2</sup> kg H2O<sup>-1</sup> as reported by Xue et al. (2015) in their global synthesis of WUE from 2000 to 2013 using Fluxnet data. Mean WUE value for our forest was 3.8 g C m<sup>-2</sup> kg H2O<sup>-1</sup>, which is higher than the mean WUE values of 1.6 to 2.3 g C m<sup>-2</sup> kg H2O<sup>-1</sup> reported by the synthesis study of Tang et al. (2014) for deciduous forests at similar latitudes. However, our mean WUE values were similar to those reported by Xie et al. (2016) in an oak-dominated forest in the Great Lakes region in Ohio, USA. This disparity in WUE values

among forest sites is attributed to several factors, such as differences in local climatic conditions, ecosystem characteristics and plant species composition.

#### 2.5.3 Variations in the Water Budget

The metric P-ET represents the net influx of water at a site, which is available water for runoff and infiltration. It is a critical measure in understanding and managing water resources in forest ecosystems (Swenson & Wahr, 2006). We observed the lowest P-ET values during years that experienced lower P such as 2016 (hot-dry), 2015 (dry), 2012 (hot-dry) and 2020 (dry). Because of the conservative or less variable nature of ET in our region due to meteorological conditions, we observed higher ET/P during hot and dry years, particularly during the growing seasons. Overall, the lowest ET/P values were observed during years with normal or wet conditions such as 2013, 2014 and 2018, leading to surplus water that was contributed to hydrological processes like runoff and infiltration (Isabelle et al., 2020). Overall, the variations in surplus water from one year to another were primarily dictated by the interannual variation in P ( $\sigma = 261.9$ ) rather than ET ( $\sigma = 45.5$ ). ET was less variable and showed low sensitivity to P, even during years characterized as hot and hot-dry. For instance, despite the low annual P in 2016 (778 mm), the annual ET of 428 mm was close to the mean annual ET of 419  $\pm$  45 mm yr<sup>-1</sup>. Furthermore, usually clear sky and high PAR during the GS in the region contributed to sustained and less variable ET at our forest site (Schwartz et al., 2006).

While our study did not present direct evidence of physiological and phenological adaptations in our deciduous forest, however, we hypothesized that high LAI and a well-stablished root system with access to deeper soil water reserves – traits associated with oak forests, may have served as a strategy to effectively handle the fluctuations in P or dry conditions and to satisfy

water demand (Matheny et al., 2017; O'Connor et al., 2021). These attributes could play a role in alleviating the water stress experienced during periods of high temperature and water stress. This perceived adaptive response of our forest aligns with the findings of previous research by Jones (2013), Lawrence et al. (2022), Lu et al. (2011), Teuling et al. (2009), and Williams et al. (2001), all of whom have highlighted the significance of these mechanisms in maintaining efficient water utilizations and minimizing water stress in forests ecosystems.

#### 2.5.4 Environmental Controls on ET and WUE

The water and carbon fluxes in forest ecosystems are influenced by a combination of physical processes associated with water supply, energy availability, and atmospheric demand (Zhang et al., 2015), along with physiological mechanism (He et al., 2022). The dominant factors controlling the variability of ET and hence WUE (GEP/ET) may vary over time. A multitude of studies in the literature have highlighted these aspects for ET (Bagley et al., 2017; Forzieri et al., 2017; Hammerle et al., 2008; Morisette et al., 2009), GEP (Yu et al., 2007) and WUE (Li et al., 2023; Y. Liu et al., 2015). Our analysis of daily ET values showed that PAR, followed by Tair were the two dominant controls on ET. REW had a secondary effect, suggesting that our deciduous forest was more energy limited than water (Das et al., 2013). However, the relative importance analysis of environmental variables on ET showed variable dependence results in extreme weather events. For example, during normal conditions or years, Tair emerged as a more influential factor (lmg = 0.479) compared to PAR (lmg = 0.257). Interestingly, the relative importance of REW and VPD exhibited variation as well, but consistently yielding negative lmg values (Table 2.5). Both soil water availability and atmospheric demand play important roles in regulating plant water-use strategies (Jung et al., 2010; Novick et al., 2016). Therefore, decline in REW due to dry soil conditions, and an increase in atmospheric demand or VPD, leads to reduction in transpiration through stomatal closure by plants to conserve water (Sulman et al., 2016).

This is further reinforced by the non-linear response of stomatal conductance to VPD, which in turn minimizes water loss (Grossiord et al., 2020). Therefore, lower ET rates observed during dry or normal conditions may be explained by the inverse relationship between soil water availability and ET (supported by PCA in Figure 2.6), which can be intensified during hot and dry periods.

Our relative importance analysis further revealed that WUE in this deciduous forest was more influenced by VPD (lmg = -0.4) and Tair (lmg = 0.3), outweighing the impact of PAR (lmg = 0.1) or REW (lmg = 0.1) at daily timescales that were negatively correlated with WUE (Table 4). The distinct pattern of VPD emerging as a primary driver of WUE was found even when analyzing daily values across the spectrum of hot and dry conditions. These results are well aligned with the recent study by Li et al., (2023), which identified VPD as the foremost control over WUE, although they identified it at half-hourly timescales. However, our results were in contrast with the findings of Li et al., (2023) who found no significant impacts of VPD on WUE. Additionally, our results supported Tang et al., (2014), suggesting a negative influence of soil water stress on WUE in a deciduous forest. The PCA further supported these findings, where VPD and WUE showed negative correlation with WUE, GEP and ET.

VPD is highly sensitive to changes in air temperature and thus it is expected to rise globally, intensifying plant water loss through transpiration (Grossiord et al., 2020). However,

photosynthetic uptake (i.e GEP) can be constrained under these circumstances due to the reduced efficiency of photosynthesis enzymes at high Ta, limiting carbon fixation (Lin et al., 2012), changes in stomatal conductance regulated by tree water availability, and nutrient availability resulting in reduced WUE (Gálvez & Tyree, 2009; Massmann et al., 2019; Wang et al., 2018). Elevated Ta can initially increase stomatal conductance, but subsequently soil water stress and excessive heat can trigger stomatal closure, reducing transpiration and impeding carbon uptake. This delicate balance between elevated Ta, ET, GEP and WUE highlights the complexity and challenges faced by forests for growth and survival in changing climate (Zhao et al., 2021).

#### 2.6 Conclusions

Analysis of water flux observations made using eddy covariance technique in a temperate deciduous forest from 2012 to 2020 showed that mean growing season (GS) and annual ET values were 367  $\pm$  40 mm and 419  $\pm$  46 mm, respectively. Overall, ET represented approximately 38% of annual P of 1148  $\pm$  262 mm yr<sup>-1</sup> over the study period. The forest had a mean P-ET value of 729  $\pm$  258 mm, indicating a positive water balance over the study period. However, a notable reduction in P-ET was observed in the growing season of 2016, where P-ET dropped 11 mm, highlighting the susceptibility of the forest to extreme weather events. Mean growing season WUE over the study period was  $3.8 \pm 0.4$  g C Kg H<sub>2</sub>O<sup>-1</sup>, with the highest WUE of 4.4 g C Kg H<sub>2</sub>O<sup>-1</sup> observed in 2014 (cool year), and the lowest values of 3.0 and 3.1 g C Kg H<sub>2</sub>O<sup>-1</sup> observed in 2012 (hot-dry year) and 2020 (dry year), respectively. An increasing trend in both annual and growing season WUE values was observed from 2012 to 2014, while a deceasing trend in WUE was observed from 2015 to

2020, when most of years experienced extreme weather events, except 2019. Both PAR and Tair were the main environmental variable governing daily ET, while VPD was the dominant driver for WUE. However, during hot and dry conditions, REW showed substantial relative importance in influencing WUE. Our study results underscore the resilience of ET and WUE in our oak-dominated forest in face of climate change and extreme weather events. These long-term flux observations will help to enrich the understanding water exchange processes in temperate deciduous forests of eastern North America and develop protocols and models to explore ways to better manage water resources in the Great Lakes region in changing climate.

## 2.7 Acknowledgements

This study was funded by Natural Sciences and Engineering Research Council (NSERC), Global Water Futures Program (GWF), and the Ontario Ministry of Environment and Climate Change (MOECC). Funding from the Canadian Foundation of Innovation (CFI) through new opportunity and Leaders Opportunity Fund and Ontario Research Fund of the Ministry of Research and Innovation is also acknowledged. In-kind support from the Long Point Region Conservation Authority (LPRCA) is also acknowledged. Finally, we acknowledge support from Zoran Nesic at the University of British Columbia (Dr. T. A. Black's group) in assistance with flux measurements at our site and thank past and present members of the Hydrometeorology and Climatology lab at McMaster University, including Robin Thorne, Brandon Burns, Michelle Kula, Eric Beamesderfer, Lejla Latifovic and Farbod Tabaei for their support in the fieldwork. We gratefully thank the editor and two anonymous reviewers for the constructive suggestions on the manuscript.

#### 2.8 References

- Anderegg, W. R. L., Konings, A. G., Trugman, A. T., Yu, K., Bowling, D. R., Gabbitas, R., Karp, D. S., Pacala, S., Sperry, J. S., Sulman, B. N., & Zenes, N. (2018). Hydraulic diversity of forests regulates ecosystem resilience during drought. *Nature*, *561*(7724), 538–541. https://doi.org/10.1038/s41586-018-0539-7
- Arain, M. A. (2022), AmeriFlux FLUXNET-1F CA-TPD Ontario Turkey Point Mature Deciduous, Ver. 3-5, AmeriFlux AMP, (Dataset). https://doi.org/10.17190/AMF/1881567
- Arain, M. A., Xu, B., Brodeur, J. J., Khomik, M., Peichl, M., Beamesderfer, E., Restrepo-Couple, N., & Thorne, R. (2022). Heat and drought impact on carbon exchange in an age-sequence of temperate pine forests. *Ecological Processes*, 11(1). https://doi.org/10.1186/s13717-021-00349-7
- Bagley, J. E., Kueppers, L. M., Billesbach, D. P., Williams, I. N., Biraud, S. C., & Torn, M. S. (2017). The influence of land cover on surface energy partitioning and evaporative fraction regimes in the U.S. Southern Great Plains. *Journal of Geophysical Research*, *122*(11), 5793–5807. https://doi.org/10.1002/2017JD026740
- Baldocchi, D. (2019). How eddy covariance flux measurements have contributed to our understanding of Global Change Biology. Global Change Biology, 26(1), 242–260. https://doi.org/10.1111/gcb.14807
- Beamesderfer, E., Arain, A., Khomik, M., Brodeur, J. J., & Burns, B. M. (2020a). Response of carbon and water fluxes to meteorological and phenological variability in two eastern North American forests of similar age but contrasting species composition- A multiyear comparison. *Journal of Geophysical Research: Biogeosciences*, 17(13), 3563–3587. https://doi.org/https://doi.org/10.5194/bg-17-3563-2020
- Beamesderfer, E., Arain, M. A., Khomik, M., Brodeur, J., & Burns, B. (2020b). Response of carbon and water fluxes to environmental variability in two Eastern North American forests of similarage but contrasting leaf-retention and shape strategies. *Biogeosciences Discussions*, 1–39. https://doi.org/10.5194/bg-2019-457
- Beamesderfer, E., Arain, M. A., Khomik, M., & Brodeur, J. J. (2020). The Impact of Seasonal and Annual Climate Variations on the Carbon Uptake Capacity of a Deciduous Forest Within the Great Lakes Region of Canada. *Journal of Geophysical Research: Biogeoscience*, 125(9). https://doi.org/10.1029/2019JG005389
- Beer, C., Ciais, P., Reichstein, M., Baldocchi, D., Law, B. E., Papale, D., Soussana, J. F., Ammann, C., Buchmann, N., Frank, D., Gianelle, D., Janssens, I. A., Knohl, A., Köstner, B., Moors, E., Roupsard, O., Verbeeck, H., Vesala, T., Williams, C. A., & Wohlfahrt, G. (2009). Temporal and among-site variability of inherent water use efficiency at the ecosystem level. *Global Biogeochemical Cycles*, 23(2), 1–13. https://doi.org/10.1029/2008GB003233
- Black, T. A. (1979). Evapotranspiration From Douglas Fir Stands Exposed to Soil Water Deficits. *Water Resources Research*, 15(1), 164–170. https://doi.org/10.1029/WR015i001p00164
- Bonan, G. B. (2008). Forests and Climate Change: Forcings, Feedbacks, and the Climate Benefits of

- Forests. Science, 320(5882), 1444–1449. https://doi.org/10.1126/science.1155121
- Bréda, N., Granier, A., & Aussenac, G. (1995). Effects of thinning on soil and tree water relations, transpiration and growth in an oak forest (Quercus petraea (Matt.) Liebl.). *Tree Physiology*, 15(5), 295–306. https://doi.org/10.1093/treephys/15.5.295
- Brodeur, J. (2014). Data-driven approaches for sustainable operation and defensible results in a long-term, multi-site ecosystem flux measurement program (Doctoral dissertation). McMaster University.
- Buras, A., Rammig, A., & S. Zang, C. (2020). Quantifying impacts of the 2018 drought on European ecosystems in comparison to 2003. *Biogeosciences*, 17(6), 1655–1672. https://doi.org/10.5194/bg-17-1655-2020
- Ciais, P., Reichstein, M., Viovy, N., Granier, A., Ogée, J., Allard, V., Aubinet, M., Buchmann, N., Bernhofer, C., Carrara, A., Chevallier, F., De Noblet, N., Friend, A. D., Friedlingstein, P., Grünwald, T., Heinesch, B., Keronen, P., Knohl, A., Krinner, G., ... Valentini, R. (2005). Europe-wide reduction in primary productivity caused by the heat and drought in 2003. *Nature*, 437, 259–533. https://doi.org/10.1038/nature03972
- Clogg, C. C., Petkova, E., & Haritou, A. (1995). Statistical Methods for Comparing Regression Coefficients Between Models. *American Journal of Sociology*, 100(5), 1261–1293. https://www.jstor.org/stable/2782277
- Condon, L. E., Atchley, A. L., & Maxwell, R. M. (2020). Evapotranspiration depletes groundwater under warming over the contiguous United States. *Nature Communications*, 11(873). https://doi.org/10.1038/s41467-020-14688-0
- Das, A. J., Stephenson, N. L., Flint, A., Das, T. J., & Van Mantgem, P. J. (2013). Climatic Correlates of Tree Mortality in Water-and Energy-Limited Forests. *PLoS ONE*, 8(7), 69917. https://doi.org/10.1371/journal.pone.0069917
- Diao, H., Wang, A., Yang, H., Yuan, F., Guan, D., & Wu, J. (2021). Responses of evapotranspiration to droughts across global forests: A systematic assessment. *Canadian Journal of Forest Research*, 51(1), 1–9. https://doi.org/10.1139/cjfr-2019-0436
- Environment and Climate Change Canada (ECCC). (2023, January). *Climate Data Online*. Https://Climate.Weather.Gc.ca. Accessed 16 January.
- Farley, K. A., Jobbagy, E. G., & Jackson, R. B. (2005). Effects of afforestation on water yield: a global synthesis with implications for policy. *Global Change Biology* (2005), 11, 1565–1576. https://doi.org/10.1111/j.1365-2486.2005.01011.x
- Forzieri, G., Alkama, R., Miralles, D. G., & Cescatti, A. (2017). Satellites reveal contrasting responses of regional climate to the widespread greening of Earth. *Science*, 356(6343), 1180–1184. https://doi.org/10.1126/science.aal1727
- Friedlingstein, P., Houghton, R. A., Marland, G., Hackler, J., Boden, T. A., Conway, T. J., Canadell, J. G., Raupach, M. R., Ciais, P., & Le Quéré, C. (2010). Update on CO2 emissions. In *Nature Geoscience* (Vol. 3, Issue 12, pp. 811–812). https://doi.org/10.1038/ngeo1022

- Gaertner, B. A., Zegre, N., Warner, T., Fernandez, R., He, Y., & Merriam, E. R. (2019). Climate, forest growing season, and evapotranspiration changes in the central Appalachian Mountains, USA. *Science of the Total Environment*, 650, 1371–1381. https://doi.org/10.1016/j.scitotenv.2018.09.129
- Gálvez, D. A., & Tyree, A. M. T. (2009). Impact of simulated herbivory on water relations of aspen (Populus tremuloides) seedlings: the role of new tissue in the hydraulic conductivity recovery cycle. *Oecologia*, 161, 665–671. https://doi.org/10.1007/s00442-009-1416-8
- Givnish, T. J. (2002). Adaptive significance of evergreen vs. deciduous leaves: solving the triple paradox. *Silva Fennica*, 36(3), 703–743. https://doi.org/https://doi.org/10.14214/sf.535
- Graf, A., Klosterhalfen, A., Arriga, N., Bernhofer, C., Bogena, H., Bornet, F., Brüggemann, N., Brümmer, C., Buchmann, N., Chi, J., Chipeaux, C., Cremonese, E., Cuntz, M., Dušek, J., El-Madany, T. S., Fares, S., Fischer, M., Foltýnová, L., Gharun, M., ... Vereecken, H. (2020). Altered energy partitioning across terrestrial ecosystems in the European drought year 2018: Energy partitioning in the drought 2018. *Philosophical Transactions of the Royal Society B: Biological Sciences*, 375(1810). https://doi.org/10.1098/rstb.2019.0524
- Granier, A., Reichstein, M., Bréda, N., Janssens, I. A., Falge, E., Ciais, P., Grünwald, T., Aubinet, M., Berbigier, P., Bernhofer, C., Buchmann, N., Facini, O., Grassi, G., Heinesch, B., Ilvesniemi, H., Keronen, P., Knohl, A., Köstner, B., Lagergren, F., ... Wang, Q. (2007). Evidence for soil water control on carbon and water dynamics in European forests during the extremely dry year: 2003. *Agricultural and Forest Meteorology*, 143(1–2), 123–145. https://doi.org/10.1016/j.agrformet.2006.12.004
- Griscom, B. W., Adams, J., Ellis, P. W., Houghton, R. A., Lomax, G., Miteva, D. A., Schlesinger, W. H., Shoch, D., Siikamäki, J. V., Smith, P., Woodbury, P., Zganjar, C., Blackman, A., Campari, J., Conant, R. T., Delgado, C., Elias, P., Gopalakrishna, T., Hamsik, M. R., ... Fargione, J. (2017). Natural climate solutions. *Proceedings of the National Academy of Sciences of the United States of America*, 114(44), 11645–11650. https://doi.org/10.1073/pnas.1710465114
- Groempings, U. (2021). *The Relative Importance of Regressors in Linear Models*. https://prof.bht-berlin.de/groemping/relaimpo/,
- Grossiord, C., Buckley, T. N., Cernusak, L. A., Novick, K. A., Poulter, B., Siegwolf, R. T. W., Sperry, J. S., & Mcdowell, N. G. (2020). *Tansley review Plant responses to rising vapor pressure deficit*. 1550–1566. https://doi.org/10.1111/nph.16485
- Hammerle, A., Haslwanter, A., Tappeiner, U., Cernusca, A., & Wohlfahrt, G. (2008). Leaf area controls on energy partitioning of a temperate mountain grassland. *Biogeosciences*, 5(2), 421–431. https://doi.org/10.5194/bg-5-421-2008
- Hammond, W. M., Williams, A. P., Abatzoglou, J. T., Adams, H. D., Klein, T., López, R., Sáenz-Romero, C., Hartmann, H., Breshears, D. D., & Allen, C. D. (2022). Global field observations of tree die-off reveal hotter-drought fingerprint for Earth's forests. *Nat Commun*, *13*, 1761. https://doi.org/10.1038/s41467-022-29289-2

- He, Q. L., Xiao, J. L., & Shi, W. Y. (2022). Responses of Terrestrial Evapotranspiration to Extreme Drought: A Review. In *Water* (Vol. 14, Issue 23). MDPI. https://doi.org/10.3390/w14233847
- Isabelle, P. E., Nadeau, D. F., Anctil, F., Rousseau, A. N., Jutras, S., & Music, B. (2020). Impacts of high precipitation on the energy and water budgets of a humid boreal forest. *Agricultural and Forest Meteorology*, 280(October 2019), 107813. https://doi.org/10.1016/j.agrformet.2019.107813
- Jasechko, S., Sharp, Z. D., Gibson, J. J., Birks, S. J., Yi, Y., & Fawcett, P. J. (2013). Terrestrial water fluxes dominated by transpiration. *Nature*, 496(7445), 347–350. https://doi.org/10.1038/nature11983
- Jones, H. G. (2013). Plants and microclimate: A quantitative approach to environmental plant physiology. In *Plants and Microclimate: A Quantitative Approach to Environmental Plant Physiology* (Vol. 9780521279). https://doi.org/10.1017/CBO9780511845727
- Jung, M., Reichstein, M., Ciais, P., Seneviratne, S. I., Sheffield, J., Goulden, M. L., Bonan, G., Cescatti, A., Chen, J., De Jeu, R., Dolman, A. J., Eugster, W., Gerten, D., Gianelle, D., Gobron, N., Heinke, J., Kimball, J., Law, B. E., Montagnani, L., ... Zhang, K. (2010). Recent decline in the global land evapotranspiration trend due to limited moisture supply. *Nature*, 467(7318), 951–954. https://doi.org/10.1038/nature09396
- Keenan, T. F., Hollinger, D. Y., Bohrer, G., Dragoni, D., Munger, J. W., Schmid, H. P., & Richardson, A. D. (2013). Increase in forest water-use efficiency as atmospheric carbon dioxide concentrations rise. *Nature*, 499(7458), 324–327. https://doi.org/10.1038/nature12291
- Khalid, S. (2016). Impact of afforestation on soil chemical and physical properties of southern Ontario forests, with a comparison to a naturally regenerated stand. [Undergraduate thesis]. McMaster University.
- Kljun, N., Kormann, R., Rotach, M. W., & Meixer, F. X. (2003). Comparison of the langrangian footprint model lpdm-b with an analytical footprint model. *Boundary-Layer Meteorology*, 106.
- Law, B. E., Falge, E., Gu, L., Baldocchi, D. D., Bakwin, P., Berbigier, P., Davis, K., Dolman, A. J., Falk, M., Fuentes, J. D., Goldstein, A., Granier, A., Grelle, A., Hollinger, D., Janssens, I. A., Jarvis, P., Jensen, N. O., Katul, G., Mahli, Y., ... Oechel, W. (2002). *Environmental controls over carbon dioxide and water vapor exchange of terrestrial vegetation*. 113(April), 97–120.
- Lawrence, D., Coe, M., Walker, W., Verchot, L., & Vandecar, K. (2022). The Unseen Effects of Deforestation: Biophysical Effects on Climate. *Frontiers in Forests and Global Change*, 5(756115). https://doi.org/10.3389/ffgc.2022.756115
- Lejeune, Q., Davin, E. L., Gudmundsson, L., Winckler, J., & Seneviratne, S. I. (2018). Historical deforestation locally increased the intensity of hot days in northern mid-latitudes. *Nature Climate Change*, 8(5), 386–390. https://doi.org/10.1038/s41558-018-0131-z
- Lemordant, L., Gentine, P., Swann, A. S., Cook, B. I., & Scheff, J. (2018). Critical impact of vegetation physiology on the continental hydrologic cycle in response to increasing CO2. *Proceedings of the National Academy of Sciences of the United States of America*, 115(16), 4093–4098. https://doi.org/10.1073/pnas.1720712115

- Li, Y., Zhang, K., & Liu, L. (2023). Water use efficiency at multi-time scales and its response to episodic drought and wet periods in a typical subtropical evergreen forest of Southeast China. *Ecological Indicators*, *151*. https://doi.org/10.1016/j.ecolind.2023.110254
- Lin, Y. S., Medlyn, B. E., & Ellsworth, D. S. (2012). Temperature responses of leaf net photosynthesis: The role of component processes. *Tree Physiology*, *32*(2), 219–231. https://doi.org/10.1093/treephys/tpr141
- Liu, X., Chen, X., Li, R., Long, F., Zhang, L., Zhang, Q., & Li, J. (2017). Water-use efficiency of an old-growth forest in lower subtropical China OPEN. https://doi.org/10.1038/srep42761
- Liu, Y., Xiao, J., Ju, W., Zhou, Y., Wang, S., & Wu, X. (2015). Water use efficiency of China's terrestrial ecosystems and responses to drought. *Scientific Reports*, 5. https://doi.org/10.1038/srep13799
- L.P.R.C.A. (2023). Long Point Region Conservation Authority. Long Point Region Conservation Authority. https://lprca.on.ca/
- Lu, N., Chen, S., Wilske, B., Sun, G., & Chen, J. (2011). Evapotranspiration and soil water relationships in a range of disturbed and undisturbed ecosystems in the semi-arid Inner Mongolia, China. *Journal of Plant Ecology*, 4(2), 49–60. https://doi.org/10.1093/jpe/rtq035
- Lumley, T. (2020). *Thomas Lumley Based on Fortran Code by Alan Miller*.
- Massmann, A., Gentine, P., & Lin, C. (2019). When Does Vapor Pressure Deficit Drive or Reduce Evapotranspiration? *Journal of Advances in Modeling Earth Systems*, 11(10), 3305–3320. https://doi.org/10.1029/2019MS001790
- Matheny, A. M., Fiorella, R. P., Bohrer, G., Poulsen, C. J., Morin, T. H., Wunderlich, A., Vogel, C. S., & Curtis, P. S. (2017). Contrasting strategies of hydraulic control in two codominant temperate tree species. *Ecohydrology*, 10(3). https://doi.org/10.1002/eco.1815
- Matthews, J. S. A., Vialet-Chabrand, S., & Lawson, T. (2020). Role of blue and red light in stomatal dynamic behaviour. In *Journal of Experimental Botany* (Vol. 71, Issue 7, pp. 2253–2269). Oxford University Press. https://doi.org/10.1093/jxb/erz563
- Moomaw, W. R., Law, B. E., & Goetz, S. J. (2020). Focus on the role of forests and soils in meeting climate change mitigation goals: Summary. *Environmental Research Letters*, 15(4). https://doi.org/10.1088/1748-9326/ab6b38
- Morisette, J. T., Richardson, A. D., Knapp, A. K., Fisher, J. I., Graham, E. A., Abatzoglou, J., Wilson, B. E., Breshears, D. D., Henebry, G. M., Hanes, J. M., & Liang, L. (2009). Tracking the rhythm of the seasons in the face of global change: Phenological research in the 21 st century. *Frontiers in Ecology and the Environment*, 7(5), 253–260. https://doi.org/10.1890/070217
- Nalevanková, P., Sitková, Z., Kučera, J., & Střelcová, K. (2020). Impact of water deficit on seasonal and diurnal dynamics of european beech transpiration and time-lag effect between stand transpiration and environmental drivers. *Water*, 12(12), 1–21. https://doi.org/10.3390/w12123437

- Novick, K. A., Ficklin, D. L., Stoy, P. C., Williams, C. A., Bohrer, G., Oishi, A. C., Papuga, S. A., Blanken, P. D., Noormets, A., Sulman, B. N., Scott, R. L., Wang, L., & Phillips, R. P. (2016). The increasing importance of atmospheric demand for ecosystem water and carbon fluxes. In *Nature Climate Change* (Vol. 6, Issue 11, pp. 1023–1027). https://doi.org/10.1038/nclimate3114
- O'Connor, J. C., Dekker, S. C., Staal, A., Tuinenburg, O. A., Rebel, K. T., & Santos, M. J. (2021). Forests buffer against variations in precipitation. *Global Change Biology*, 27(19), 4686–4696. https://doi.org/10.1111/gcb.15763
- Oki, T., & Kanae, S. (2006). Global Hydrological Cycles and World Water Resources. *Science*, 313(5790), 1068–1072. https://doi.org/10.1126/science.1128845
- Pan, S., Tian, H., Dangal, S. R. S., Yang, Q., Yang, J., Lu, C., Tao, B., Ren, W., & Ouyang, Z. (2014). Earth's Future Responses of global terrestrial evapotranspiration to climate change and increasing atmospheric CO 2 in the 21st century. https://doi.org/10.1002/2014EF000263
- Papale, D., Reichstein, M., Aubinet, M., Canfora, E., Bernhofer, C., Kutsch, W., Longdoz, B., Rambal, S., Valentini, R., Vesala, T., & Yakir, D. (2006). Towards a standardized processing of Net Ecosystem Exchange measured with eddy covariance technique: algorithms and uncertainty estimation. *Biogeosciences*, 3(4), 571–583. https://doi.org/10.5194/bg-3-571-2006
- Peichl, M., Arain, M. A., & Brodeur, J. J. (2010). Agricultural and Forest Meteorology Age effects on carbon fluxes in temperate pine forests. *Agricultural and Forest Meteorology*, 150(7–8), 1090–1101. https://doi.org/10.1016/j.agrformet.2010.04.008
- Schwartz, M. D., Ahas, R., & Aasa, A. (2006). Onset of spring starting earlier across the Northern Hemisphere. *Global Change Biology*, 12(2), 343–351. https://doi.org/10.1111/j.1365-2486.2005.01097.x
- Seneviratne, S. I., Corti, T., Davin, E. L., Hirschi, M., Jaeger, E. B., Lehner, I., Orlowsky, B., & Teuling, A. J. (2010). Investigating soil moisture-climate interactions in a changing climate: A review. In *Earth-Science Reviews* (Vol. 99, Issues 3–4, pp. 125–161). https://doi.org/10.1016/j.earscirev.2010.02.004
- Shuttleworth, W. (2012). *Terrestrial Hydrometeorology* (Vol. 1). John Wiley and Sons. https://doi.org/10.1002/9781119951933
- Sulman, B. N., Roman, D. T., Yi, K., Wang, L., Phillips, R. P., & Novick, K. A. (2016). High atmospheric demand for water can limit forest carbon uptake and transpiration as severely as dry soil. *Geophysical Research Letters*, 43(18), 9686–9695. https://doi.org/10.1002/2016GL069416
- Swenson, S., & Wahr, J. (2006). *Estimating Large-Scale Precipitation Minus Evapotranspiration from GRACE Satellite Gravity Measurements*. Journal of Hydrometeorology, 7:252-270. DOI: https://doi.org/10.1175/JHM478.1
- Tang, X., Li, H., Desai, A. R., Nagy, Z., Luo, J., Kolb, T. E., Olioso, A., Xu, X., Yao, L., Kutsch, W., Pilegaard, K., Köstner, B., & Ammann, C. (2014). How is water-use efficiency of terrestrial ecosystems distributed and changing on Earth? *Scientific Reports*, 4, 1–11.

- https://doi.org/10.1038/srep07483
- Teuling, A. J., Hirschi, M., Ohmura, A., Wild, M., Reichstein, M., Ciais, P., Buchmann, N., Ammann, C., Montagnani, L., Richardson, A. D., Wohlfahrt, G., & Seneviratne, S. I. (2009). A regional perspective on trends in continental evaporation. *Geophysical Research Letters*, 36(2), 1–5. https://doi.org/10.1029/2008GL036584
- Teuling, A. J., Seneviratne, S. I., Stöckli, R., Reichstein, M., Moors, E., Ciais, P., Luyssaert, S., Van Den Hurk, B., Ammann, C., Bernhofer, C., Dellwik, E., Gianelle, D., Gielen, B., Grünwald, T., Klumpp, K., Montagnani, L., Moureaux, C., Sottocornola, M., & Wohlfahrt, G. (2010). Contrasting response of European forest and grassland energy exchange to heatwaves. *Nature Geoscience*, 3(10), 722–727. https://doi.org/10.1038/ngeo950
- Vilhar, U. (2016). Comparison of drought stress indices in beech forests: A modelling study. *IForest*, 9(4), 635–642. https://doi.org/10.3832/ifor1630-008
- Wang, M., Chen, Y., Wu, X., & Bai, Y. (2018). Forest-Type-Dependent Water Use Efficiency Trends Across the Northern Hemisphere. *Geophysical Research Letters*, 45(16), 8283–8293. https://doi.org/10.1029/2018GL079093
- Williams, M., Law, B. E., Anthoni, P. M., & Unsworth, M. H. (2001). Use of a simulation model and ecosystem flux data to examine carbon-water interactions in ponderosa pine. *Tree Physiology*, 21(5), 287–298. https://doi.org/10.1093/treephys/21.5.287
- Xie, J., Chen, J., Sun, G., Zha, T., Yang, B., Chu, H., Liu, J., Wan, S., Zhou, C., Ma, H., Bourque, C. P. A., Shao, C., John, R., & Ouyang, Z. (2016). Ten-year variability in ecosystem water use efficiency in an oak-dominated temperate forest under a warming climate. *Agricultural and Forest Meteorology*, 218–219, 209–217. https://doi.org/10.1016/j.agrformet.2015.12.059
- Xue, B. L., Guo, Q., Otto, A., Xiao, J., Tao, S., & Li, L. (2015). Global patterns, trends, and drivers of water use efficiency from 2000 to 2013. *Ecosphere*, 6(10). https://doi.org/10.1890/ES14-00416.1
- Yu, G., Song, X., Wang, Q., Liu, Y., Guan, D., Yan, J., Sun, X., Zhang, L., & Wen, X. (2007). Water-use efficiency of forest ecosystems in eastern China and its relations to climatic variables. https://doi.org/10.1111/j
- Zhang, K., Kimball, J. S., Nemani, R. R., Running, S. W., Hong, Y., Gourley, J. J., & Yu, Z. (2015). Vegetation Greening and Climate Change Promote Multidecadal Rises of Global Land Evapotranspiration. *Scientific Reports*, 5. https://doi.org/10.1038/srep15956
- Zhao, J., Feng, H., Xu, T., Xiao, J., Guerrieri, R., Liu, S., Wu, X., He, X., & He, X. (2021). Physiological and environmental control on ecosystem water use efficiency in response to drought across the northern hemisphere. *Science of the Total Environment*, 758. https://doi.org/10.1016/j.scitotenv.2020.143599
- Zhao, M., A, G., Liu, Y., & Konings, A. G. (2022). Evapotranspiration frequently increases during droughts. *Nature Climate Change*, 12(11), 1024–1030. https://doi.org/10.1038/s41558-022-01505-3

Zheng, H., Wang, Q., Zhu, X., Li, Y., & Yu, G. (2014). Hysteresis responses of evapotranspiration to meteorological factors at a diel timescale: Patterns and causes. *PLoS ONE*, *9*(6). https://doi.org/10.1371/journal.pone.00988

Table 2.1: Characteristics of the deciduous forest site

Parameter	Value/Remark				
Latitude (°N)	42.635°				
Longitude (°W)	80.558°				
Elevation (m)	265				
Previous land use	Naturally regenerated on abandoned agricultural land with infill plantation and forest management.				
Age (in 2020)	73-110 years				
Mean diameter at breast or 1.3 m height, DBH (cm)	25.4				
Tree density (trees ha <sup>-1</sup> )	504				
Mean tree height (m)	25.7				
Leaf area index, LAI (m <sup>2</sup> m <sup>-2</sup> )	8.0				
Dominant tree species	Quercus alba L.				
Secondary and understory tree species	Acer saccharum Marshall., Acer rubrum L., Fagus grandifolia Ehrh., Quercus velutina Lam., Quercus rubra L., Fraxinus americana L.				
Ground vegetation	Maianthemum canadense Desf., Aplectrum hyemale (Muhl. Ex Willd.), Equisetum L.				
Soil type, texture and drainage characteristics	Brunisolic grey-brown luvisol, >90% sand, which is well-drained with Low-to-moderate soil water holding capacity				
Soil bulk density (g m <sup>-3</sup> )	1.15				
30-year mean <sup>b</sup> annual temperature (°C)	8.0 (±1.6)				
30-year mean <sup>b</sup> annual precipitation (mm)	997				

a Classified by the Canadian Soil Classification Scheme and FAO World Reference Base (Present & Acton, 1984).

b 30-year mean (1981-2010) climate normal was calculated using data from weather station at Delhi, located approximately 20 km north of the site (Environment and Climate Change Canada, 2021).

**Table 2.2:** Mean annual values of meteorological variables (air temperature, Tair; vapor pressure deficit, VPD; photosynthetic active radiation, PAR; soil temperature, Ts at the 5 cm and 100 cm depths and soil moisture, SM for 0-30 soil layer and relative extractable water, REW). Growing season values are given in parenthesis. Characterization of years include hot years (2018), dry year (2015, 2017, 2020), hot and dry years (2012, 2016) and normal year (2013, 2014, 2019).

Year	Ta (°C)	VPD (kPa)	PAR (μmol m <sup>-2</sup> s <sup>-1</sup> )	Ts <sub>5cm</sub> (°C)	Ts <sub>100cm</sub> (°C)	$\theta_{0-30}$ (m <sup>3</sup> m <sup>-3</sup> )	REW
			$286.9 \pm 186.9$			$0.10 \pm 0.03$	$0.61 \pm 0.23$
2012	11.8 (18.7)	$0.57 \pm 0.42 \ (0.82)$	(398.3)	$10.3 \pm 6.9 (15.7)$	$10.1 \pm 4.2 (13.2)$	(0.08)	(0.47)
			$266.6 \pm 173.4$			$0.11 \pm 0.03$	$0.67 \pm 0.17$
2013	9.2 (17.3)	$0.35 \pm 0.26 \ (0.50)$	(366.0)	$9.2 \pm 7.5 (15.6)$	$9.2 \pm 4.8  (13.0)$	(0.10)	(0.61)
			$280.5 \pm 175.1$			$0.11 \pm 0.03$	$0.68 \pm 0.21$
2014	8.0 (17.3)	$0.33 \pm 0.25 \ (0.49)$	(380.1)	$8.8 \pm 7.3 (15.4)$	$8.6 \pm 4.8  (12.5)$	(0.10)	(0.62)
			$285.2 \pm 173.0$			$0.10 \pm 0.04$	$0.60 \pm 0.24$
2015	9.2 (17.9)	$0.35 \pm 0.27 \ (0.52)$	(386.9)	$9.5 \pm 7.2 (15.8)$	$9.3 \pm 4.8  (12.8)$	(0.09)	(0.55)
			$287.4 \pm 181.0$			$0.10 \pm 0.04$	$0.57 \pm 0.27$
2016	10.6 (18.4)	$0.42 \pm 0.34  (0.61)$	(393.7)	$10.2 \pm 7.1 (16.1)$	$10.1 \pm 4.5 (13.2)$	(0.07)	(0.38)
			$270.5 \pm 175.4$			$0.10 \pm 0.04$	$0.62 \pm 0.23$
2017	10.0 (17.4)	$0.36 \pm 0.28 \ (0.51)$	(365.5)	$10.0 \pm 6.8 (15.7)$	$9.7 \pm 4.4 (13.3)$	(0.08)	(0.49)
			$266.0 \pm 178.4$			$0.11 \pm 0.04$	$0.65 \pm 0.24$
2018	9.7 (18.4)	$0.33 \pm 0.33 \ (0.50)$	(358.5)	$9.5 \pm 7.7 (16.1)$	$9.3 \pm 5.1 (13.4)$	(0.09)	(0.52)
			$275.9 \pm 178.8$			$0.11 \pm 0.03$	$0.66 \pm 0.22$
2019	9.1 (17.2)	$0.29 \pm 0.25 \ (0.42)$	(372.4)	$9.2 \pm 7.4 (15.5)$	$9.1 \pm 4.9 (12.9)$	(0.10)	(0.57)
			$317.3 \pm 205.6$			$0.11 \pm 0.04$	$0.67 \pm 0.24$
2020	10.6 (17.7)	$0.37 \pm 0.31 \ (0.53)$	(432.6)	$9.9 \pm 6.8 (15.4)$	$9.5 \pm 4.5 (12.9)$	(0.09)	(0.52)
			$281.8 \pm 14.8$			$0.11 \pm 0.03$	$0.64 \pm 0.04$
Mean	9.7 (17.8)	$0.37 \pm 0.08 \ (0.54)$	(383.8)	$9.6 \pm 0.5  (15.7)$	$9.4 \pm 4.7 \ (13.0)$	(0.09)	(0.53)

a The standard deviation (sd) is provided next to the mean of each metric.

b Growing season is time period when GEP was above zero.

**Table 2.3:** Annual and growing season water fluxes from 2012 to 2020: Numbers in parenthesis indicate values in growing season, which is time period when GEP > 0. Characterization of years include hot year (2018), dry year (2015, 2017, 2020), hot and dry years (2012, 2016) and normal year (2013, 2014, 2019).

Year	GSL	P (mm)	ET (mm)	GEP (g C m <sup>-2</sup> )	ET/P (mm)	P-ET (mm)	WUE (g C m <sup>-2</sup> kgH <sub>2</sub> O <sup>-1</sup> )
2012	194 (April 14 to Oct. 25)	1001 (616)	429 (371)	1123	0.43 (0.60)	572 (245)	2.6 (3.0)
2013	159 (April 27 to Nov. 03)	1266 (680)	392 (351)	1387	0.31 (0.52)	874 (329)	3.5 (4.0)
2014	181 (April 30 to Oct. 28)	1429 (590)	359 (315)	1382	0.25 (0.53)	1070 (275)	3.8 (4.4)
2015	182 (April 29 to Oct. 28)	811 (500)	365 (321)	1346	0.45 (0.64)	446 (179)	3.7 (4.2)
2016	192 (April 29 to Nov. 7)	778 (383)	428 (372)	1417	0.55 (0.97)	350 (11)	3.3 (3.8)
2017	191 (May 01 to Nov. 08)	1153 (582)	423 (362)	1440	0.37 (0.62)	730 (220)	3.4 (4.0)
2018	192 (April 30 to Nov. 8)	1649 (933)	410 (360)	1310	0.25 (0.39)	1239 (573)	3.2 (3.6)
2019	192 (April 30 to Nov. 08)	1122 (592)	445 (399)	1517	0.40 (0.67)	677 (193)	3.4 (3.8)
2020	193 (April 28 to Nov. 07)	1126 (597)	521 (456)	1412	0.46 (0.76)	605 (141)	2.7 (3.1)
Mean ± Std	$187\pm10$	$1148 \pm 262$ (608 ± 139)	$419 \pm 45$ $(367 \pm 40)$	1370 ± 103	$0.38 \pm 0.10 \\ (0.63 \pm 0.16)$	$729 \pm 258$ (241 ± 145)	$3.3 \pm 0.4$ $(3.8 \pm 0.4)$

<sup>&</sup>lt;sup>a</sup> growing season length (GSL), Precipitation (P), evapotranspiration (ET), runoff plus infiltration (P-ET), the ratio of ET to P (ET/P) and water use efficiency (WUE) calculated as a ratio of gross ecosystem productivity (GEP) and ET.

<sup>&</sup>lt;sup>b</sup> ET/P < 1 indicates an efficient water use by the ecosystem.

<sup>&</sup>lt;sup>c</sup> P - ET > 0 indicates that more water is available than what the ecosystem consumes for ET, potentially contributing to runoff, infiltration, or streamflow.

**Table 2.4:** Multivariate regression analysis (MLR) of standardized daily water uses efficiency (WUE) across different dry-hot conditions (2012-2020) regressed against standardized explanatory variables, including vapor pressure deficit (VPD), air temperature (Tair), photosynthetic active radiation (PAR), and relative extractable water (REW). The analysis aims to identify the variables that best explain the model's performance under varying dry and hot conditions. Significance levels are indicated as follows: [0-0.001] = "\*\*"; (0.001-0.01] = "\*"; (0.01-0.05] = ""; (0.05-0.1] = "."; (0.1-1] = "."

		Estimate	Std. Error	t Value	Pr (> t )	Significance	
All	Intercept	-0.30	0.04	-7.33	0.00	***	WUE
	VPD	-0.40	0.03	-13.53	< 2e-16	***	
	Tair	0.71	0.05	13.64	< 2e-16	***	
	PAR	-0.15	0.04	-4.14	0.00	***	
	REW	-0.13	0.03	-5.11	0.00	***	
	Intercept	0.00	0.13	0.00	1.00		
Н	VPD	-0.37	0.13	-2.76	0.01	**	
	Tair	-0.31	0.14	-2.24	0.03		
	PAR	-	-	-	-		
	REW	-0.44	0.14	-3.15	0.00	**	
	Intercept	0.00	0.10	0.00	1.00		
D	VPD	-0.28	0.10	-2.69	0.01	**	
	Tair	-	-	-	-		
	PAR	-	-	-	-		
	REW	-0.30	0.10	-2.96	0.00	**	
	Intercept	0.00	0.09	0.00	1.00		
	VPD	-0.44	0.10	-4.36	0.00	***	
H	Tair	-	-	-	-		
	PAR	-0.25	0.10	-2.48	0.02	*	
	REW	-0.15	0.10	-1.56	0.12		
	Intercept	0.00	0.06	0.00	1.00		
	VPD	-0.51	0.06	-8.54	0.00	***	
Z	Tair	-0.10	0.06	-1.65	0.10		
	PAR	-0.18	0.06	-3.03	0.00	**	
	REW	-0.16	0.06	-2.59	0.01	*	

**Table 2.5:** Relative importance analysis results for multivariate regression of standardized daily evapotranspiration (ET), gross ecosystem productivity (GEP), and water use efficiency (WUE) against standardized explanatory variables (VPD, Tair, PAR, and REW) across various dry-hot conditions.

		lmg			Proportion of variance explained by model			
		ET	GEP	WUE	ET	GEP	WUE	
All	Intercept				69.83%	73.03%	23.90%	
	VPD	0.22	0.13	0.41				
	Tair	0.33	0.44	0.34				
	PAR	0.33	0.23	0.15				
	REW	0.13	0.21	0.11				
н	Intercept				27.72%	33.65%	27.12%	
	VPD	0.25	0.36	0.37				
	Tair	0.39		0.18				
	PAR	0.37	0.30					
	REW		0.34	0.46				
Q	Intercept				19.05%	40.01%	12.54%	
	VPD	0.24	0.59	0.44				
	Tair	0.41	0.30					
	PAR	0.35	0.02					
	REW		0.08	0.56				
E GH	Intercept				33.18%	27.64%	32.02%	
	VPD	0.19	0.83	0.61				
	Tair							
	PAR	0.56		0.33				
	REW	0.25	0.17	0.06				
Z	Intercept				41.56%	38.40%	32.37%	
	VPD	0.18	0.58	0.79				
	Tair	0.58	0.30	0.01				
	PAR	0.11		0.15				
	REW	0.13	0.12	0.04				

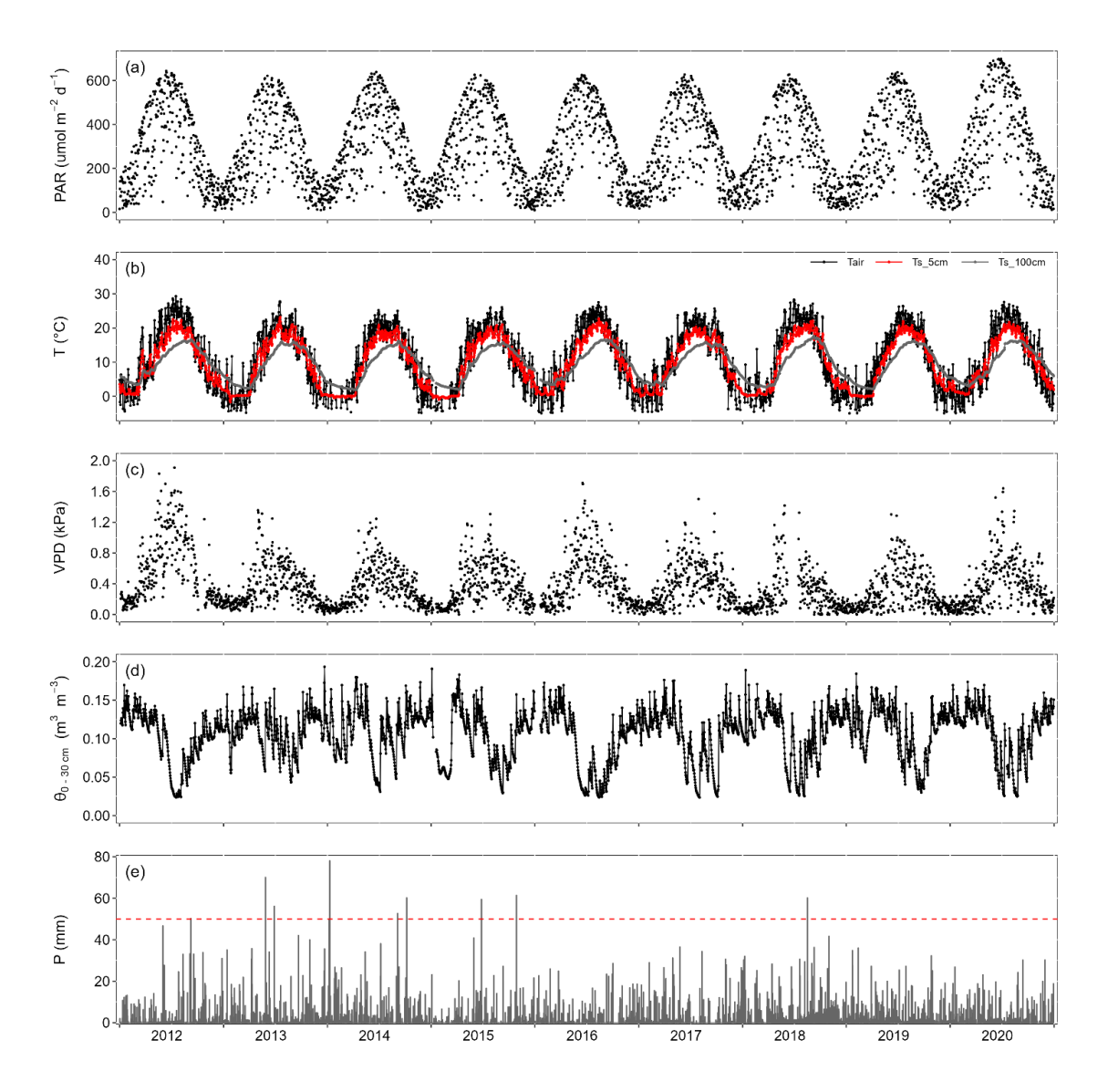


**Figure 2.1:** The interannual course of meteorological conditions from January 2012 to December 2020. (a) daily mean downward photosynthetic active radiation, PAR; (b) daily mean air Temperature, Ta, soil temperature in upper 2 cm (Ts5) and 100 cm (Ts100) layer; (c) daily mean vapour pressure deficit, VPD; and (d) daily mean volumetric water content in the 30 cm soil layer,  $\theta$ 0-30cm. The dotted line in panel (e) represents episodes of elevated precipitation. Characterization of years include hot year (2018), dry year (2015, 2017, 2020), hot and dry years (2012, 2016) and normal year (2013, 2014, 2019).

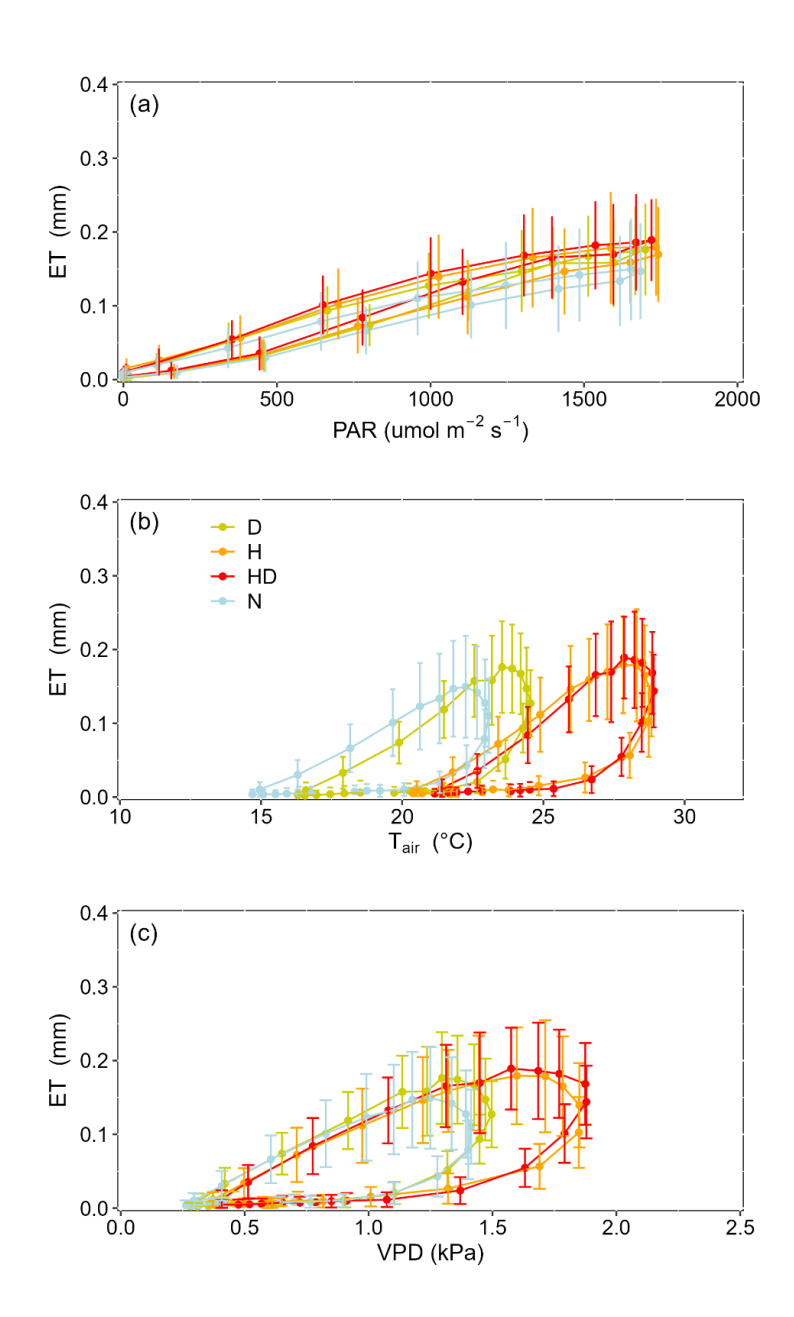


**Figure 2.2:** Hysteresis of ET to environmental controls. Ensemble half hourly diurnal relationships over the study period between evapotranspiration (ET) and air temperature, Ta (a) ET and vapor pressure deficit, VPD (b) and photosynthetically active radiation, PAR (c) for dry (yellow), hot (orange), concurrent hot and dry (red) and normal (grey) for days when Tair  $\geq$  15 °C, PAR  $\geq$  500  $\mu$ mol m<sup>-2</sup> and VDP  $\geq$  0.5 kPa from 2012 to 2021. Error bars indicating standard deviation. ET-Tair and ET-vpd relationship show clockwise-loops.

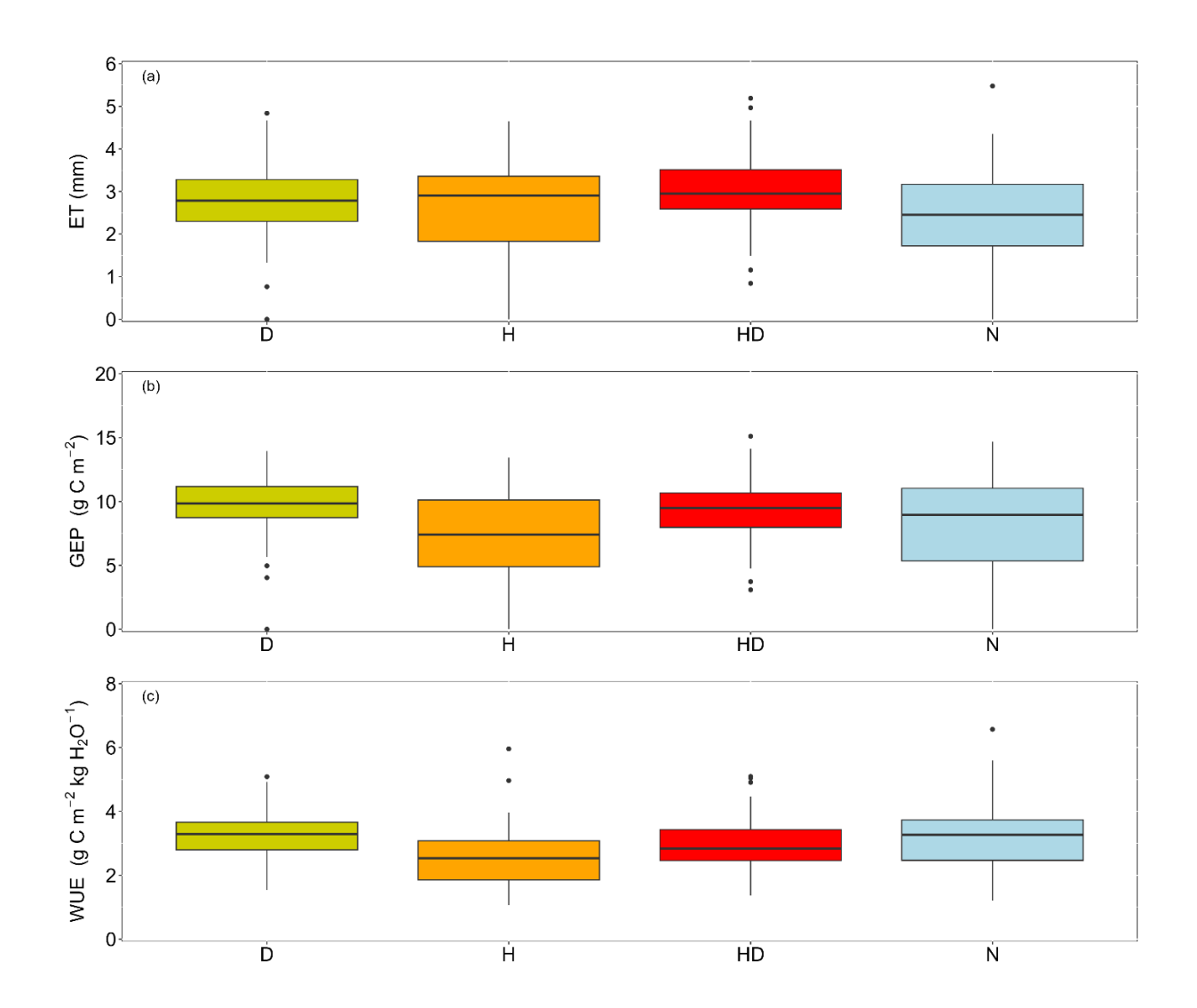


**Figure 2.3:** Response of evapotranspiration (ET), gross ecosystem productivity (GEP) and water use efficiency (WUE) to hot, dry, hot and dry and normal conditions. Daily box plots of (a) ET (b) GEP, and (c) WUE for Dry (D) when REW  $\leq$  0.4, Hot (H) when Tmax  $\geq$  27.5, Concurrent Hot and Dry (HD) when both Tmax  $\geq$  27.5 and REW  $\leq$  0.4, and Normal (N) conditions for days when Tair  $\geq$  15 °C, PAR  $\geq$  500  $\mu$ mol m<sup>-2</sup> and VDP  $\geq$  0.5 kPa from 2012 to 2021. Results from the Wilcoxon Rank-Sum test indicated significant differences were observed in ET between HD and N conditions, as well as D and N conditions. Significant differences were noted in GEP between H and HD, D, and N conditions, as well as HD and D, N conditions (see Table 2.3).

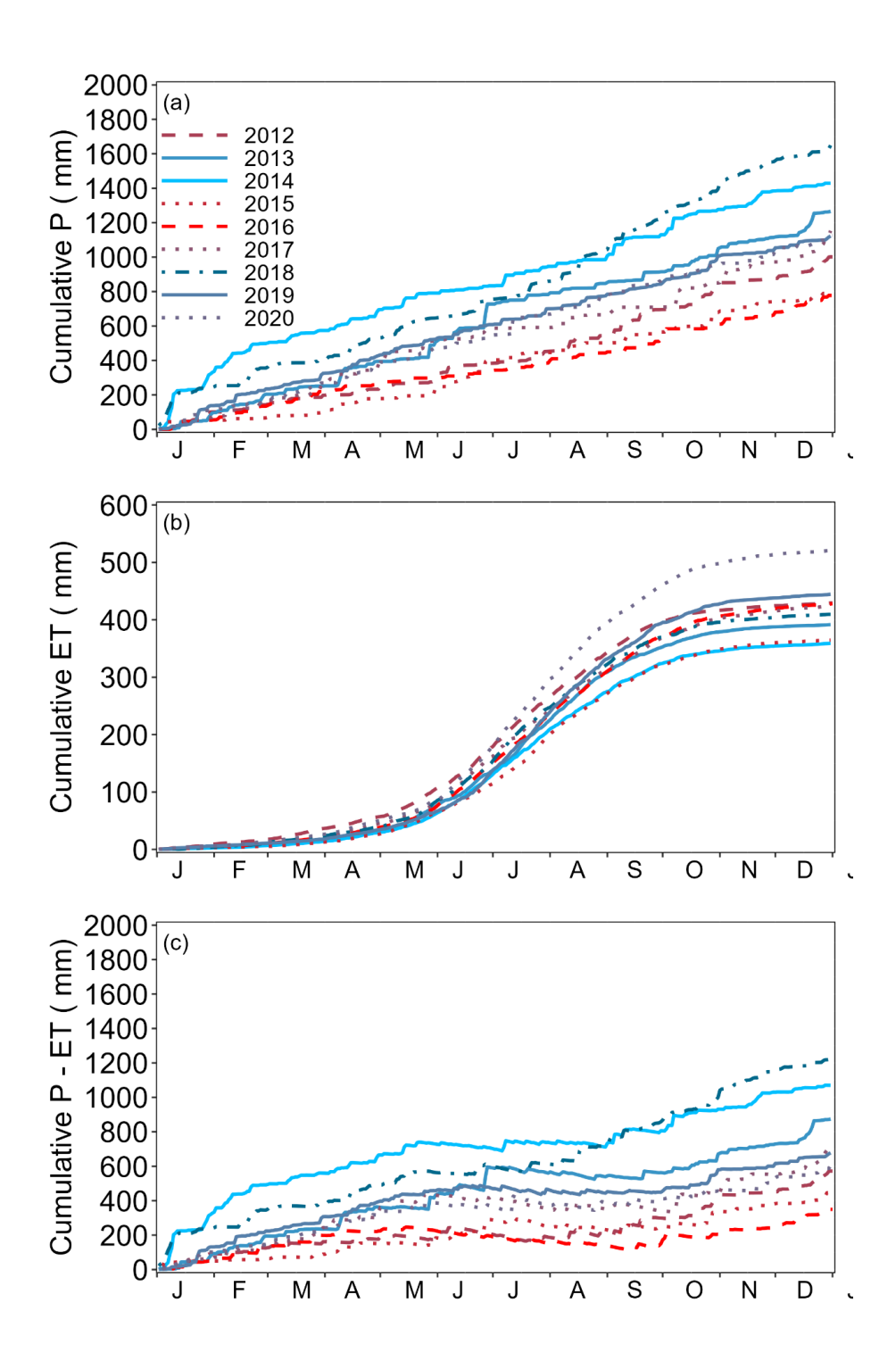


**Figure 2.4:** Cumulative water fluxes from 2012 to 2020. (a) Cumulative daily evapotranspiration (ET); (b) daily precipitation (P); and (c) surplus water (P-ET) for the period 2012-2020. Characterization of years include hot year (2018), dry year (2015, 2017, 2020), hot and dry years (2012, 2016) and normal year (2013, 2014, 2019).

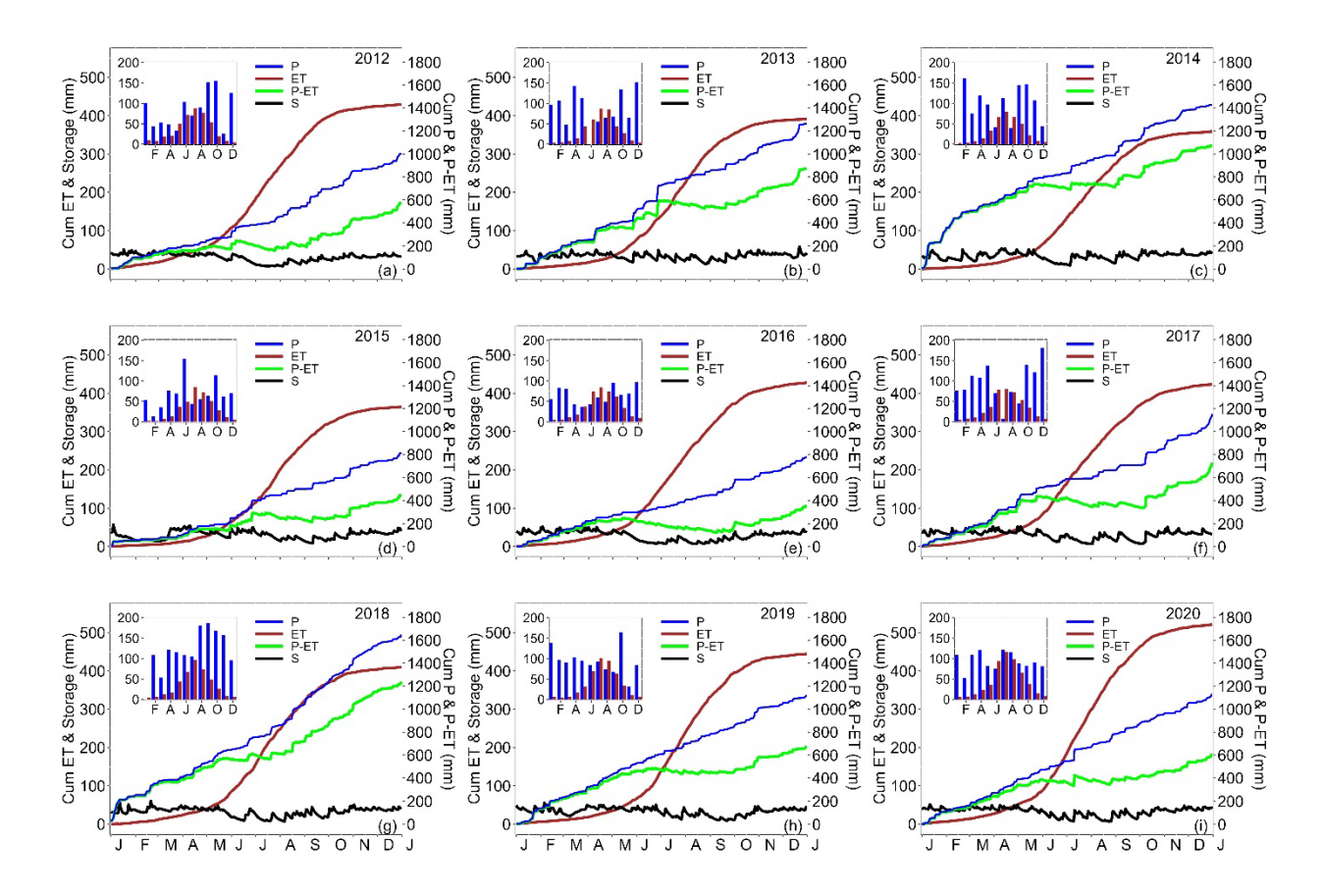


**Figure 2.5:** Water budget of the forest. Cumulative daily values of precipitation (P) (blue line), evapotranspiration (ET) (brown line), and P-ET (green line) from 2012 to 2020. A notable difference between years is evident: 2018 (hot year) exhibits higher P-ET, 2016 (hot and dry year) shows lower P-ET, 2014 (normal year with lower temperature) displays lower ET, 2015 (dry conditions) reflects lower ET, and 2020 demonstrates higher ET. Additionally, the inset includes bars representing monthly total P and ET in mm, along with the mean monthly values of soil water storage (S) (black line).

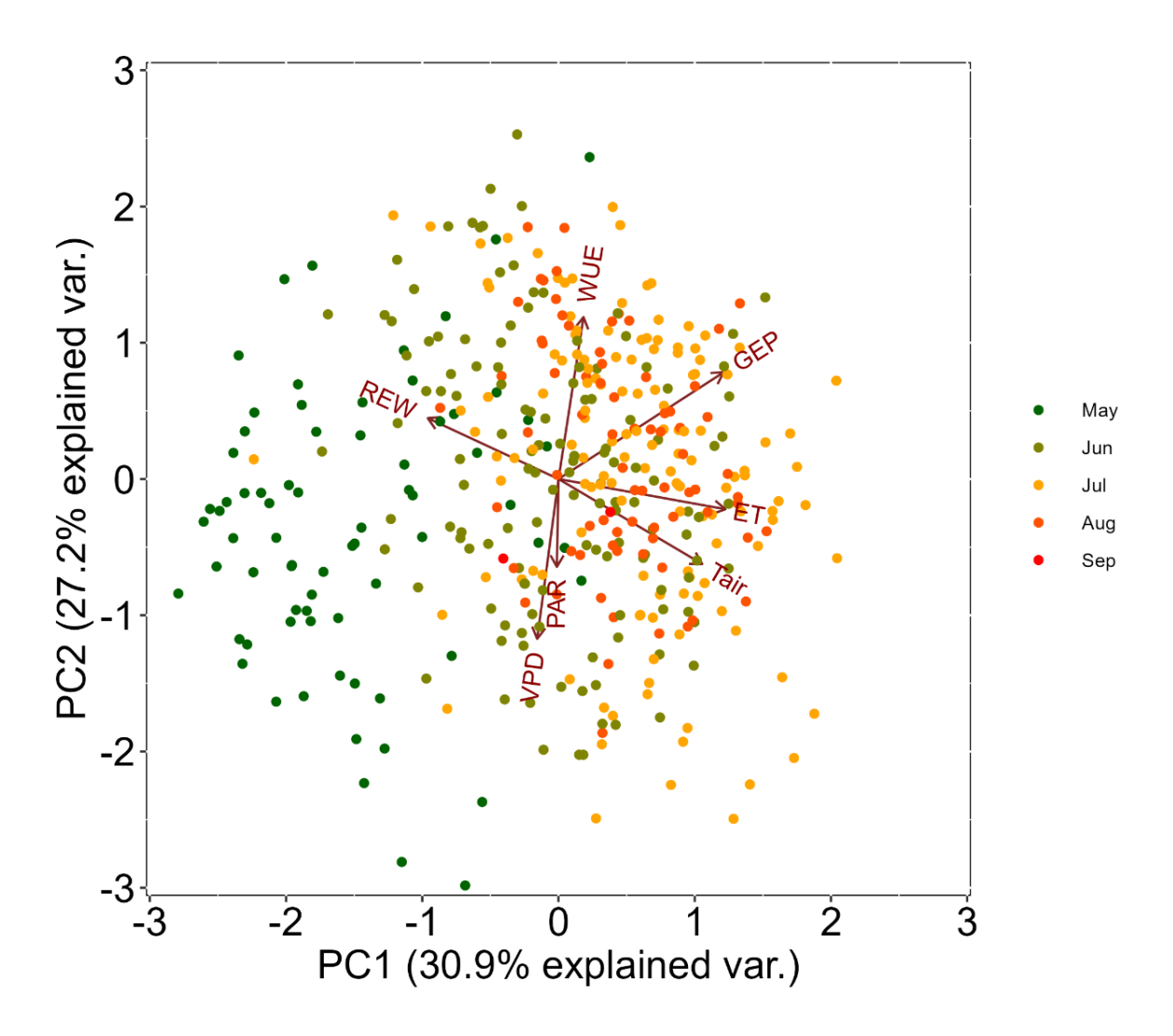


**Figure 2.6:** Principal Component Analysis (PCA) applied to daily profiles of various variables across the growing season. These variables include photosynthetically active radiation (PAR), air temperature (Tair), vapor pressure deficit (VPD), relative extractable water (REW) for the 0 to 30 cm soil layer, gross ecosystem productivity (GEP), evapotranspiration (ET), and water use efficiency (WUE). The first two principal components, PC1 and PC2, accounted for 30.9% and 27.2% of the total variance, respectively. To gain a clearer insight into the influence of available water, we filtered out days when meteorological drivers, such as radiation, held greater sway over fluxes (Tair > 15°C, PAR > 500, VPD > 0.5 kPa). This approach enables a more focused examination of the water-related effects on the variables under consideration.

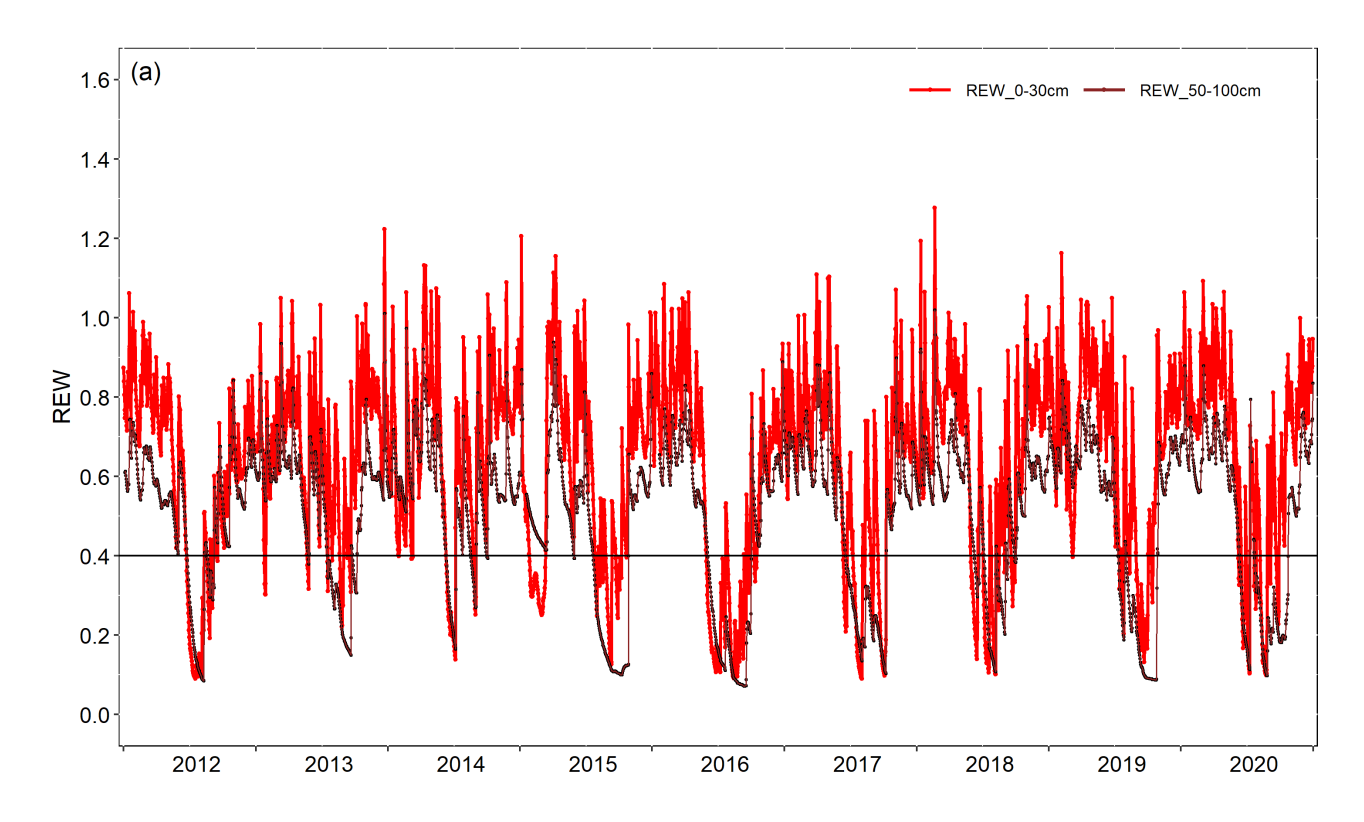


**Figure 2.7:** Daily relative extractable water (REW) expressing soil moisture relative to field capacity and wilting point for 0 to 30 cm and 50 to 100 cm soil layers.

#### **CHAPTER 3:**

# DROUGHT IMPACTS ON WATER FLUXES AND WATER-USE EFFICIENCY IN AN AGE-SEQUENCE OF TEMPERATE CONIFER FORESTS

## 3.1 Abstract

Evapotranspiration (ET) from temperate forests plays a significant role in the regional and global water cycles. However, extreme weather events such as heat, and drought are affecting the water use and water use efficiency (WUE) of these forests. Climate change impacts may be more severe in plantation forests where the age of the forest plays a significant role, impacting how these forests respond to environmental stresses. This study presents fourteen years (2008 to 2021) of water flux data measured using the eddy covariance technique in an age sequence (83, 48, and 20 years as of 2021) of eastern white pine (*Pinus strobus* L.) forests in the Great Lakes region in southern Ontario, Canada. The mean annual ET values were  $465 \pm 41$ ,  $466 \pm 32$ , and  $403 \pm 21$  mm yr<sup>-1</sup> in the 83-, 48-, and 20-year-old stands, respectively. Mean annual gross ecosystem productivity (GEP) was 1585  $\pm$ 100,  $1660 \pm 115$ , and  $1634 \pm 331$  g C m<sup>-2</sup> yr<sup>-1</sup>. Mean annual WUE was  $3.4 \pm 0.4$ ,  $3.6 \pm 0.4$ , and  $4.0 \pm 0.4$ 0.8 g C kg H<sub>2</sub>O yr<sup>-1</sup> in the 83-, 48-, and 20-year-old stands, respectively. Lower ET and higher GEP explained the highest WUE observed in the youngest stand. Air temperature (Tair) was identified as the dominant control on monthly ET in all three different-aged stands, while drought reduced ET in the late summer. Similarly, Tair was the dominant control on monthly GEP and WUE in the three forest stands. Net radiation (Rn) and leaf area index (LAI) had a secondary influence on ET at this same timescale, although their relative importance varied according to the season and forest age. The oldest forest exhibited lower sensitivity to drought, indicating higher resilience to dry conditions.

Furthermore, a decline in the ET/Precipitation (P) ratio was observed in all three stands over three consecutive drought years from 2015 to 2017. WUE during these consecutive drought years increased, with the youngest stand generally having the highest WUE. These long-term flux observations study will help to enhance our understanding of water exchanges in different-aged temperate plantation forests in Eastern North America, contributing to a better understanding of their responses to extreme weather events. This data and analysis will help to better manage plantation forest to develop strategies for managing water resources and ensuring water security in the region under changing climate.

## 3.2 Introduction

Forest evapotranspiration (ET) is a key component of the water cycle in terrestrial ecosystems, encompassing evaporation from the soil surface, wet canopy, and transpiration from plant's stomata. Moreover, ET plays a crucial role in the interactions between the Earth's surface and the atmosphere, significantly influencing local and regional climates (Katul et al., 2012; Restrepo-Coupe et al., 2021; Zhao et al., 2021). ET also facilitates the carbon dioxide (CO2) uptake through photosynthesis (Allen et al., 1989) and hence contributes in mitigating climate change (Moomaw et al., 2020). At the ecosystem level, the interplay between carbon uptake through photosynthesis and water evaporation is quantified by the ratio of gross ecosystem productivity (GEP) to ET, known as water use efficiency (WUE) (Giles-Hansen et al., 2021). WUE is widely used as a key metric or indicator to explore the carbon-water relationship in ecosystems.

Climate change and its related factors such as altered rainfall patterns, changes in energy availability, and variations in soil moisture, has the potential to disrupt the balance of water and energy in

ecosystems (Valipour et al., 2020), as well as ecological processes, such as photosynthesis, ecosystem respiration, carbon allocation and light- and water-use (Schlesinger et al., 2016; Wolf et al., 2013). Such imbalances can significantly impact the productivity and WUE of forest ecosystems. Therefore, it is important to fully understand the effects of climate change and extreme weather events on forest ecosystems (Zhang et al., 2023).

Over the past few decades, more intense and prolonged droughts have been observed across the world (IPCC, 2021). The exacerbation of these droughts is attributed to elevated temperature which has caused changes in precipitation pattern and increases water vapor deficit, leading to enhanced ET rates (IPCC, 2021). This relationship between warmer temperature and heightened atmospheric demand plays a significant role in the frequency, duration, and intensity of droughts. Understanding these interconnected atmospheric, hydrological and biological processes is vital for developing effective strategies and sustainable forest management practices to mitigate the impacts of droughts and safeguard the growth and resilience of forest ecosystems in changing climate (Guauque-Mellado et al., 2022).

Temperate forests are a major carbon sink and vital component of global carbon cycle. They significantly contribute to the local and regional water balance (Jasechko et al., 2013; Schlesinger & Jasechko, 2014). In eastern North America, planting monoculture forests has been a well-established practice to restore degraded agriculture lands that were once forests (Griscom et al., 2017; OMNR, 1986). As these monoculture forest plantations develop and grow, they undergo many natural and human disturbances including wildfires, wind through, insect infestations, thinning treatments and timber harvests (Franklin et al., 2002; Kulakowski et al., 2011). However, during their initial growth stages, these monoculture forests are more susceptible to extreme weather events such as droughts

due to the lack of species diversity and uniform and partially-developed root systems, which limits their ability to access water from different soil layers (Bauhus et al., 2010; Messier et al., 2022). However, studies in the literature have reported contrasting findings regarding the impact of drought on forest ET and WUE. Some studies report a decrease in ET during drought events, which can be attributed to insufficient precipitation, soil water depletion, and stomatal closure (Ge et al., 2014; Law et al., 2002; Guauque-Mellado et al., 2022). While other studies suggest that forest ET either remained stable during droughts (Liu et al., 2018) or increased in some deep rooted forests due to availability of more radiation and higher temperature (Arango Ruda & Arain, 2024; Bevacqua et al., 2021; Xie et al., 2016). This variability in ET responses to drought is influenced by species composition (Anderegg et al., 2018), deployed forest management practices (del Campo et al., 2022; Xu et al., 2020) and the intensity and duration of the drought event as well as regional climate (Diao et al., 2021). Moreover, the age of the forest significantly influences ET and its response to environmental conditions (Delzon & Loustau, 2005; Peichl, Arain, Ullah, et al., 2010; Skubel et al., 2015). Mature forests, with their higher species diversity and deep roots tend to be more resilient to dry conditions (Anderegg et al., 2018 Haberstroh et al., 2021). The access to deeper water sources, reduces water stress and helps in maintaining carbon uptake during dry periods (Lawrence et al., 2022). However, the canopy of mature forests is exposed to more sunlight, warmer temperatures, higher humidity deficit, and may increase evaporative demand to cool their canopy, while experiencing hydrologic or water transport limitations (Seneviratne et al., 2010; Niinemets, 2010). On the other hand, younger stands which higher tree density, smaller heights, lower roughness lengths and shallow roots may be more sensitivity and vulnerable to drought stress due to higher competition for water and nutrients (Arain et al., 2022; Chen et al., 2020). However, the mechanisms that cause variations in forest water use and growth in responses to drought across different forest ages are not well understood in the literature.

In this study, the effects of dry soil conditions or droughts on water flux dynamics of three eastern white pine (*Pinus strobous* L.) forest of different ages (83, 48, and 20 years as of 2021) in the Great Lakes region of eastern North America is investigated utilizing the eddy covariance flux, meteorological and hydrological data from 2008 to 2021. This study aimed to achieve three primary objectives: (1) to quantify seasonal and year-to-year variations in ET, GEP, and WUE across an age-sequence of white pine forest; (2) to identify the primary environmental controls influencing ET, GEP, and WUE; and (3) to assess the impact of dry conditions or seasonal droughts on ET in white pine forest of varying ages. By examining the long-term eddy covariance fluxes and environmental drivers, this study contributes to our understanding of how conifer forests of different age respond to drought and extreme weather events. These findings will provide valuable insights for restoration, conservation and sustainable management of plantations or afforested forest ecosystems.

## 3.3 Materials and Methods

## 3.3.1 Study Site

The research sites comprise three eastern white pine forests (*Pinus strobus* L.) that were planted in 1939, 1974, and 2002 north of Lake Erie in southern Ontario, Canada. As of 2021, these stands were 83, 48, and 20 years old, respectively, and they are situated within a 20 km radius of each other at approximately the same latitude (Table 3.1). These research sites are part of the Turkey Point Environmental Observatory (TPEO) and have been associated with various networks including the Global Water Futures Observatory (GWFO) program, former Fluxnet-Canada/Canadian Carbon Program, AmeriFlux, global Fluxnet and US-Canada Global Centre for climate change impacts on

transboundary waters. Within these networks, they are referred to as CA-TP1 (Arain, 2023), CA-TP3 (Arain, 2022), and CA-TP4 (Arain, 2018) sites, respectively. In certain studies, these forests have also been identified as TP02, TP74, and TP39, which correspond to the years when they were initially established, that is, 2002, 1974, and 1939, respectively.

The 83-year-old and 48-year-old forests were planted with young white pine trees in areas that were previously oak-savanna lands that had been cleared. The 20-year-old forest was planted with white pine seedlings on a former agricultural land that had been left unused for several years before the planting initiated. The species composition at the 83-year-old forest includes 82% white pine, 11% balsam fir (Abies balsamifera L. Mill) and 7% native Carolinian species - oak (Quercus velutina L., Quercus alba L.), red maple (Acer rubrum L.), wild black cherry (Prunus serotina Ehrh.), and white birch (Betula papyrifera). The understory includes young white pine trees of varying heights, ranging from 0.5 to 6 meters as well as black oak, balsam fir, and black cherry trees. The ground cover vegetation consists of various plant species including bracken fern (Pteridium aquilinum), moss (Polytrichum spp.), blackberry (Rubus spp.), poison ivy (Rhus radicans), and Canada mayflower (Maianthenum canadense). The 83-year-old forest was partially but uniformly thinned in 1983, where 104.76 m3 ha<sup>-1</sup> wood volume was removed from 38.6 ha (Ontario Ministry of Natural Resources and Forestry records). A second partial thinning was performed in 2012 at this site, where one third of trees were harvested, reducing the stand density from 413 trees ha<sup>-1</sup> to  $321 \pm 111$  trees ha<sup>-1</sup> while also reducing the basal area by 13%. The species composition of the 48-year-old stand is predominantly white pine (94%) with 5% jack pine (Pinus banksiana) and 1% of another tree's species such as oak. The ground vegetation in this stand is largely comprised of bryophyte species. This stand was also partially thinned in 2021, when every fourth row, plus a few trees from either side of the row were

removed by machine harvesting with the aim of overall removal of about a third of the basal area. The 20-year-old is exclusively comprised of white pine trees. There is almost no understory vegetation due to dense tree canopy. However, this has started to change because of the die out of lower branches allowing more light to ground surface. Non-thinning activity has been performed at this site.

The terrain at all three forests is mostly flat, with slopes ranging from 0.5% to 3.0%. The soil consists of approximately 98% sand and falls under the category of lacustrine-derived Brunisolic grey brown luvisols according to the Canadian System of Soil Classification as described by (Presant & Acton, 1984). These soils have relatively low ability to retain water, as indicated in Table 1 and suggested by McLaren et al. (2008) and Khalid (2016).

Water level measurements in a well at the 83- forest, which is also in proximity to 48-year-old stand indicate that the water table depth is approximately 6–7 m with an underlying clay layer at about 10 m depth. The 20-year-old site lacks direct water level measurements, but it is located near Big Creek, where the stream surface water level is approximately 5–6 m below the surrounding ground elevation during peak stream flow. Additional details about the sites can be found in Table 1 and in Arain et al., (2022), Chan et al., 2018; Peichl et al., (2010), and Restrepo & Arain (2005).

Data from the Environment and Climate Change Canada weather stations in Delhi, Ontario, located about 19 to 22 km north-northwest of the study sites, indicate that the region experiences a warm and humid continental climate. Over the 29-year period (1991-2020), the average annual temperature was 8.4 °C, with an average annual precipitation of 965 mm. Approximately 13% of this precipitation falls as snow (Environment and Climate Change Canada (ECCC), 2023).

## 3.3.2 Eddy Covariance Flux and Meteorological Measurements

Energy, water vapor, and CO<sub>2</sub> fluxes were measured at all three sites from 2008 to 2021 using closed-path eddy covariance (EC) systems. The EC systems were comprised of a sonic anemometer (CSAT3, Campbell Scientific Inc., USA), infrared gas analyzer (LI-7000, LI-COR Inc., USA), climate control box, heated 4 m sampling tube and desktop computers housed in trailer or huts as described by Arain et al. (2022). In all three EC systems, air was sampled at 20 Hz and IRGAs were calibrated on biweekly to monthly intervals. CO<sub>2</sub> storage (Sc) in the air column below the EC sensors was calculated using CO2 concentrations measured by the IRGAs at the top (28-34 m at 83-year-old and 16-20 m at 48-year old site) and mid-canopy (14 m at 83-year-old and 8 m at 48-year old site) heights (LI-820/LI-800, LI-COR Inc., USA). Storage fluxes were not calculated for the younger site due to smaller air column height below EC sensor. See Arain et al. (2022) for further details.

Meteorological variables were measured at the three forest sites, including downwelling and upwelling shortwave and longwave radiation (CNR1, Kipp and Zonen Inc., Netherlands) at 83-year old site and net radiation (NR-Lite, Kipp and Zonen Inc., Netherlands) at 48-, and 20-year-old stands, downward and upward photosynthetically active radiation (PAR↓ and PAR↑) (LI-200S, LI-COR Inc., USA), air temperature (Tair) and relative humidity (HMP45C, Campbell Scientific Inc., USA) and wind speed and direction (05103-10, R.M. Young Co., USA).

Soil moisture (CS-615/616, Campbell Scientific Inc., USA) was measured at two locations at 5, 10, 20, 50, and 100 cm depths at the 83-year-old site and 5, 10, 20, and 50 cm depths at 48-year-old and

20-year-old sites. Soil moisture measurements at these two locations are considered representative of the forest's soil water status and drought conditions due to the homogeneous soil texture, topography and vegetation characteristics.

Precipitation (P) was measured at the 83-year-old site and the adjacent 48-year-old site using an accumulation rain gauge (model T200B, Geonor, Campbell Scientific Inc., USA) and a tipping-bucket rain gauge (model TE525, Texas Instruments Inc., USA) in an open area near the sites. At the 20-year-old site, a heated all-season tipping-bucket rain gauge (model 52202, R.M. Young Co., USA) was utilized. To ensure data accuracy, P measurements were cross validated with data obtained from the Environment and Climate Change Canada weather station at Delhi, Ontario. All flux, meteorological and soil data were sampled every 5 seconds and averaged at half-hour intervals.

# 3.3.3 Data Processing and Data Quality Control

The quality control of flux and meteorological data was performed following the Fluxnet Canada Research Network (FCRN) guidelines as described in Brodeur (2014) and Papale et al. (2006). Flux and meteorological data cleaning consisted of removing values above or below predefined upper and lower thresholds and removing erroneous values due to instrument malfunction, power failure, instruments calibration, and data quality control. A friction velocity (u\*) threshold of 0.5 was applied to daytime and nighttime flux data to remove erroneous flux values during low turbulence periods (Arain et al., 2022; Peichl et al., 2010). A three-dimensional Lagrangian footprint model was used to calculate flux footprints for each half-hourly measurement (Kljun et al., 2003). Fluxes were retained within 80% of the cumulative flux threshold. Subsequently, data filling was performed through linear interpolation for smaller gaps (a few hours) and data from other TPEO EC flux sites and the ECCC weather station in Delhi, Ontario

(Brodeur, 2014).

Half-hourly GEP values were estimated by adding measured net ecosystem productivity NEP (Fc + Sc) and modelled daytime ecosystem respiration (RE) derived using non-linear regression model applied to half-hourly nighttime NEP data as a function of soil temperature (Ts) at 5 cm depth and volumetric water content in the 0–30 cm soil layer. Missing GEP values were modelled using a rectangular hyperbolic function that was fitted to bin-averaged, half-hourly GEP and PAR data (Beamesderfer et al., 2020). Further details of flux data gap filling are given in Arain et al. (2022), Chan et al. (2018) and Peichl, Arain, & Brodeur (2010).

The energy budget closure estimated using daily mean values was  $0.80 \, (R^2 = 0.89)$ ,  $0.79 \, (R^2 = 0.94)$ , and  $0.71 \, (R^2 = 0.95)$  for the 83-, 48-, and 20-year site, respectively. These values indicate proximity to energy balance closure, which is reliable enough for conducting seasonal and annual ET analyses. The best energy balance closure was observed in the spring at all three sites (slope<sub>83y</sub> = 0.86, slope<sub>48y</sub> = 0.92, slope<sub>20y</sub> = 0.93), while the lowest energy balance closure was observed in winter (slope<sub>83y</sub> = 0.75, slope<sub>48y</sub> = 0.81, slope<sub>20y</sub> = 0.85), primarily due to the lower magnitude of winter fluxes.

# 3.3.4 Leaf Area Index

Leaf area index (LAI) is a key descriptor of biomass conditions in forests and is used to quantify the transpiring leaf surface (Hammerle et al., 2008; Liang et al., 2014). The 16-day 250 m resolution leaf area index (LAI) was obtained from MODIS satellite platform of the USGS EARTHDATA portal (https://lpdaacsvc.cr.usgs.gov/appeears/). For each site, the 250-meter pixel containing the flux tower was retrieved for the study period from 2008 to 2021. The surrounding pixels in the area had the similar LAI values as the central pixel where the tower is located. LAI displayed significant

differences among the three forests (Table 3.3). The 20-year-old stand exhibited lower LAI levels with mean LAI value of 2.34 m<sup>2</sup> m<sup>-2</sup>, while the 48- and 83-year-old forests showed mean LAI values of 3.90, and 4.41 m<sup>2</sup> m<sup>-2</sup>, respectively. Higher levels of LAI at the two older stands is reflective of their larger photosynthetic capacity. The reader is informed that Arain et al. (2022) have reported higher LAI values for all three sites based on ground level measurements.

# 3.3.5 Water Availability and Drought Characterization

The precipitation minus evapotranspiration (P-ET) was utilized to represent the net water influx at each stand and is regarded as the water available for runoff and infiltration. P-ET is a crucial measure for comprehending and managing water resources in forest ecosystems (Swenson and Wahr, 2006).

Site-specific soil water status or dry conditions were characterized based on Relative Extractable Water (REW); an eco-physiological drought indicator used to quantify the proportion of soil water that is available for plant uptake. It is also referred as Water Holding Capacity or Plant Available Water in the literature. REW was calculated for each site following Arain et al. (2022) as:

$$REW = \frac{VWC - VWC_{wp}}{VWC_{fc} - VWC_{wp}} \tag{5}$$

Where VWC is the measured soil water content in m<sup>3</sup> m<sup>-3</sup> for the 0 to 30 cm soil layer, VWC<sub>wp</sub> is the soil volumetric soil water content at wilting plant point (0.01 m<sup>3</sup> m<sup>-3</sup>), and VWC<sub>fc</sub> is the volumetric soil water content at field capacity (0.16 m<sup>3</sup> m<sup>-3</sup>). The expression VWC<sub>fc</sub> - VWC<sub>wp</sub> is the difference between the soil water reserve at field capacity and the permanent wilting point. VWC in 0 to 30 cm soil layer was assumed to be representative of deeper soil column based one of our previous study at 83- and 48-year old sites which showed similar VWC values for upper (0-20 cm) and deeper (50-100 cm).

cm) soil layers in these sandy well drained soils (Fig. S3.2). Dry periods were defined based on a REW value of  $\leq 0.4$  (Granier et al., 2007; Vilhar, 2016), and the number of days under these conditions was quantified for each month at each site.

For each site, an evaporative index was calculated as the ratio of ET to P (ET/P). It represents the fraction of P consumed by ET and helps in characterizing the influence of land cover and climate on water balance (Diao et al., 2021).

## 3.3.6 Statistical Analysis

Considering regional climate seasonality, the seasons were classified by calendar months with spring encompassing April and May, summer encompassing June to September, fall encompassing October and November, and winter encompassing December to March. To enhance interpretation ET along with environmental variables (Rn, Tair, REW, VPD) time series were standardized ( $\mu$ =0,  $\sigma$ =1) throughout the study period, facilitating dataset feature comparison. The slope of linear relationships between daily ET and environmental variables indicated ET sensitivity to climate anomalies, reflecting the direct impact of climate constraints on ET (Arain et al., 2022). In monthly data, negative correlation with standardized Tair, VPD and Rn values, indicated stress conditions for the respective variables, while positive correlation with standardized REW values suggested drought stress. Daily anomalies were grouped over bi-weekly periods for sensitivity index calculation following (Xu et al., 2020).

A multiple linear regression analysis was performed to investigate the impact of biotic and abiotic factors on ET, GEP, and WUE. The study considered standardized (z-scored) variables, including Rn, Tair, REW, VPD, and leaf area index (LAI). Standardization allowed for a quantitative

comparison of the regression coefficients (Clogg et al., 1995). Furthermore, we assessed the relative significance of each variable using the package "relaimpo" in R (Groempings, 2021). The selection of variables for multivariate modeling involved filtering based on collinearity using the variance inflation factor (VIF), an indicator of collinearity dependent on the correlation coefficient (R<sub>i</sub>) between each variable and the remaining variable in the model as follow

$$VIF = 1/(1 - R_i^2) (6)$$

Variables with VIF values >10 were usually considered highly collinear and removed from the set of variables, while variable with 5>VIF>3 had an admissible degree of collinearity (Guerrieri et al., 2016; Zhao et al., 2021). In addition, the set of variables providing the model with the lower Akaike Information Criterion (AIC) score was used to select the model that minimizes overfitting as a higher number of parameters is going to result in an improvement in the goodness of the fit (Akaike, 1974).

Based on the methodology described in Anderegg et al., (2018), we conducted a multiple linear regression analysis to identify the resilience of forest age to drought stresses by calculating a drought coupling and a drought sensitivity index. This method was modified from Novick et al. (2016) and Sulman et al. (2016). The drought coupling is the coefficient of determination from a standardized linear model of ET as a function of VPD, soil moisture, and their interaction for days when Tair ≥ 15°C, photosynthetic active radiation (PAR) > 500 μmol m<sup>-2</sup> s<sup>-1</sup>, and VPD > 0.5 kPa. Likewise, the drought sensitivity was the sum of the absolute coefficients, including the interaction term of soils moisture and VPD. These criteria ensured that the analysis focused on days with dominant transpiration, minimal leaf area changes, and when water fluxes were influenced by water availability (Anderegg et al., 2018a).

#### 3.4 Results

#### 3.4.1 Environmental Conditions

Meteorological variables over the study period from 2008 to 2021 are shown in Figure 3.1. Net radiation (Rn) had high values during the growing season, particularly in the summer of 2011, 2016, and 2020 due to clear sky conditions (Fig. 3.1a). Prior to 2016, the older forest had consistently higher levels of Rn than the younger stands. However, after 2016 the seasonal pattern of Rn in the 83- and 48-year-old sites closely matched. It may partly be due to their proximity and gradual buildup of above ground biomass at the 48-year-old stand influencing radiation. Rn levels at the 20-year-old site exhibited more variation, with consistently lower levels than the older stands. The higher air temperature (Tair) was observed in summer, particularly in July and August (Fig. 3.1b), with notable peaks in 2011, 2012, 2016, 2018, and 2020. Overall, Tair in all three stands followed a similar pattern. VPD exhibited high values during the growing seasons in 2011, 2012, and 2016 at the three sites (~ 1 kPa). The lowest VPD values were observed in 2009 (~ 0.6 kPa) in all three stands. Notably, VPD consistently remained higher at the 83-year-old stand after the thinning in the winter of 2012 with VPD being particularly high in 2020 (Fig. 3.1c). The annual P showed lower values in 2009 (995) mm), 2010 (896 mm), 2015 (811 mm) and 2016 (778 mm), while it reached its highest level in 2018 (1649 mm) (Table 3.2). Volumetric Water Content (VWC) displayed peak values in early spring due to snowmelt, gradually declined as foliage developed and photosynthesis and ET started and reached the lowest values in late growing season, particularly around July-August. VWC increased again in the fall due to higher P and lower atmospheric demand (Fig. 3.1d). All three forest sites experienced consecutive drought conditions in the summers of 2015, 2016, and 2017. The respective ET/P values for these years were 0.83, 0.98, and 1.31, with P-ET values of 54 mm, 4.3 mm, and -61.3 mm. These values are the averages of ET/P and P-ET across stands for each year. The years 2008, 2013, 2014, 2018, and 2019 had fewer or no periods showing dry conditions.

# 3.4.2 Forest Age and Water Dynamics

ET displayed distinct variation across multiple years (Table 3.3, Fig. 3.2). The two older forests consistently demonstrated similar annual ET totals over the study period, ranging from 395 to 536 mm. In comparison, the 20-year-old stand had annual ET values ranging from 373 to 443 mm over the same period. The highest annual ET values of 536 mm and 514 mm were observed in 2010 at the 83- and 48-year-old forests, respectively (Table 3.3, Fig. 3.2). In general, the oldest forest exhibited greater year-to-year variation in ET, while the younger forest showed relatively lower variability. In the summer, the 83-year-old trees had a higher average ET of  $300 \pm 25$  mm over the study period compared to the younger trees. Meanwhile, the 48-year-old trees had higher ET values of  $91 \pm 11$  mm during spring and  $54 \pm 7$  mm during fall. Over the study period, mean annual ET was  $465 \pm 41$ ,  $466 \pm 32$  and  $403 \pm 21$  mm yr1 at the 83-, 48- and 20-year old forests, respectively. The mean annual ET in the two older stands was about 62 to 63 mm higher compared to that in 20-year-old forest.

ET decreased during dry periods (REW  $\leq$  0.4; Fig. 3.3), with 20-year-old forest consistently exhibiting lower ET levels compared to both older forests. The Wilcoxon signed-rank test indicated a significant difference in ET among the three stands (not shown). The test also revealed significant differences in ET between wet and dry conditions (Fig. 3.3, Table S3.2), with the 48- and 20-year-old forests showing notably higher contrasts in ET values between these conditions (Fig. 3.3). These results suggested that younger forests were less resilient to dry conditions compared to the 83-year-old stand.

Forest water availability (P-ET) was constrained in dry years (Table 3.2, Fig. 3.2). The highest annual P-ET occurred in 2018 and 2014, corresponding with high P values (Table 3.2). Over the study period, the 20-year-old forest had the highest P-ET ( $716 \pm 241$  mm), compared to the 83- and 48-year-old stands which had P-ET values of  $655 \pm 242$  and  $654 \pm 227$  mm, respectively. Overall, more severe reductions in P-ET were associated with greater precipitation shortfalls, warm temperatures and the influence of canopy expansion on ET.

## 3.4.3 Evapotranspiration and Environmental Controls

Results from the MLR analysis of monthly ET values with explanatory variables of Rn, Tair, LAI, and REW showed varied performance among these different age forests (Table 3.4). The oldest forest exhibited the highest model performance (R<sup>2</sup>=0.73, p-value: < 0.001), indicating a strong and significant relationship between the environmental variables and ET. The 48-year-old forest also demonstrated a robust relationship (R<sup>2</sup>=0.69, p-value: < 0.001), while the 20-year-old plantation exhibited lower but still substantial explanatory power (R<sup>2</sup>=0.58, p-value: < 0.001). These results suggest that forest age influences how well the measured variables correlate, with the younger forest showing a less consistent or whicker response.

In terms of relative importance at monthly timescales, Tair emerged as the most important predictor of monthly ET across all forest stands, with lmg values of 0.26, 0.37, and 0.38 for the 83-, 48-, and 20-year-old, respectively. Rn also played a significant role across all forests, with lmg values of 0.20, 0.28, and 0.26 for the 83-, 48-, and 20-year-old. While LAI was relevant at 83-year-old (lmg = 0.22) and the 48-year-old (lmg = 0.33) stands, its importance lessened in the youngest forest (lmg = 0.20), due to smaller LAI, limiting light exposure (Table 3.4).

The regression analysis of monthly standardized (std) values of environmental controls regressed against monthly standardized ET for different seasons showed that in spring and fall, Tair had a positive and significant correlation with ET across all sites, with summer std correlation being significant only in the older forest (Fig. 3.4a). Significant positive correlations between std of ET and Rn were observed at the 83- and 48-year-old throughout seasons, while at the 20-year-old, it was significant only in fall (Fig. 3.4b). Positive significant correlations between std of ET and VPD were noted in spring and fall for the two oldest forests, with non-significant correlations during summer across all forests (Fig. 3.4d). When examining the relationship between ET and REW, negative significant correlations were found in fall and spring.

In addition, the sensitivity analysis of environmental stressors conducted at a daily time scale showed negative sensitivity values for environmental variables (e.g., dET/dTair < 0) (Fig. 3.5). During the transition from July to August in summer, all three stands exhibited reduction in std ET with std Tair values (dET/dTair<0). Notably, the sensitivity of ET to Tair was more pronounced in the younger forest, spanning from early summer (June) to the end of the summer in September (Fig. 3.5a). Negative sensitivity values for REW are shown in Figure 3.5d and indicate stress conditions for ET (dET/REW<0). In summer, drought stresses (REW) consistently influenced ET across all three stands, particularly in June and July (Fig. 3.5d). Although, the sensitivity was stronger for the 48-year-old stand.

The daily-scale regression model, incorporating VPD, soil moisture (SM) and their interaction, emerged as a robust indicator of the forests' response to drought stress (Fig. 3.6). The 20-year-old forest showed higher coupling (Fig. 3.6b) and higher sensitivity (Fig. 3.6d) to drought compared to the older forest counterparts. These findings signify a less constrained variation (indicative of lower

resilience) in ET within the younger forest, as explained by the fluctuation in VPD and VMC. This analysis indicated how the age of the forest acts as a buffer to influence the ET response to soil water deficit and evaporative demand (Fig. 3.6a, b). Overall, the results stated in this study showed that age significantly influenced how forests responded to drought stress, where younger forests exhibited greater sensitivity and coupling to drought.

# 3.4.4 Water Use Efficiency (WUE)

The seasonal and annual fluctuations in GEP and WUE across the three different stands are shown in Table 3.3. The 83-year-old stand, displayed the lower mean GEP value of 1585±100 g C m<sup>-2</sup> yr<sup>-1</sup>, as compared to the 48-year-old stand which exhibited relatively higher productivity with mean GEP value of 1660±115 g C m<sup>-2</sup> yr<sup>-1</sup>. Over the study period, GEP of the younger forest constantly increased, surpassing the older counterparts in 2015 with an annual GEP value of 1923 g C m<sup>-2</sup> yr<sup>-1</sup>. In 2016, dry conditions led to decreased GEP in all three stands, however, the younger stand consistently outperformed the older forests, except in 2018. The highest productivity was observed in the youngest forest in 2020 with annual GEP of 2272 g C m<sup>-2</sup> yr<sup>-1</sup>. Similarly, the productivity of the older forests was lower than that of the 48-year-old stand, except in 2018 and 2021. Overall, seasonal dry conditions, resulted in decreased GEP values across all three stands (Fig. 3.3).

Similar patterns were observed in the WUE of these forests (Table 3.4). The 20-year-old stand consistently exhibited higher WUE and had mean WUE of 4 g C kg H<sub>2</sub>O<sup>-1</sup> over the study period, followed by the 48-year-old forest at 3.6 g C kg H<sub>2</sub>O<sup>-1</sup>. WUE of the youngest forest increased as the forest matured and the canopy expanded, indicating a positive correlation between WUE and forest growth. WUE increased during dry conditions, likely due to a greater reduction in ET levels across the three stands compared to the rate of decrease in photosynthetic productivity (Fig. 3.3). The results

from the MLR analysis indicated that Tair was the better predictor of WUE at the three stands at monthly time scale (Table 3.4). Interestingly, the  $\beta$  coefficients indicated a significant negative association of Rn and LAI with WUE, unlike the response of ET and GEP to Rn. The lmg values reported for the three stands were 0.59, 0.54, and 0.66 for the 83-, 48-, and 20-year-olds, respectively. LAI also played a significant role, with lmg values of 0.23, 0.21, and 0.17 for the 83-, 48-, and 20-year-olds.

## 3.5 Discussion

# 3.5.1 Forest Age and Water Dynamics

Forest age plays an important role in determining the magnitude of water fluxes in terrestrial forest ecosystems (Cornish and Vertessy, 2001). Among all three different forest ages, ET rates were consistently lower at the 20-year-old, while the 83- and the 48-year-old stands displayed comparatively higher ET rates. The ET rates of the 48-year-old stand surpassed those of the oldest forest after 39 years of its establishment, marking a shift in water flux dynamics in 2013. However, this higher ET in the 48-year-old stand did not consistently outpace the rates observed in the 83-year-old forest in the subsequent years. Previous research has highlighted notable variations in ET patterns linked to forest age, influenced by factors such as tree physiology, including leaf, sapwood area dynamics (Cornish and Vertessy, 2001), and developed root systems (O'Connor et al., 2021). Both, older forests consistently maintained higher LAI and hence ET. Indeed, LAI was generally the second most important control in explaining the variability of not only ET across forests but also for GEP and WUE at the monthly timescale (Table 3.4).

The study results revealed a decreasing trend in ET for the 83-year-old and 48-year-old stands (Fig.

S3.3), likely due to increasing forest age and tree height (Teuling & Hoek van Dijke, 2020). In contrast, the younger stand showed an increasing trend (Fig. S3.3). Reduced interannual variability of ET in the younger stands can be ascribed to factors such as the homogeneity of vegetation, where the structure of the stand is more uniform and homogeneous than the older stand, resulting in a more consistent ET, as the vegetation is at a similar growth stage and responds similarly to environmental conditions. In contrast, higher ET variability in the mature stand may be attributed to canopy complexity stemming from a denser array of tree sizes and species as well as canopy gaps due to natural tree mortality and self-thinning. Additionally, the more well-established root system in older forest may yield varied responses to soil moisture contributing to increased variability (O'Connor et al., 2021).

In comparison with other forests, the 83- and 48-year-old stands exhibited ET values of 441 mm yr<sup>-1</sup> and 458 mm yr<sup>-1</sup>, respectively, which was higher than the mean annual ET of 419±46 mm yr<sup>-1</sup> reported by Arango Ruda and Arain (2024) for a deciduous forest in the same region between 2012 to 2020. Contrarily, the 20-year-old stand exhibited a lower mean annual ET of 406±21 mm yr<sup>-1</sup>. The mean annual ET in our study was much higher than 226±8 mm yr<sup>-1</sup> recorded in a *Pinus palustris* Mill. forests in the United States (Guerrieri et al., 2016) and 349±3 mm yr<sup>-1</sup> observed in a boreal forest in Western Canada from 2017 to 2020 (Nicholls & Carey, 2021). However, these values fell below those reported for tropical forests of 1316±192 mm yr<sup>-1</sup> (Paca et al., 2019).

ET is the most important and the largest component of water balance in vegetation ecosystem, accounting for 59-67% of total P utilization over the land (Bonan, 2015; Wang & Dickinson, 2012). Our study results showed that these different age forest have made and important contribution to water supply in the region, where P-ET was positive and ET/P < 1 across the years, with interannual

mean values ranging from 654 to 716 mm yr<sup>-1</sup> (Table 3.2) (Krishnan et al., 2012). On an annual basis, the oldest forest exhibited an ET/P interannual mean of 0.43, which was higher than values observed in the 20-year-old stand (ET/P=0.38), and a deciduous temperate forest in the region (i.e. 0.38, Arango Ruda and Arain, 2024). This index increased in years that experience dry conditions such as in 2010 and 2015. ET/P at these temperate pine stands was lower than the  $2.19 \pm 0.37$  ratio reported by Nicholls and Carey (2021) for a boreal forest.

# 3.5.2 Water Use Efficiency (WUE)

Significant variations in stand productivity were found among the three stands (Table 3.3). In particular, the 48-year-old often exhibited higher GEP than the older forest. The younger forest exhibited an incremental trend in GEP, surpassing the values observed in the older stands in 2017 at the age of 17 years. This pattern is consistent with the well-documented growth trajectory of white pine trees, which experience a surge in growth during their initial years, peaking around 20 years. Subsequently, the growth rate begins to decline, ultimately influencing productivity (Burns and Honkala, 1990). By the age of 55, the growth rate of white pines trees is almost equal in all sites (Burns and Honkala, 1990), which may explain the relatively similar GEP rates of the two older stands (Table 3.3). Moreover, sandy soils, a thicker A horizon, past crop cultivations and little competition from other tree species due to mono-culture nature of these plantation forest, contribute to favorable conditions that support the rapid growth of these white pine forests (Burns and Honkala, 1990).

The analysis showed that in the youngest forest, GEP had a greater influence on WUE compared to the older forests (Table S3.1). However, overall, WUE was strongly linked to ET in all three stands (Table S3.1). The lower ET in the younger forest led to optimized WUE across consecutive years, as

opposed to the older coniferous forest. Notably, as productivity increased over the years within the youngest stand, WUE increased from 2.34 g C m<sup>-2</sup> kg H<sub>2</sub>O in 2008 to 5.36 g C m<sup>-2</sup> kg H<sub>2</sub>O in 2019. Conversely, the 83-year-old forest, with access to more water due to the deeper root system, experienced a decrease in WUE due to higher ET (Fernández et al., 2009). Overall, the 20-year-old forest performed better in maximizing forest carbon storage while conserving water resources (Hubbard et al., 2010), indicating that younger forests are more sustainable and efficient ecosystems regarding carbon sequestration and water utilization.

WUE values for our stands fell within the range observed for needleleaf evergreen forests (3-4 g C m<sup>-2</sup> kg<sup>-1</sup> H<sub>2</sub>O) (Tang et al., 2014). Overall, pine plantations have larger WUE than deciduous forests (Li et al., 2023). These findings aligned with this pattern, as WUE ranged from 3.4 to 4 g C m<sup>-2</sup> kg H<sub>2</sub>O in these forests in comparison with those reported by Arango Ruda and Arain (2024) for a temperate deciduous forest at the same region, which recorded a WUE of 3.3 g C m<sup>-2</sup> kg H<sub>2</sub>O. Coniferous forests are more conservative at water use, which explains the rationale behind their elevated WUE.

# 3.5.3 Evapotranspiration and Environmental Controls

The Intergovernmental Panel on Climate Change (IPCC) has projected a significant increase in global temperatures by mid-century, which is anticipated to have profound implications for plant ecosystems worldwide (IPCC, 2021). This warming is often associated with increasing Rn and decreasing relative humidity, which in turn impact processes like ET rates (IPCC, 2021). Therefore, the finding here of monthly ET dependence on temperature in white pine plantations (Table 3.4), reveal the susceptibility of these ecosystems to changing climate.

Recent research by Aguilos et al. (2021) underscores the dependency of ET on solar energy availability and temperature. This study with particularly focus on forest ecosystems of varying ages advances these arguments (Table 3.4). These findings highlight the susceptibility of plantation or managed forests to climate change-induced alterations in environmental factors. Additionally, variables like WUE and GEP are also influenced by these changes (Table 3.4). For instance, a negative correlation was found between Rn and WUE, suggesting reduced WUE due to heightened radiation leading to increased ET rates without a proportional rise in carbon uptake (Teuling et al., 2010)

Soil moisture and atmospheric water demand are recognized as critical factors affecting vegetation productivity and water utilization, especially during periods of hydrological stress (Jung et al., 2010; Klos et al., 2018; Novick et al., 2016). Although VPD is increasingly acknowledged for its role in regulating carbon and water fluxes within vegetation (Novick et al., 2016), this study did not observe a significant response of ET, GEP, and WUE to VPD variations (Table 3.4). Similarly, responses to low soil moisture levels were not as strong as these responses were Rn and Tair, However, a decrease in ET was seen during dry conditions across the stands, with younger stands displaying a stronger signal (Fig. 3.3). This discrepancy may be attributed to differences in root depth, sapwood area, forest age, and canopy extent among stands (Anderegg et al., 2018); Cairns et al., 1997; Granier et al., 2000; Peichl & Arain, 2007). Indeed, forest age appears to influence the sensitivity of ET to variations in soil moisture and atmospheric demand (Fig. 3.6), with older forests exhibiting lower coupling to drought conditions. This variation is likely attributed to differences in forest structure, plant composition, and physiological traits related to water transport (Anderegg et al., 2018).

Contrary to ET response, enhanced WUE was observed during dry conditions across the three forest

ages, potentially due to larger reductions in ET rather than GEP, aligning with findings from previous studies for WUE during moderate and short-term drought (Liu et al., 2015). Furthermore, meteorological drought may not necessarily decrease forest WUE when groundwater remains sufficient, as demonstrated by Aguilos et al., (2021).

A decrease in ET suggests reduced water loss through evaporation and transpiration, demonstrating the stands capacity for water conservation (Jung et al., 2010). Simultaneously, the observed increase in WUE indicates that these stands are becoming more efficient in utilizing available water resources, facilitating better adaptation to drought conditions (Yang et al., 2016). Hence, our findings hold significance for the better understating of the processes and ways forest ecosystems may respond to climate change.

#### 3.6 Conclusions

This study examines the seasonal and year-to-year variations in water and carbon fluxes over a 14-year period (2008-2021). The measurements were taken using eddy covariance in a series of temperate white pine (*Pinus strobus* L.) forests of different ages (83, 48, and 20 years) in southern Ontario, Canada. The youngest white pine forest stood out for its lowest water use (403 mm yr<sup>-1</sup>), higher productivity (1634 g C m<sup>-2</sup> yr<sup>-1</sup>), and higher WUE (4 g C kg H<sub>2</sub>O yr<sup>-1</sup>) over the study period, in comparison to the older stands. This indicates that younger forests are more sustainable and efficient ecosystems regarding carbon sequestration and water utilization. ET variability increased with forest age, with the oldest forest showing the greatest year-to-year fluctuations. The lower year-to-year variation in ET of the younger stands likely stems from the uniformity of vegetation, which results in more consistent ET as the stands are at a similar growth stage and respond similarly to

environmental conditions. The ET/P ratio remained consistently below 1 for all years across all forests, where the older stands had a higher ET/P ratio (0.43) compared to the youngest forest (0.38). Late summer drought conditions reduced ET, but the oldest forest showed greater drought resilience, likely due to its well-established root system accessing deeper soil water. The water available across the stands was positive across the years with interannual mean values ranging from 654 to 716 mm yr<sup>-1</sup>, indicating an overall consistent contribution to the local water supply. The most significant impact on ET and GEP was caused by Tair, followed by LAI. This reflects how susceptible these ecosystems are to changes in environmental conditions and the effect of age affects through variations in the vegetation cover. This long-term observation enhances our understanding of water flux dynamics in plantation forests of varying ages and provides valuable insights into their response to future climate change. These findings have relevance for the restoration and conservation of plantation and managed forests, helping to develop sustainable forestry practices and climate adaptation strategies.

## 3.7 Acknowledgements

Funding was provided by the Natural Sciences and Engineering Research Council (NSERC) Discovery and NSERC Alliance Mission grants and Global Water Futures (GWF) Program – Southern Forests Water Futures and GWF Observatory, Ontario Ministry of Environment and Climate Change (MOECC) as well as Social Science and Humanities Research Council (SSHRC) through Global Centre for Climate Change in Transnational Waters grants awarded to M.A. Arain. Past funding from the Canadian Foundation of Innovation (CFI), Ontario Innovation Trust (OIT), Ontario Ministry of Research and Innovation (MRI) is also acknowledged. In-kind support from the Ontario Ministry of Natural Resources and Forestry (OMNRF), St Williams Conservation Reserve Community Council

(SWCRCC), the Normandale Fish Culture Station, Long Point Waterfowl Research and Education Centre, Long Point Eco-Adventures, Ontario Power Generation (OPG), Norfolk County, and McMaster University is acknowledged. The authors acknowledge Bruce Whitside and family for providing access to the 20-year-old site located on their property. Finally, we acknowledge support from Zoran Nesic at the University of British Columbia (Dr. T. A. Black's group) in flux measurements and Jason Brodeur (McMaster University) for flux data handing and past and present members of the Hydrometeorology and Climatology lab at McMaster University, including Natalia Restrepo-Couple, Jason Brodeur, Myroslava Khomik, Matthias Peichl, Robin Thorne, Michelle Kula, Janell Trant, Eric Beamesderfer, Brandon Burns, Lejla Latifovic, Farbod Tabaei and Nur Hussain for their support in the fieldwork and data collection.

#### 3.8 References

- Aguilos, M., Sun, G., Noormets, A., Domec, J. C., McNulty, S., Gavazzi, M., Prajapati, P., Minick, K. J., Mitra, B., & King, J. (2021). Ecosystem productivity and evapotranspiration are tightly coupled in loblolly pine (Pinus taeda I.) plantations along the coastal plain of the southeastern U.S. Forests, 12(8). https://doi.org/10.3390/f12081123
- Akaike, H. (1974). A new look at the statistical model identification. In IEEE TRANSACTIONS ON AUTOMATIC CONTROL (Issue 6, pp. 215–222).
- Anderegg, W. R. L., Konings, A. G., Trugman, A. T., Yu, K., Bowling, D. R., Gabbitas, R., Karp, D. S., Pacala, S., Sperry, J. S., Sulman, B. N., & Zenes, N. (2018a). Hydraulic diversity of forests regulates ecosystem resilience during drought. Nature, 561(7724), 538–541. https://doi.org/10.1038/s41586-018-0539-7
- Arain, A. (2018). AmeriFlux BASE CA-TP4 Ontario Turkey Point 1939 Plantation White Pine, Ver. 4-5, AmeriFlux AMP, (Dataset).
- Arain, A. (2022). AmeriFlux FLUXNET-1F CA-TP3 Ontario Turkey Point 1974 Plantation White Pine, Ver. 3-5, AmeriFlux AMP, (Dataset).
- Arain, A. (2023). AmeriFlux FLUXNET-1F CA-TP1 Ontario Turkey Point 2002 Plantation White Pine, Ver. 3-5, AmeriFlux AMP, (Dataset).
- Arain, A., Xu, B., Brodeur, J. J., Khomik, M., Peichl, M., Beamesderfer, E., Restrepo-Couple, N., & Thorne, R. (2022). Heat and drought impact on carbon exchange in an age-sequence of temperate pine forests. Ecological Processes, 11(1). https://doi.org/10.1186/s13717-021-00349-7
- Arain, M. A., & Restrepo-Coupe, N. (2005). Net ecosystem production in a temperate pine plantation in southeastern Canada. Agricultural and Forest Meteorology, 128(3–4), 223–241. https://doi.org/10.1016/j.agrformet.2004.10.003
- Arango Ruda, E., & Arain, M. A. (2024). Impacts of heat and drought on the dynamics of water fluxes in a temperate deciduous forest from 2012 to 2020. Agricultural and Forest Meteorology, 344, 109791. https://doi.org/10.1016/J.AGRFORMET.2023.109791
- Bauhus, J., van der Meer, P. J., & Kanninen, M. (2010). Ecosystem goods and services from plantation forests. In Earthscan.
- Beamesderfer, E., Arain, A., Khomik, M., Brodeur, J. J., & Burns, B. M. (2020). Response of carbon and water fluxes to meteorological and phenological variability in two eastern North American forests of similar age but contrasting species composition- A multiyear comparison. Journal of Geophysical Research: Biogeosciences, 17(13), 3563–3587.

- https://doi.org/https://doi.org/10.5194/bg-17-3563-2020
- Bevacqua, E., De Michele, C., Manning, C., Couasnon, A., Ribeiro, A. F. S., Ramos, A. M., Vignotto, E., Bastos, A., Blesić, S., Durante, F., Hillier, J., Oliveira, S. C., Pinto, J. G., Ragno, E., Rivoire, P., Saunders, K., van der Wiel, K., Wu, W., Zhang, T., & Zscheischler, J. (2021). Guidelines for Studying Diverse Types of Compound Weather and Climate Events. Earth's Future, 9(11). https://doi.org/10.1029/2021EF002340
- Black, T. A. (1979). Evapotranspiration From Douglas Fir Stands Exposed to Soil Water Deficits. Water Resources Research, 15(1), 164–170. https://doi.org/10.1029/WR015i001p00164
- Bonan, G. B. (2015). Ecological Climatology: Concepts and Applications (3rd ed.). Cambridge University Press. https://doi.org/10.1017/CBO9781107339200
- Brodeur, J. (2014). Data-driven approaches for sustainable operation and defensible results in a long-term, multi-site ecosystem flux measurement program. McMaster University.
- Burns, R. M., & Honkala, B. (1990). Silvics of North America: 1. Conifers; 2. Hardwoods. Agriculture Handbook 654. (Vol. 1). U.S. Department of Agriculture, Forest Service. https://www.srs.fs.usda.gov/pubs/misc/ag 654/volume 1/vol1 table of contents.htm
- Cairns, M. A., Brown, S., Helmer, E. H., & Baumgardner, G. A. (1997). Root Biomass Allocation in the World's Upland Forests. In Source: Oecologia (Vol. 111, Issue 1).
- Chan, F. C. C., Altaf Arain, M., Khomik, M., Brodeur, J. J., Peichl, M., Restrepo-Coupe, N., Thorne, R., Beamesderfer, E., McKenzie, S., Xu, B., Croft, H., Pejam, M., Trant, J., Kula, M., & Skubel, R. (2018). Carbon, water and energy exchange dynamics of a young pine plantation forest during the initial fourteen years of growth. Forest Ecology and Management, 410(September 2017), 12–26. https://doi.org/10.1016/j.foreco.2017.12.024
- Chen, Z., Yu, G., & Wang, Q. (2020). Effects of climate and forest age on the ecosystem carbon exchange of afforestation. Journal of Forestry Research, 31, 365–374. https://doi.org/10.1007/s11676-019-00946-5
- Clogg, C. C., Petkova, E., & Haritou, A. (1995). Statistical Methods for Comparing Regression Coefficients Between Models. American Journal of Sociology, 100(5), 1261–1293. https://www.jstor.org/stable/2782277
- Cornish, P. M., & Vertessy, R. A. (2001). Forest age-induced changes in evapotranspiration and water yield in a eucalypt forest [Article]. Journal of Hydrology (Amsterdam), 242(1), 43–63. https://doi.org/10.1016/S0022-1694(00)00384-X
- Delzon, S., & Loustau, D. (2005). Age-related decline in stand water use: Sap flow and transpiration in a pine forest chronosequence. Agricultural and Forest Meteorology, 129(3–4), 105–119. https://doi.org/10.1016/j.agrformet.2005.01.002

- Diao, H., Wang, A., Yang, H., Yuan, F., Guan, D., & Wu, J. (2021). Responses of evapotranspiration to droughts across global forests: A systematic assessment. Canadian Journal of Forest Research, 51(1), 1–9. https://doi.org/10.1139/cjfr-2019-0436
- Environment and Climate Change Canada (ECCC). (2023, January). Climate Data Online. Https://Climate.Weather.Gc.ca. Accessed 16 January.
- Fernández, M. E., Gyenge, J., & Schlichter, T. (2009). Water flux and canopy conductance of natural versus planted forests in Patagonia, South America. Trees Structure and Function, 23(2), 415–427. https://doi.org/10.1007/s00468-008-0291-y
- Franklin, J. F., Spies, T. A., Pelt, R. Van, Carey, A. B., Thornburgh, D. A., Berg, D. R., Lindenmayer, D. B., Harmon, M. E., Keeton, W. S., Shaw, D. C., Bible, K., & Chen, J. (2002). Disturbances and structural development of natural forest ecosystems with silvicultural implications, using Douglas-fir forests as an example. Forest Ecology and Management, 155(1–3), 399–423. https://doi.org/10.1016/S0378-1127(01)00575-8
- Ge, Z. M., Kellomäki, S., Zhou, X., & Peltola, H. (2014). The role of climatic variability in controlling carbon and water budgets in a boreal Scots pine forest during ten growing seasons. Boreal Environ. Res., 19(3), 181–194.
- Giles-Hansen, K., Wei, X., & Hou, Y. (2021). Dramatic increase in water use efficiency with cumulative forest disturbance at the large forested watershed scale. Carbon Balance and Management, 16(1), 1–15. https://doi.org/10.1186/s13021-021-00169-4
- Granier, A., Biron, P., & Lemoine, D. (2000). Water balance, transpiration and canopy conductance in two beech stands. Agricultural and Forest Meteorology, 100(4), 291–308. https://doi.org/10.1016/S0168-1923(99)00151-3
- Granier, A., Reichstein, M., Bréda, N., Janssens, I. A., Falge, E., Ciais, P., Grünwald, T., Aubinet, M., Berbigier, P., Bernhofer, C., Buchmann, N., Facini, O., Grassi, G., Heinesch, B., Ilvesniemi, H., Keronen, P., Knohl, A., Köstner, B., Lagergren, F., ... Wang, Q. (2007). Evidence for soil water control on carbon and water dynamics in European forests during the extremely dry year: 2003. Agricultural and Forest Meteorology, 143(1–2), 123–145. https://doi.org/10.1016/j.agrformet.2006.12.004
- Griscom, B. W., Adams, J., Ellis, P. W., Houghton, R. A., Lomax, G., Miteva, D. A., Schlesinger, W. H., Shoch, D., Siikamäki, J. V., Smith, P., Woodbury, P., Zganjar, C., Blackman, A., Campari, J., Conant, R. T., Delgado, C., Elias, P., Gopalakrishna, T., Hamsik, M. R., ... Fargione, J. (2017). Natural climate solutions. Proceedings of the National Academy of Sciences of the United States of America, 114(44), 11645–11650. https://doi.org/10.1073/pnas.1710465114
- Groempings, U. (2021). The Relative Importance of Regressors in Linear Models. https://prof.bht-berlin.de/groemping/relaimpo/,

- Guauque-Mellado, D., Rodrigues, A., Terra, M., Mantovani, V., Yanagi, S., Diotto, A., & de Mello, C. (2022). Evapotranspiration under Drought Conditions: The Case Study of a Seasonally Dry Atlantic Forest. Atmosphere, 13(6). https://doi.org/10.3390/atmos13060871
- Guerrieri, R., Lepine, L., Asbjornsen, H., Xiao, J., & Ollinger, S. V. (2016). Evapotranspiration and water use efficiency in relation to climate and canopy nitrogen in U.S. forests. Journal of Geophysical Research: Biogeosciences, 121(10), 2610–2629. https://doi.org/10.1002/2016JG003415
- Haberstroh, S., Caldeira, M. C., Lobo-do-Vale, R., Martins, J. I., Moemken, J., Pinto, J. G., & Werner, C. (2021). Nonlinear plant–plant interactions modulate impact of extreme drought and recovery on a Mediterranean ecosystem. New Phytologist, 231(5), 1784–1797. https://doi.org/10.1111/nph.17522
- Hammerle, A., Haslwanter, A., Tappeiner, U., Cernusca, A., & Wohlfahrt, G. (2008). Leaf area controls on energy partitioning of a temperate mountain grassland. Biogeosciences, 5(2), 421–431. https://doi.org/10.5194/bg-5-421-2008
- Hubbard, R. M., Stape, J., Ryan, M. G., Almeida, A. C., & Rojas, J. (2010). Effects of irrigation on water use and water use efficiency in two fast growing Eucalyptus plantations. Forest Ecology and Management, 259(9), 1714–1721. https://doi.org/10.1016/J.FORECO.2009.10.028
- IPCC. (2021). Climate Change 2021: The Physical Science Basis. Contribution of Working Group I to the Sixth Assessment Report of the Intergovernmental Panel on Climate Change.
- Jasechko, S., Sharp, Z. D., Gibson, J. J., Birks, S. J., Yi, Y., & Fawcett, P. J. (2013). Terrestrial water fluxes dominated by transpiration. Nature, 496(7445), 347–350. https://doi.org/10.1038/nature11983
- Jung, M., Reichstein, M., Ciais, P., Seneviratne, S. I., Sheffield, J., Goulden, M. L., Bonan, G., Cescatti, A., Chen, J., De Jeu, R., Dolman, A. J., Eugster, W., Gerten, D., Gianelle, D., Gobron, N., Heinke, J., Kimball, J., Law, B. E., Montagnani, L., ... Zhang, K. (2010a). Recent decline in the global land evapotranspiration trend due to limited moisture supply. Nature, 467(7318), 951–954. https://doi.org/10.1038/nature09396
- Katul, G. G., Oren, R., Manzoni, S., Higgins, C., & Parlange, M. B. (2012). Evapotranspiration: A process driving mass transport and energy exchange in the soil-plant-atmosphere-climate system. In Reviews of Geophysics (Vol. 50, Issue 3). Blackwell Publishing Ltd. https://doi.org/10.1029/2011RG000366
- Khalid, S. (2016). Impact of afforestation on soil chemical and physical properties of southern Ontario forests, with a comparison to a naturally regenerated stand. [Undergraduate thesis]. McMaster University.
- Kljun, N., Kormann, R., Rotach, M. W., & Meixer, F. X. (2003). Comparison of the langrangian footprint model lpdm-b with an analytical footprint model. Boundary-Layer Meteorology,

106.

- Klos, P. Z., Goulden, M. L., Riebe, C. S., Tague, C. L., O'geen, A. T., Flinchum, B. A., Safeeq, M., Conklin, M. H., Hart, S. C., Berhe, A. A., Hartsough, P. C., Holbrook, W. S., & Bales, R. C. (2018). Subsurface plant-accessible water in mountain ecosystems with a Mediterranean climate. Wiley Interdisciplinary Reviews: Water, 5(3). https://doi.org/10.1002/WAT2.1277
- Krishnan, P., Meyers, T. P., Scott, R. L., Kennedy, L., & Heuer, M. (2012). Energy exchange and evapotranspiration over two temperate semi-arid grasslands in North America. Agricultural and Forest Meteorology, 153, 31–44. https://doi.org/10.1016/J.AGRFORMET.2011.09.017
- Kulakowski, D., Bebi, P., & Rixen, C. (2011). interacting effects of land use change, climate change and suppression of natural disturbances on landscape forest structure in the Swiss Alps [Article]. Oikos, 120(2), 216–225. https://doi.org/10.1111/j.1600-0706.2010.18726.x
- Lawrence, D., Coe, M., Walker, W., Verchot, L., & Vandecar, K. (2022). The Unseen Effects of Deforestation: Biophysical Effects on Climate. Frontiers in Forests and Global Change, 5(756115). https://doi.org/10.3389/ffgc.2022.756115
- Liu, X., Sun, G., Mitra, B., Noormets, A., Gavazzi, M. J., Domec, J. C., Hallema, D. W., Li, J., Fang, Y., King, J. S., & McNulty, S. G. (2018). Drought and thinning have limited impacts on evapotranspiration in a managed pine plantation on the southeastern United States coastal plain. Agricultural and Forest Meteorology, 262, 14–23. https://doi.org/10.1016/J.AGRFORMET.2018.06.025
- Liu, Y., Xiao, J., Ju, W., Zhou, Y., Wang, S., & Wu, X. (2015). Water use efficiency of China's terrestrial ecosystems and responses to drought. Scientific Reports, 5. https://doi.org/10.1038/srep13799
- Li, Y., Zhang, K., & Liu, L. (2023). Water use efficiency at multi-time scales and its response to episodic drought and wet periods in a typical subtropical evergreen forest of Southeast China. Ecological Indicators, 151. https://doi.org/10.1016/j.ecolind.2023.110254
- McLaren, J. D., Arain, M. A., Khomik, M., Peichl, M., & Brodeur, J. (2008). Water flux components and soil water-atmospheric controls in a temperate pine forest growing in a well-drained sandy soil. Journal of Geophysical Research: Biogeosciences, 113(4), 1–16. https://doi.org/10.1029/2007JG000653
- Messier, C., Bauhus, J., Sousa-Silva, R., Auge, H., Baeten, L., Barsoum, N., Bruelheide, H., Caldwell, B., Cavender-Bares, J., Dhiedt, E., Eisenhauer, N., Ganade, G., Gravel, D., Guillemot, J., Hall, J. S., Hector, A., Hérault, B., Jactel, H., Koricheva, J., ... Zemp, D. C. (2022). For the sake of resilience and multifunctionality, let's diversify planted forests! Conservation Letters, 15(1), 1–8. https://doi.org/10.1111/conl.12829
- Moomaw, W. R., Law, B. E., & Goetz, S. J. (2020). Focus on the role of forests and soils in meeting climate change mitigation goals: Summary. Environmental Research Letters, 15(4).

- https://doi.org/10.1088/1748-9326/ab6b38
- Nicholls, E. M., & Carey, S. K. (2021). Evapotranspiration and energy partitioning across a forest-shrub vegetation gradient in a subarctic, alpine catchment. Journal of Hydrology, 602(July), 126790. https://doi.org/10.1016/j.jhydrol.2021.126790
- Niinemets, U. (2010). review of light interception in plant stands from leaf to canopy in different plant functional types and in species with varying shade tolerance [Article]. Ecological Research, 25(4), 693–714. https://doi.org/10.1007/s11284-010-0712-4
- Novick, K. A., Ficklin, D. L., Stoy, P. C., Williams, C. A., Bohrer, G., Oishi, A. C., Papuga, S. A., Blanken, P. D., Noormets, A., Sulman, B. N., Scott, R. L., Wang, L., & Phillips, R. P. (2016a). The increasing importance of atmospheric demand for ecosystem water and carbon fluxes. In Nature Climate Change (Vol. 6, Issue 11, pp. 1023–1027). https://doi.org/10.1038/nclimate3114
- O'Connor, J. C., Dekker, S. C., Staal, A., Tuinenburg, O. A., Rebel, K. T., & Santos, M. J. (2021). Forests buffer against variations in precipitation. Global Change Biology, 27(19), 4686–4696. https://doi.org/10.1111/gcb.15763
- Ontario Ministry of Natural Resources [OMNR]. (1986). Evergreen challenge: the agreement forest story.
- Paca, V. H. da M., Espinoza-Dávalos, G. E., Hessels, T. M., Moreira, D. M., Comair, G. F., & Bastiaanssen, W. G. M. (2019). The spatial variability of actual evapotranspiration across the Amazon River Basin based on remote sensing products validated with flux towers. Ecological Processes, 8(1). https://doi.org/10.1186/s13717-019-0158-8
- Papale, D., Reichstein, M., Aubinet, M., Canfora, E., Bernhofer, C., Kutsch, W., Longdoz, B., Rambal, S., Valentini, R., Vesala, T., & Yakir, D. (2006). Towards a standardized processing of Net Ecosystem Exchange measured with eddy covariance technique: algorithms and uncertainty estimation. Biogeosciences, 3(4), 571–583. https://doi.org/10.5194/bg-3-571-2006
- Peichl, M., & Arain, M. A. (2007). Allometry and partitioning of above- and belowground tree biomass in an age-sequence of white pine forests. Forest Ecology and Management, 253(1–3), 68–80. https://doi.org/10.1016/J.FORECO.2007.07.003
- Peichl, M., Arain, M. A., & Brodeur, J. J. (2010). Agricultural and Forest Meteorology Age effects on carbon fluxes in temperate pine forests. Agricultural and Forest Meteorology, 150(7–8), 1090–1101. https://doi.org/10.1016/j.agrformet.2010.04.008
- Peichl, M., Arain, M. A., Ullah, S., & Moore, T. R. (2010). Carbon dioxide, methane, and nitrous oxide exchanges in an age-sequence of temperate pine forests. Global Change Biology, 16(8), 2198–2212. https://doi.org/10.1111/j.1365-2486.2009.02066.x

- Peichl, M., Brodeur, J. J., Khomik, M., & Arain, M. A. (2010). Biometric and eddy-covariance based estimates of carbon fluxes in an age-sequence of temperate pine forests. Agricultural and Forest Meteorology, 150(7–8), 952–965. https://doi.org/10.1016/j.agrformet.2010.03.002
- Presant, E., & Acton, C. (1984). The Soils of the Regional Municipality of Haldimand-Norfolk. Report No. 57.
- Restrepo-Coupe, N., Albert, L. P., Longo, M., Baker, I., Levine, N. M., Mercado, L. M., da Araujo, A. C., Christoffersen, D., Costa, M. H., Fitzjarrald, D. R., Galbraith, D., Imbuzeiro, H., Malhi, Y., von Randow, C., Zeng, X., Moorcroft, P., & Saleska, S. R. (2021). Understanding water and energy fluxes in the Amazonia: Lessons from an observation-model intercomparison. Glob Change Biol, 27, 1802–1819. https://doi.org/10.1111/gcb.15555
- Restrepo, N. C., & Arain, M. A. (2005). Energy and water exchanges from a temperate pine plantation forest. Hydrological Processes, 19(1), 27–49. https://doi.org/10.1002/hyp.5758
- Schlesinger, W. H., Dietze, M. C., Jackson, R. B., Phillips, R. P., Rhoades, C. C., Rustad, L. E., & Vose, J. M. (2016). Forest biogeochemistry in response to drought [Article]. Global Change Biology, 22(7), 2318–2328. https://doi.org/10.1111/gcb.13105
- Schlesinger, W. H., & Jasechko, S. (2014). Transpiration in the global water cycle. Agricultural and Forest Meteorology, 189–190, 115–117. https://doi.org/10.1016/J.AGRFORMET.2014.01.011
- Skubel, R., Arain, M. A., Peichl, M., Brodeur, J. J., Khomik, M., Thorne, R., Trant, J., & Kula, M. (2015). Age effects on the water-use efficiency and water-use dynamics of temperate pine plantation forests. Hydrological Processes, 29(18), 4100–4113. https://doi.org/10.1002/hyp.10549
- Sulman, B. N., Roman, D. T., Yi, K., Wang, L., Phillips, R. P., & Novick, K. A. (2016). High atmospheric demand for water can limit forest carbon uptake and transpiration as severely as dry soil. Geophysical Research Letters, 43(18), 9686–9695. https://doi.org/10.1002/2016GL069416
- Swenson, S., & Wahr, J. (2006). Estimating Large-Scale Precipitation Minus Evapotranspiration from GRACE Satellite Gravity Measurements.
- Tang, X., Li, H., Desai, A. R., Nagy, Z., Luo, J., Kolb, T. E., Olioso, A., Xu, X., Yao, L., Kutsch, W., Pilegaard, K., Köstner, B., & Ammann, C. (2014). How is water-use efficiency of terrestrial ecosystems distributed and changing on Earth? Scientific Reports, 4, 1–11. https://doi.org/10.1038/srep07483
- Teuling, A. J., & Hoek van Dijke, A. J. (2020). Forest age and water yield. In Nature (Vol. 578, Issue 7762, pp. E16–E18). Nature Publishing Group. https://doi.org/10.1038/s41586-019-1306-0
- Teuling, A. J., Seneviratne, S. I., Stöckli, R., Reichstein, M., Moors, E., Ciais, P., Luyssaert, S., Van

- Den Hurk, B., Ammann, C., Bernhofer, C., Dellwik, E., Gianelle, D., Gielen, B., Grünwald, T., Klumpp, K., Montagnani, L., Moureaux, C., Sottocornola, M., & Wohlfahrt, G. (2010). Contrasting response of European forest and grassland energy exchange to heatwaves. Nature Geoscience, 3(10), 722–727. https://doi.org/10.1038/ngeo950
- Valipour, M., Bateni, S. M., Gholami Sefidkouhi, M. A., Raeini-Sarjaz, M., & Singh, V. P. (2020). Complexity of Forces Driving Trend of Reference Evapotranspiration and Signals of Climate Change. Atmosphere, 11(10), 1081. https://doi.org/10.3390/atmos11101081
- Vilhar, U. (2016). Comparison of drought stress indices in beech forests: A modelling study. IForest, 9(4), 635–642. https://doi.org/10.3832/ifor1630-008
- Wang, K., & Dickinson, R. E. (2012). A review of global terrestrial evapotranspiration: Observation, modeling, climatology, and climatic variability. In Reviews of Geophysics (Vol. 50, Issue 2). Blackwell Publishing Ltd. https://doi.org/10.1029/2011RG000373
- Wolf, S., Eugster, W., Ammann, C., Häni, M., Zielis, S., Hiller, R., Stieger, J., Imer, D., Merbold, L., & Buchmann, N. (2013). Contrasting response of grassland versus forest carbon and water fluxes to spring drought in Switzerland [Article]. Environmental Research Letters, 8(3), 35007–35012. https://doi.org/10.1088/1748-9326/8/3/035007
- Xie, J., Chen, J., Sun, G., Zha, T., Yang, B., Chu, H., Liu, J., Wan, S., Zhou, C., Ma, H., Bourque, C. P. A., Shao, C., John, R., & Ouyang, Z. (2016). Ten-year variability in ecosystem water use efficiency in an oak-dominated temperate forest under a warming climate. Agricultural and Forest Meteorology, 218–219, 209–217. https://doi.org/10.1016/j.agrformet.2015.12.059
- Xu, B., Arain, M. A., Black, T. A., Law, B. E., Pastorello, G. Z., & Chu, H. (2020). Seasonal variability of forest sensitivity to heat and drought stresses: A synthesis based on carbon fluxes from North American forest ecosystems. Global Change Biology, 26(2), 901–918. https://doi.org/10.1111/gcb.14843
- Yang, Y., Guan, H., Batelaan, O., McVicar, T. R., Long, D., Piao, S., Liang, W., Liu, B., Jin, Z., & Simmons, C. T. (2016). Contrasting responses of water use efficiency to drought across global terrestrial ecosystems. Scientific Reports, 6. https://doi.org/10.1038/srep23284
- Zhang, Z., Zhang, L., Xu, H., Creed, I. F., Blanco, J. A., Wei, X., Sun, G., Asbjornsen, H., & Bishop, K. (2023). Forest water-use efficiency: Effects of climate change and management on the coupling of carbon and water processes. In Forest Ecology and Management (Vol. 534). Elsevier B.V. https://doi.org/10.1016/j.foreco.2023.120853
- Zhao, J., Feng, H., Xu, T., Xiao, J., Guerrieri, R., Liu, S., Wu, X., He, X., & He, X. (2021). Physiological and environmental control on ecosystem water use efficiency in response to drought across the northern hemisphere. Science of the Total Environment, 758. https://doi.org/10.1016/j.scitotenv.2020.143599

**Table 3.1:** Site characteristics of the 83-year-old, 48-year-old, and 20-year-old forests of the Turkey Point Observatory.

Site	83-year-old	48-year-old	20-year-old
Stand age (start/end)	64/83	29/49	1/21
Tower location	42.7102, -80.3574	42.7074, -80.3485	42.6617, -80.5599
Elevation (m)	184	184	265
Plantation year	1939	1974	2002
Average canopy height (m)	23.4 (22.9)	16.2	6.85
Tree density (trees ha <sup>-1</sup> )	321 (413)	1583	1567
Leaf area index, LAI (m <sup>2</sup> m <sup>-2</sup> )	3.25	2.90	1.59
Average diameter at 1.3 m	38.99 (37.2)	17.90	15.76
height, DBH (cm)			
Stand basal area (m <sup>2</sup> ha <sup>-1</sup> )	36.00 (40.90)	40.00 (26.80)	31.80
Above ground biomass (t C	129.62 (143.80)	86.68	44.67
_ha <sup>-1</sup> )			
Soil texture	Fine sand	Fine sand	Fine sand
Soil drainage	Well-drained	Well-drained	Well-drained
Classification	Brunisolic grey	Brunisolic grey	Brunisolic grey
	brown luvisol	brown luvisol	brown luvisol
Proportion of sand (%)	98	85	93
Bulk density (g cm <sup>-3</sup> )	1.36	1.38	1.44

Note: Numbers in brackets indicate pre-thinning data.

**Table 3.2:** Annual and seasonal water balance at three white pine stands of different age. Precipitation (P), the ratio of ET to P (ET/P), and runoff plus infiltration (P-ET). YR, SPR, SUM and FAL represent yearly, spring, summer and fall totals.

	runo11 pius ini1		P (mm		<u> </u>		ET/P (r			P-ET (mm)			
Year	Site	VD		Season		YR		Season		YR		Season	
		YR	SPR	SUM	FAL		SPR	SUM	FAL		SPR	SUM	FAL
	83-year-old					0.46	0.59	0.96	0.37	616	57	16	91
2008	48-year-old	1140	139	364	144	0.42	0.60	0.83	0.35	658	56	63	93
	20-year-old					0.36	0.75	0.62	0.32	733	35	136	98
	83-year-old					0.48	0.54	0.89	0.32	522	84	35	93
2009	48-year-old	995	182	336	135	0.49	0.55	0.91	0.38	506	83	29	85
	20-year-old					0.38	0.49	0.64	0.30	622	93	120	95
	83-year-old					0.60	0.62	0.96	0.30	360	62	13	144
2010	48-year-old	896	164	345	207	0.57	0.73	0.88	0.28	382	45	41	149
	20-year-old					0.49	0.66	0.72	0.24	459	56	97	158
	83-year-old					0.38	0.27	0.94	0.21	807	199	20	209
2011	48-year-old	1293	272	332	265	0.35	0.28	0.84	0.24	841	195	54	200
	20-year-old					0.30	0.28	0.70	0.18	907	195	101	216
	83-year-old					0.49	1.16	0.73	0.25	508	-13	111	136
2012	48-year-old	1001	82	416	181	0.49	1.27	0.67	0.26	515	-22	136	133
	20-year-old					0.37	1.12	0.47	0.23	628	-10	222	140
	83-year-old					0.37	0.31	0.77	0.25	799	177	93	150
2013	48-year-old	1266	257	407	199	0.38	0.37	0.73	0.32	779	161	111	136
	20-year-old					0.32	0.31	0.58	0.29	863	178	170	142
	83-year-old					0.29	0.29	0.86	0.19	1009	155	48	205
2014	48-year-old	1429	217	339	255	0.31	0.41	0.82	0.18	989	127	60	208
	20-year-old					0.28	0.39	0.71	0.18	1028	133	97	209
	83-year-old					0.54	0.61	0.88	0.25	376	57	38	132
2015	48-year-old	811	146	317	175	0.53	0.59	0.84	0.30	384	60	52	123
	20-year-old					0.51	0.55	0.77	0.33	396	66	72	117
	83-year-old					0.52	0.83	1.07	0.37	372	14	-17	86
2016	48-year-old	778	80	246	135	0.51	0.98	0.89	0.45	382	1	28	74
	20-year-old					0.52	0.85	0.99	0.43	370	12	2	77

Ph.D. Thesis – E. Arango Ruda McMaster – School of Earth, Environment & Society

	83-year-old					0.36	0.33	1.34	0.18	733	165	-67	215
2017	48-year-old	1153	246	196	262	0.39	0.39	1.32	0.21	706	151	-62	207
	20-year-old					0.38	0.38	1.28	0.22	710	152	-55	206
	83-year-old					0.29	0.34	0.53	0.15	1178	156	273	276
2018	48-year-old	1649	237	581	326	0.31	0.41	0.57	0.16	1134	139	249	273
	20-year-old					0.24	0.36	0.42	0.12	1249	151	338	286
	83-year-old					0.38	0.37	0.87	0.22	699	125	41	153
2019	48-year-old	1122	198	319	196	0.41	0.39	0.93	0.26	662	120	21	144
	20-year-old					0.35	0.36	0.77	0.23	732	127	73	150
	83-year-old					0.39	0.35	0.70	0.32	687	133	120	117
2020	48-year-old	1127	203	400	173	0.41	0.42	0.69	0.37	666	118	122	109
	20-year-old					0.38	0.39	0.64	0.32	701	123	145	118
	83-year-old					0.51	0.81	0.76	0.18	494	23	102	226
2021	48-year-old	1009	118	433	277	0.46	0.78	0.69	0.15	547	26	135	235
	20-year-old					0.38	0.51	0.55	0.17	624	58	193	231
	83-year-old					0.43 ±	0.53 ±	0.88 ±	0.25 ±	654±	100±	59 ±	160±
	65-year-old					0.09	0.26	0.19	0.07	242	68	80	58
$Mean \pm \sigma$	48-year-old	1119 ±	181 ±	359 ±	209 ±	0.43 ±	0.58 ±	0.83 ±	0.28 ±	654±	90 ±	74±	155±
(2008-2021)	70-year-olu	237	63	91	209 <u>1</u> 59	0.08	0.28	0.18	0.09	227	64	73	60
	20-year-old	237				0.38 ±	0.53 ±	0.71 ±	0.25 ±	716±	98±	<b>122</b> ±	160±
	20-ycai-0iu					0.08	0.24	0.22	0.08	241	63	95	61

**Table 3.3:** Annual and seasonal water use efficiency in three white pine stands of different age. Evapotranspiration (ET), gross ecosystem productivity (GEP) and water use efficiency (WUE) calculated as a ratio of gross ecosystem productivity (GEP) to ET. YR, GS, SPR, SUM and FAL represent yearly, growing seasons, spring, summer and fall totals. Leaf area index (LAI) values are also given.

			ET (	(mm)			(	GEP			W	/UE		LAI
Year	ar Site		YR Se			YR		Season		YR	Season			
		YK	SPR	SUM	FAL	YK	SPR	SUM	FAL	YK	SPR	SUM	FAL	SUM
	83-year-old	524	82	348	53	1547	267	1108	171	3.0	3.3	3.2	3.2	4.2
2008	48-year-old	482	83	301	51	1443	274	1005	162	3.0	3.3	3.3	3.2	3.8
	20-year-old	407	104	227	46	953	251	586	112	2.3	2.4	2.6	2.4	2.6
	83-year-old	473	97	301	43	1444	284	985	157	3.1	2.9	3.3	3.7	3.8
2009	48-year-old	489	99	307	51	1485	300	1005	157	3.0	3.0	3.3	3.1	3.5
	20-year-old	373	88	216	40	1137	262	706	131	3.0	3.0	3.3	3.3	2.3
	83-year-old	536	102	332	62	1576	317	1079	156	2.9	3.1	3.2	2.5	4.3
2010	48-year-old	514	119	304	58	1739	387	1133	187	3.4	3.2	3.7	3.2	4.4
	20-year-old	437	109	248	49	1430	333	881	169	3.3	3.1	3.6	3.5	2.0
	83-year-old	485	73	312	55	1437	243	1006	176	3.0	3.3	3.2	3.2	4.5
2011	48-year-old	452	77	278	64	1566	305	1051	196	3.5	4.0	3.8	3.0	4.4
	20-year-old	386	77	231	48	1462	314	929	185	3.8	4.1	4.0	3.8	2.8
	83-year-old	493	94	305	44	1454	283	966	136	2.9	3.0	3.2	3.1	4.1
2012	48-year-old	487	104	280	48	1672	382	1022	172	3.4	3.7	3.6	3.6	3.5
	20-year-old	374	92	194	41	1485	359	852	164	4.0	3.9	4.4	4.0	2.2
	83-year-old	467	79	314	49	1506	237	1097	166	3.2	3.0	3.5	3.4	4.4
2013	48-year-old	487	96	295	63	1668	315	1137	206	3.4	3.3	3.8	3.3	3.5
	20-year-old	403	79	237	57	1578	354	1011	196	3.9	4.5	4.3	3.4	2.6
	83-year-old	420	63	290	49	1606	259	1187	154	3.8	4.1	4.1	3.1	5.0
2014	48-year-old	440	90	278	46	1700	323	1173	195	3.9	3.6	4.2	4.2	4.7
	20-year-old	401	84	242	45	1844	378	1217	219	4.6	4.5	5.0	4.9	3.0
2015	83-year-old	434	89	279	43	1708	309	1169	210	3.9	3.5	4.2	4.9	4.0
2015	48-year-old	426	86	266	52	1895	364	1246	261	4.4	4.3	4.7	5.0	3.6

Ph.D. Thesis – E. Arango Ruda McMaster – School of Earth, Environment & Society

	20-year-old	414	80	246	58	1923	394	1198	286	4.6	5.0	4.9	4.9	2.1
	83-year-old	405	66	263	49	1619	278	1081	214	4.0	4.2	4.1	4.3	5.0
2016	48-year-old	395	78	218	61	1639	324	987	265	4.1	4.1	4.5	4.3	4.0
	20-year-old	407	67	244	58	1757	345	1016	303	4.3	5.1	4.2	5.2	1.9
	83-year-old	420	82	263	47	1706	330	1173	179	4.1	4.0	4.5	3.8	4.4
2017	48-year-old	447	96	258	55	1644	379	1037	195	3.7	4.0	4.0	3.5	4.0
	20-year-old	443	94	251	56	1825	419	1105	248	4.1	4.4	4.4	4.4	2.3
	83-year-old	471	81	309	49	1646	256	1239	148	3.5	3.2	4.0	3.0	4.1
2018	48-year-old	516	98	333	52	1604	267	1148	179	3.1	2.7	3.4	3.4	4.1
	20-year-old	400	86	243	40	1557	293	1053	177	3.9	3.4	4.3	4.4	2.1
	83-year-old	423	73	278	42	1541	258	1121	155	3.6	3.5	4.0	3.7	4.2
2019	48-year-old	460	78	298	52	1692	305	1180	197	3.7	3.9	4.0	3.8	3.7
	20-year-old	390	72	246	46	2001	384	1307	263	5.1	5.4	5.3	5.8	2.3
	83-year-old	439	70	280	56	1637	256	1146	194	3.7	3.6	4.1	3.5	4.2
2020	48-year-old	461	85	278	65	1833	342	1198	242	4.0	4.0	4.3	3.7	3.7
	20-year-old	426	80	255	55	2272	436	1402	323	5.3	5.5	5.5	5.9	2.1
	83-year-old	514	95	331	51	1768	316	1208	195	3.4	3.3	3.6	3.9	5.5
2021	48-year-old	461	92	298	42	1666	320	1090	206	4.3	3.5	3.7	5.0	3.9
	20-year-old	385	59	240	46	1650	305	1009	247	3.6	5.1	4.2	5.4	2.5
	83-year-old	465	82	300	5	1585	278	1112	172	3.4	3.4	3.7	3.5	4.4
Mean		±41	±12	±25	±5	±100	±29	±80	±23	±0.4	±0.4	±0.4	±0.6	±0.4
± σ	48-year-old	466	04 .44	285		1660	328	4404 .00	201	3.6	3.6	3.9	3.7	3.9
(2008-	•	±32	91 ±11	±26	54 ±7	±115	±37	1101 ±80	±32	±0.4	±0.4	±0.4	±0.6	±0.4
2021)	20-year-old	403 ±21	84 ±13	237 ±15	49 ±7	1634 ±331	345 ±54	1019 ±216	216 ±62	4.0 ±0.8	4.2 ±0.9	4.3 ±0.8	4.4 ±1.0	2.3 ±0.3
		<b>T41</b>	±13	±13	サブエ/	±JJI	±34	<b>±210</b>	±02	±0.0	±0.9	±υ.δ	±1.U	±0.3

**Table 3.4:** Multivariate regression analysis regressing monthly average evapotranspiration (ET) against the explanatory variables, including vapor pressure deficit (VPD), air temperature (Tair), net radiation (Rn), relative extractable water (REW) and leaf area index (LAI) from 2008 to 2021. Significance code are: [0-0.001] = '\*\*\*; (0.001-0.01] = '\*\*'; (0.01-0.05] = '\*'; (0.05-0.1] = '.'; (0.1-1] = '.'

	Forest	Regressor	Estimate	Std. Error	t Value	<b>Pr(&gt; t )</b>	Significance	lmg
		Intercept	0.000	0.026	0.000	1.000		
	plo	Tair	0.536	0.075	7.152	0.000	***	0.261
	83-year-old	Rn	0.360	0.056	6.454	0.000	***	0.200
	-ye	LAI	0.242	0.056	4.323	0.000	***	0.220
	83	VPD	-0.217	0.078	-2.778	0.006	**	0.185
		REW	-0.099	0.042	-2.388	0.018	*	0.135
	pI	Intercept	0.000	0.036	0.000	1.000		
ET	48-year-old	Tair	0.445	0.093	4.800	0.000	***	0.377
	-yea	LAI	0.274	0.082	3.343	0.001	**	0.335
	48	Rn	0.217	0.064	3.397	0.001	***	0.287
		Intercept	0.000	0.049	0.000	1.000		
	-old	Tair	0.622	0.112	5.538	0.000	***	0.382
	20-year-old	Rn	0.209	0.094	2.207	0.029	*	0.260
	y-0.	LAI	-0.133	0.093	-1.428	0.155		0.175
	7	REW	-0.108	0.076	-1.417	0.158		0.183
		Intercept	0.000	0.021	0.000	1.000		
	plo	Tair	0.615	0.061	10.146	< 2e- 16	***	0.276
	ear-	Rn	0.237	0.045	5.258	0.000	***	0.176
	83-year-old	LAI	0.168	0.045	3.710	0.000	***	0.209
	∞	REW	-0.143	0.034	-4.253	0.000	***	0.148
		VPD	-0.125	0.063	-1.981	0.049	*	0.191
4	_	Intercept	0.000	0.025	0.000	1.000		
GEP	-old	Tair	0.589	0.065	9.096	0.000	***	0.340
	ear	LAI	0.127	0.061	2.089	0.038	*	0.262
	48-year-old	Rn	0.157	0.044	3.558	0.000	***	0.223
	4	REW	-0.145	0.038	-3.849	0.000	***	0.175
	plo	Intercept	0.000	0.044	0.000	1.000		
	.r-0	Tair	0.807	0.088	9.141	0.000	***	0.511
	20-year-	REW	-0.216	0.067	-3.21	0.002	**	0.271
	20.	LAI	-0.188	0.082	-2.293	0.023	*	0.217
	pld	Intercept	0.000	0.040	0.000	1.000		
WUE	83-year-old	Tair	1.293	0.096	13.445	< 2e- 16	***	0.595
	83-	Rn	-0.249	0.068	-3.655	0.000	***	0.174

Ph.D. Thesis – E. Arango Ruda McMaster – School of Earth, Environment & Society

	LAI	-0.298	0.082	-3.631	0.000	***	0.231
	Intercept	0.000	0.043	0.000	1.000		
48-year-old	Tair	1.299	0.112	11.602	< 2e- 16	***	0.539
yea	Rn	-0.270	0.076	-3.537	0.001	***	0.152
-84	LAI	-0.197	0.105	-1.877	0.062	•	0.214
	REW	0.134	0.065	2.054	0.042	*	0.096
-5	Intercept	-0.005	0.051	-0.093	0.926		
20-year-old	Tair	1.269	0.113	11.181	< 2e- 16	***	0.663
0-y	Rn	-0.331	0.098	-3.393	0.001	***	0.163
72	LAI	-0.336	0.104	-3.244	0.001	**	0.174

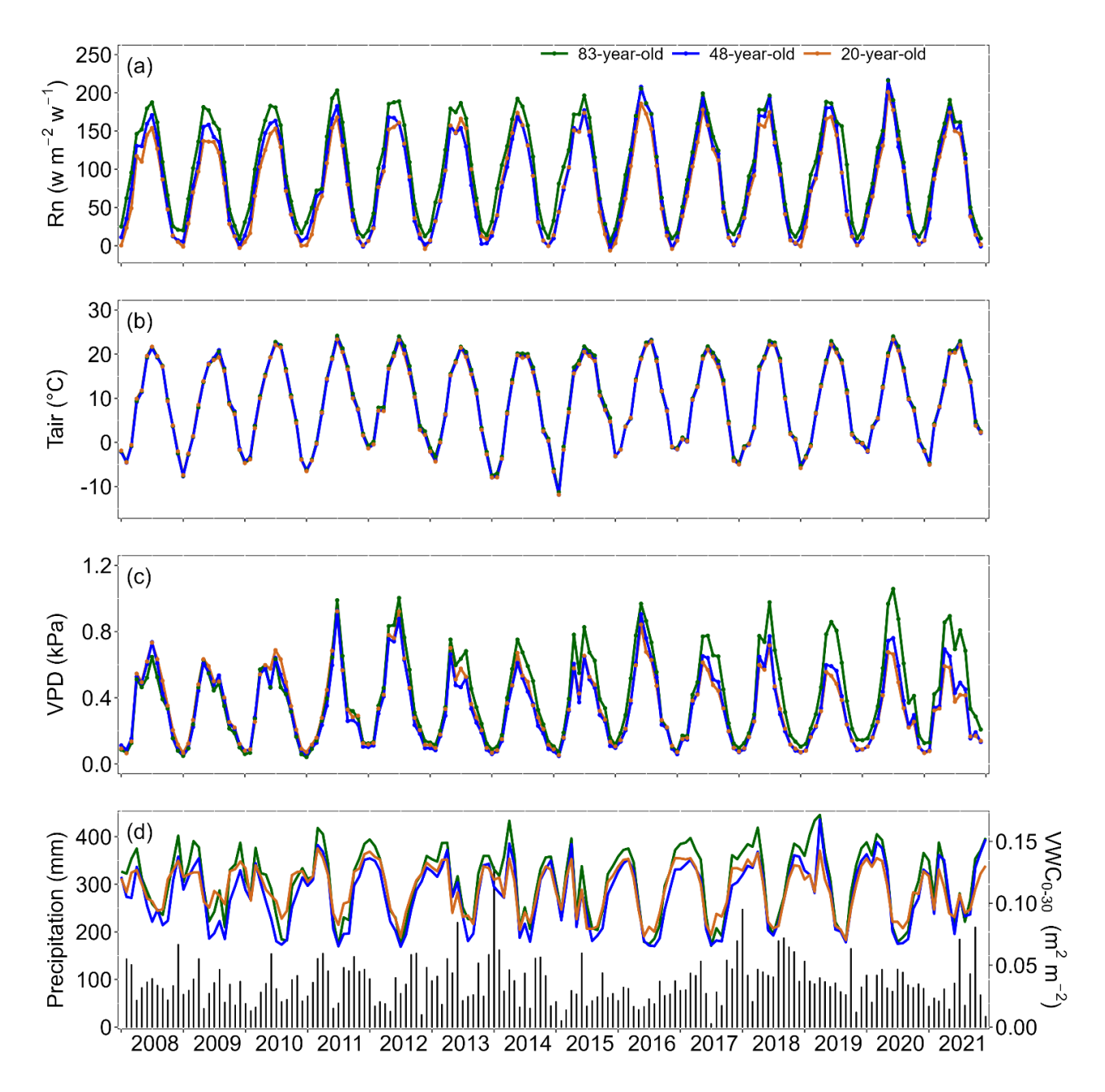


**Figure 3.1**: Inter-annual variability (2008–2021) of monthly averages of net radiation (Rn), air temperature (Tair), vapor pressure deficit (VPD), relative extractable water (REW) and monthly total precipitation (P).

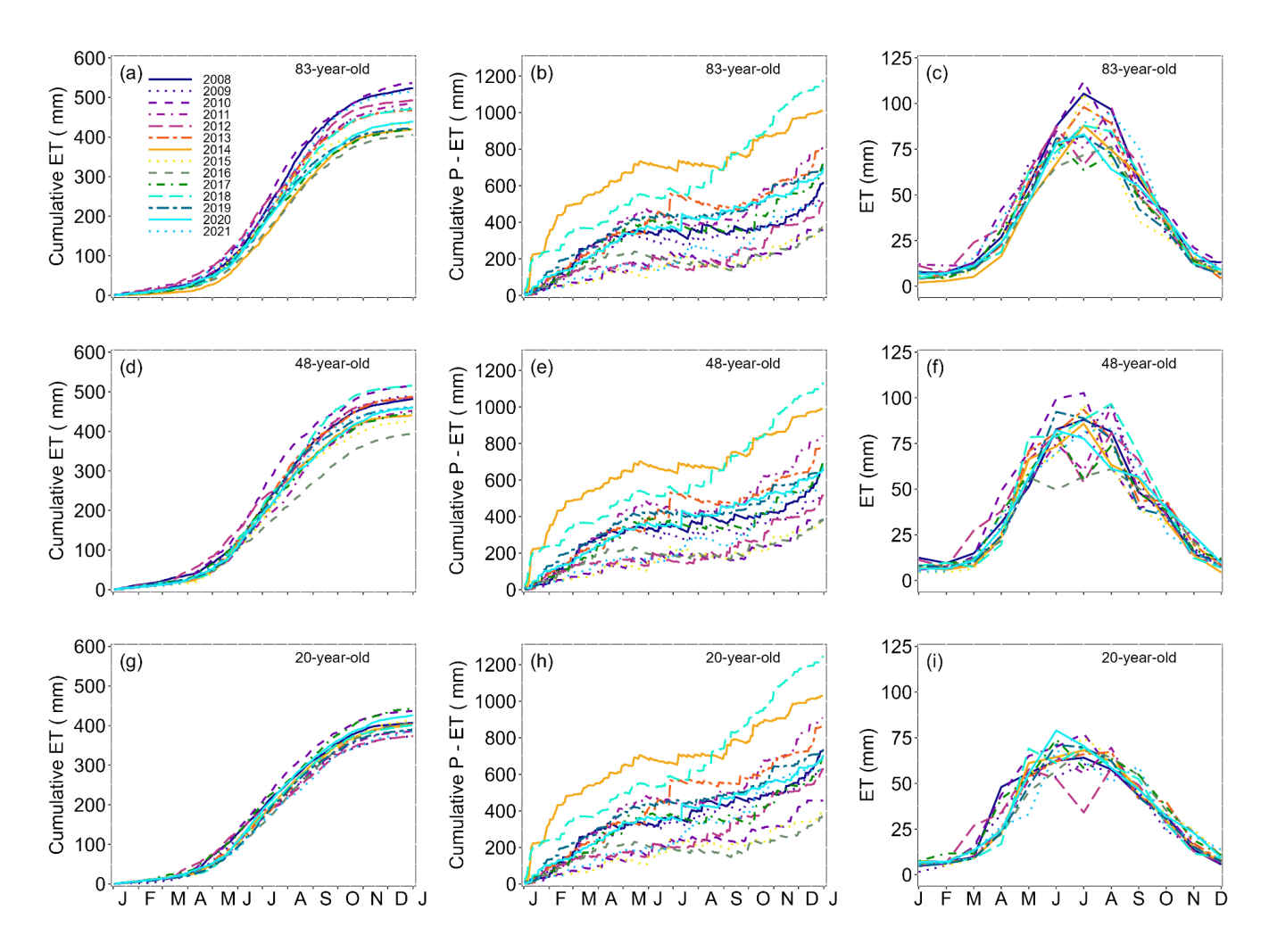


**Figure 3.2**: Cumulative daily values of evapotranspiration (ET), runoff plus infiltration (P-ET) and monthly total ET in mm for the 84-Year Conifer (a-c), 49-Year Conifer (d-f) and 21-Year Conifer (g-i) from 2008 to 2021.

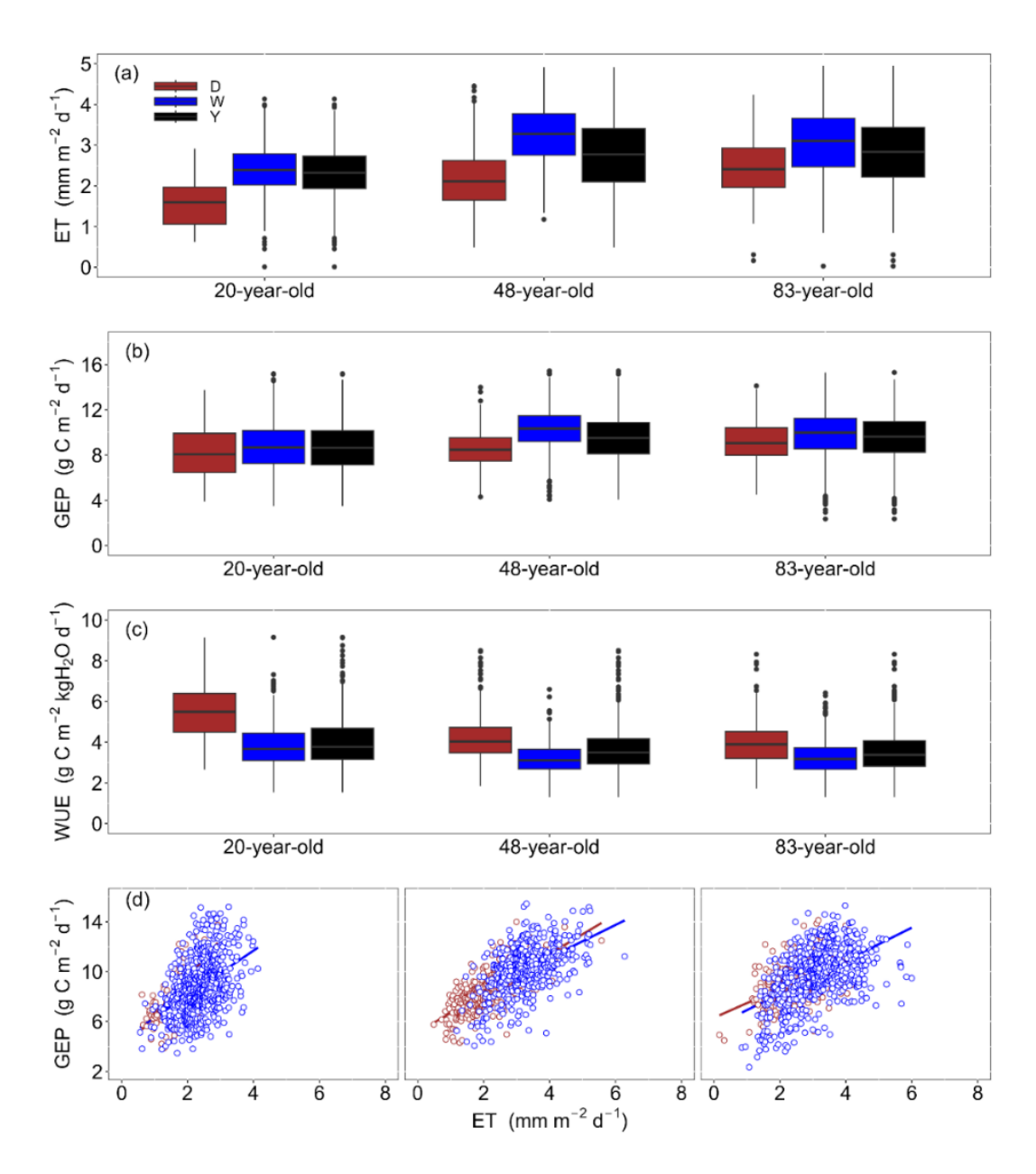


**Figure 3.3**: Comparison of (a) daily evapotranspiration (ET), (b) gross ecosystem productivity (GEP) and (c) water use efficiency (WUE) under Wet (REW0-30 > 0.4) and Dry (REW0-30  $\leq$  0.4) conditions for the 20-Year Conifer, 48-Year Conifer and 83-Year Conifer when Tair $\geq$ 15C, PAR $\geq$ 500 µmmol and VPD $\geq$ 0.5 kPa for gap-filled values. The Wilcoxon signed-rank test indicated significant difference in ET, GEP, and WUE for dry and wet conditions at all the sites. (d) The coupling between GEP and ET, WUE, is better explained by ET rather than GEP at the three sites (ET $_{lmg83}$  = 0.8, ET $_{lmg48}$  = 0.8, ET $_{lmg20}$  = 0.6).

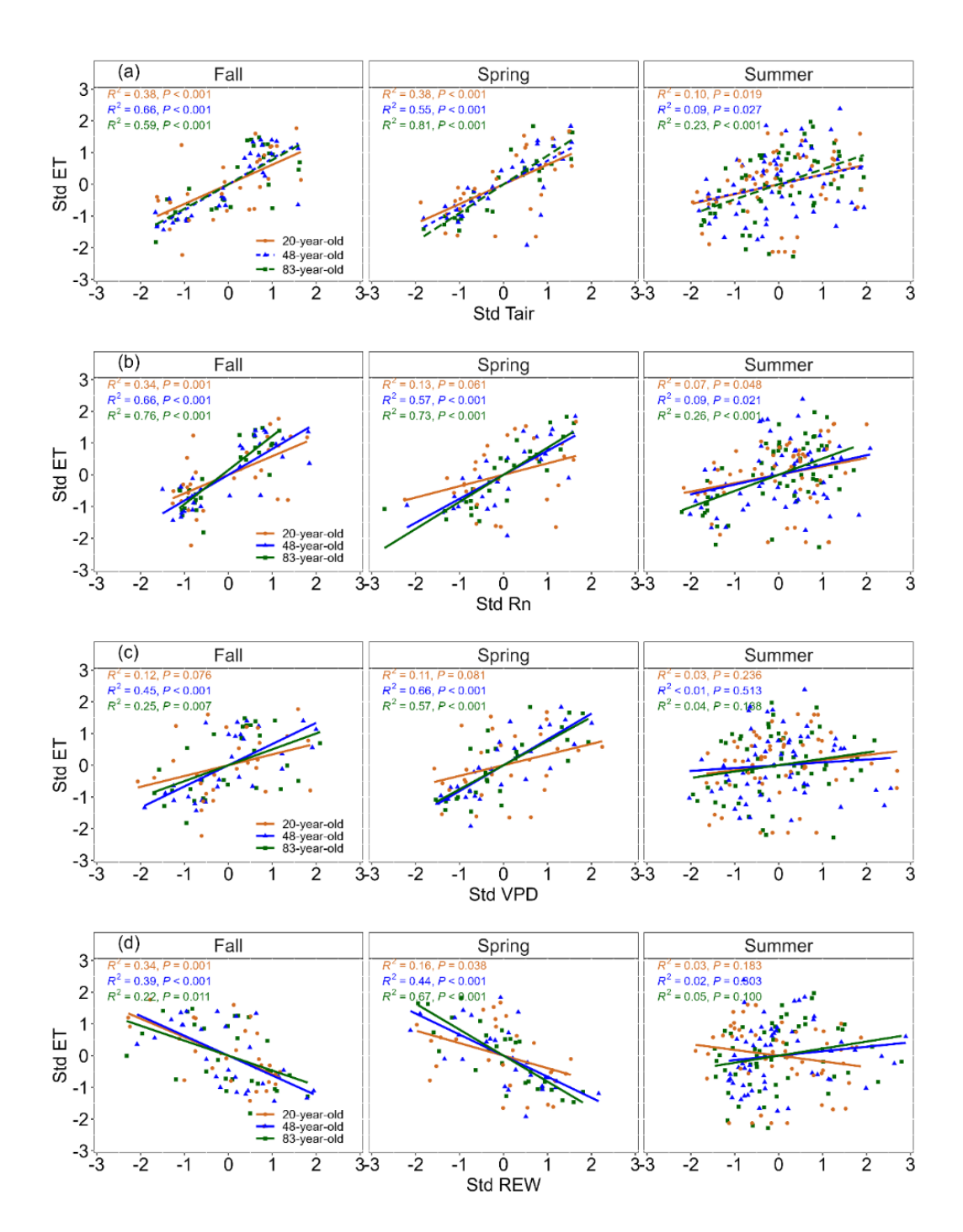


**Figure 3.4**: Sensitivity of ET to environmental variables. Correlations between standardized monthly evapotranspiration (ET) and (a) monthly standardized net radiation (Rn), (b) monthly standardized air temperature (Tair), (c) monthly standardized vapor pressure deficit (VPD), and (d) monthly standardized relative extractable water (REW) in spring (AM), summer (JJAS) and autumn (ON) in the 83-, 48-, and 20-Year Conifer using gap ET and gap GEP.

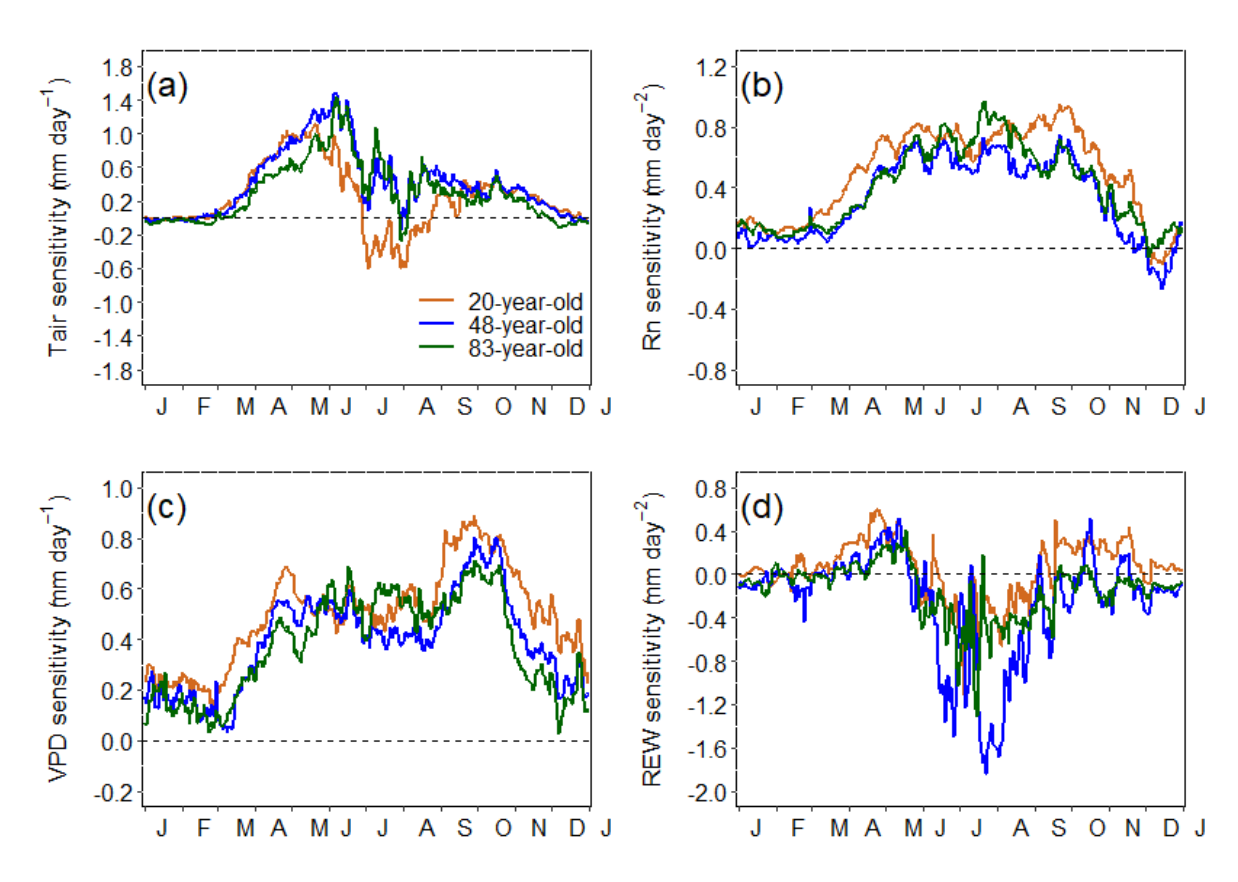


**Figure 3.5**: Daily sensitivities of evapotranspiration to air temperature (a), net radiation (b), vapor pressure deficit (c) and relative extractable water (d) in the 83-, 48-, and 20-Year Conifer using gap filled ET (using day and night values). Curves show the mean sensitivity in the 15 day moving windows. Data were standardized to remove forest growth and long-term climate variability impacts. When the flux vs climate variable correlation for 15 day moving averages was significant (p < 0.05), the slope of the regression showed the effect of climate constraints on the water use of the forests following Schwalm et al. 2010 and Wu & Chen 2013. The response in GEP can be found at Arain et al., 2022.

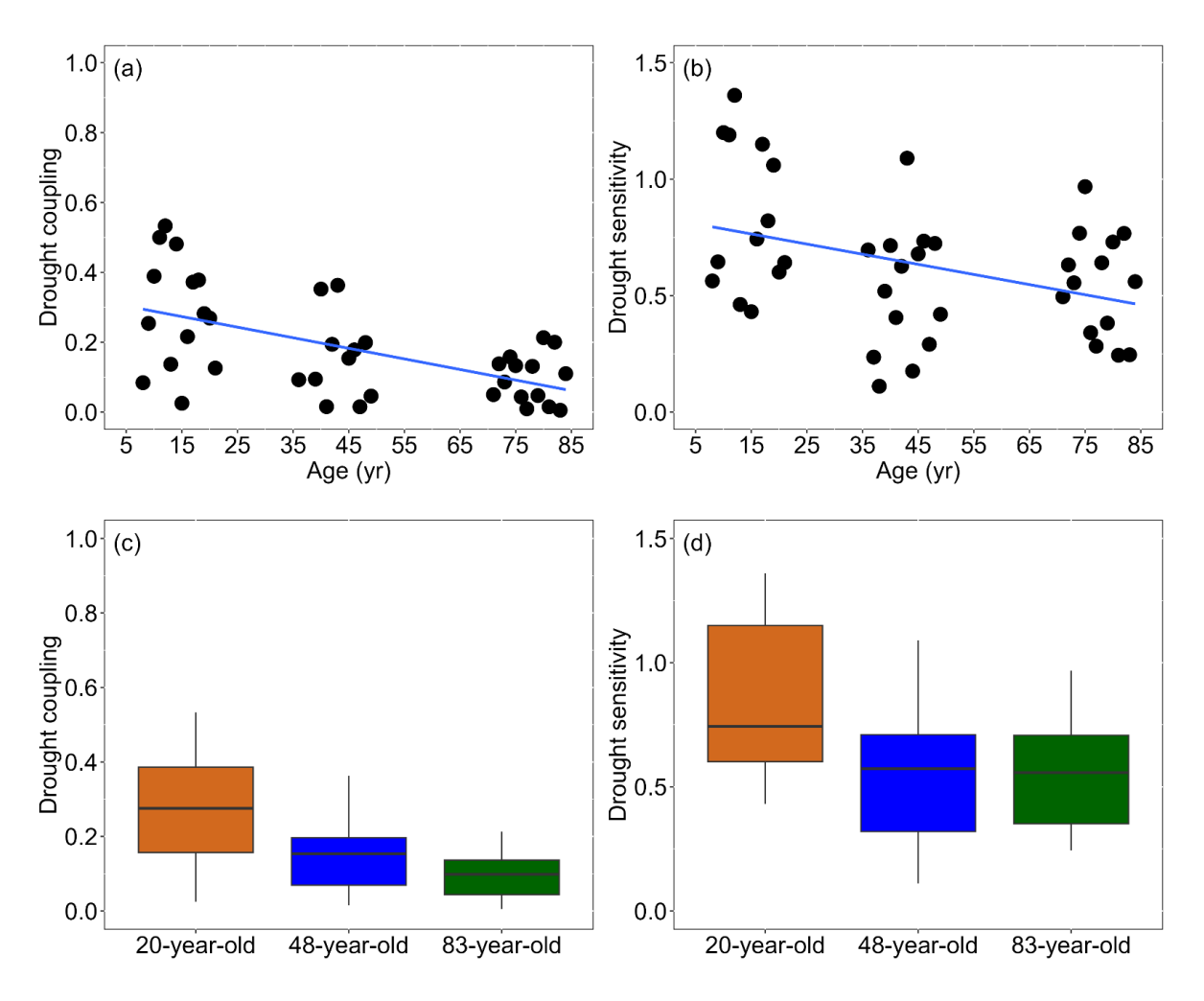


**Figure 3.6**: Forest evapotranspiration (ET) sensitivity to drought as a function of age. (a-b) Drought coupling is expressed as the percentage of explained variation (R<sup>2</sup>). (c-d) Drought sensitivity is expressed as the summed absolute values of standardized coefficients of drought variables regressed against evapotranspiration (ET) as a function of daily VPD, soil moisture (SM) and their interaction. The drought coupling and sensitivity were both obtained for each year.

**Table S3.1:** Contribution of ET and GEP to WUE. Multivariate regression analysis regressing daily standardized WUE against the explanatory variables, including daily standardized ET and daily standardized GEP. Significance code are: [0-0.001] = '\*\*\*'; (0.001-0.01] = '\*\*'; (0.01-0.05] = '\*'; (0.05-0.1] = '.'; (0.1-1] = '.'. The relative importance (lmg) of each predictor variable in explaining the variability in WUE is also shown.

	Forest	Regressor	Estimate	Std. Error	t Value	Pr(> t )	Significance	lmg
	<b>.</b>	Intercept	0.000	0.015	0.000	1.000		
	Year ifer	ET	-0.877	0.018	-49.450	<2e-16	***	0.779
	83-Year Conifer	GEP	0.573	0.018	32.300	<2e-16	***	0.221
더		Intercept	0.000	0.011	0.000	1.000		
WUE	8-Year onifer	ET	-1.165	-1.165	-78.070	<2e-16	***	0.821
	48-, Con	GEP	0.694	0.015	46.48	<2e-16	***	0.179
		Intercept	0.000	0.010	0.000	1.000		
	20-Year Conifer	ET	-0.965	0.011	-85	<2e-16	***	0.612
		GEP	0.827	0.011	72.86	<2e-16	***	0.388

**Table S3.2:** ET, GEP and WUE show significant differences during dry and wet conditions. Results for the non-parametric Wilcoxon signed-rank test to test for difference in ET, GEP, and WUE between dry and wet conditions.

Site	ET (mm	)	GEP		WUE		
Site	W p-value		W	p-value	W	p-value	
83-Year Conifer	135509	< 2.2e-16	112972	0.000	55546	< 2.2e-16	
48-Year Conifer	132970	< 2.2e-16	117617	< 2.2e-16	32245	< 2.2e-16	
20-Year Conifer	46165	0.000	31319	0.019	8756	0.000	

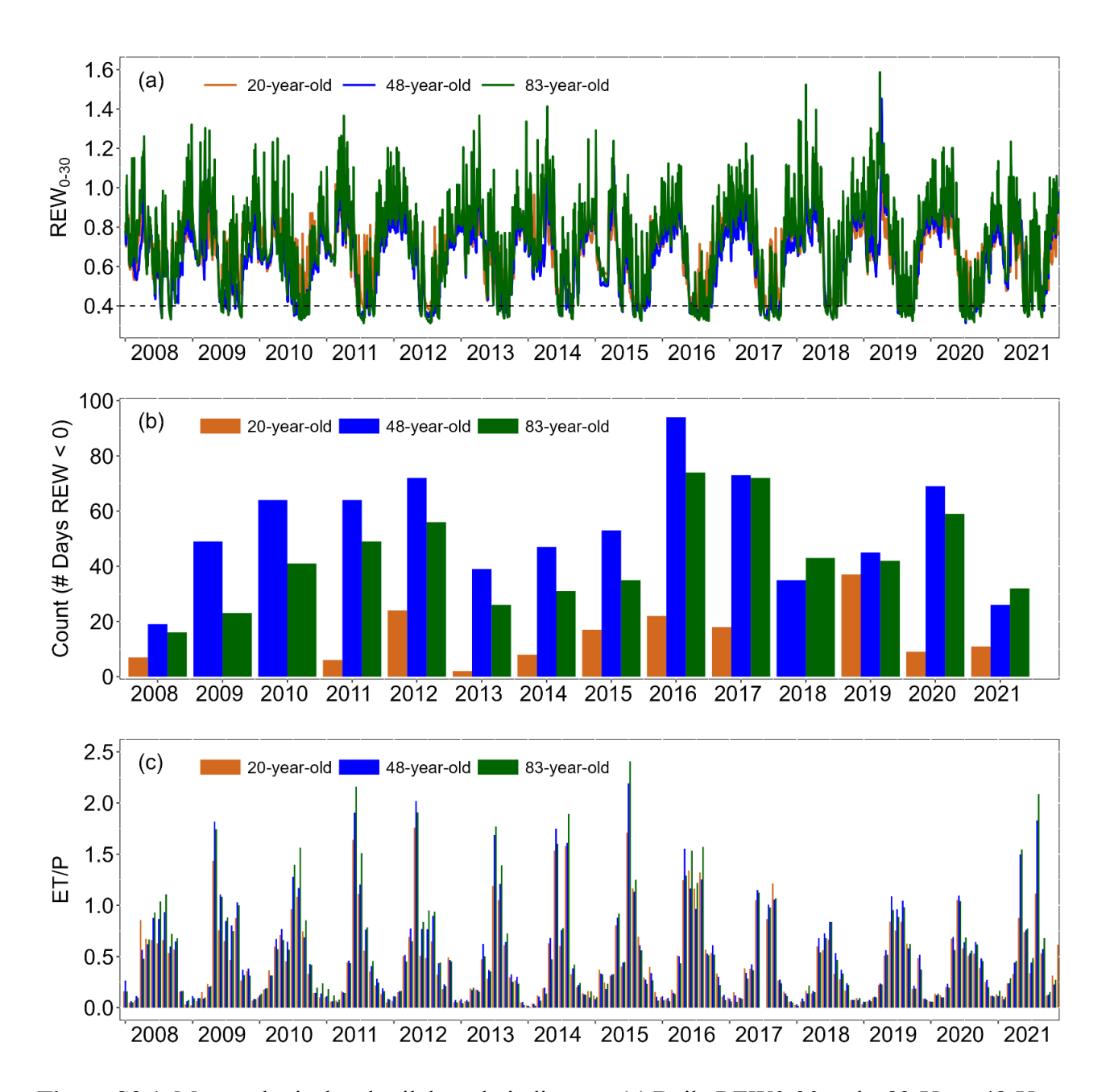


**Figure S3.1**: Meteorological and soil drought indicators. (a) Daily REW0-30 at the 83-Year, 48-Year, and 20-Year stand; (b) Bars represent the number of days per year when REW0-30 was lower than 0.4; (c) Monthly ratio of ET to P calculated from 2008 to 2021.

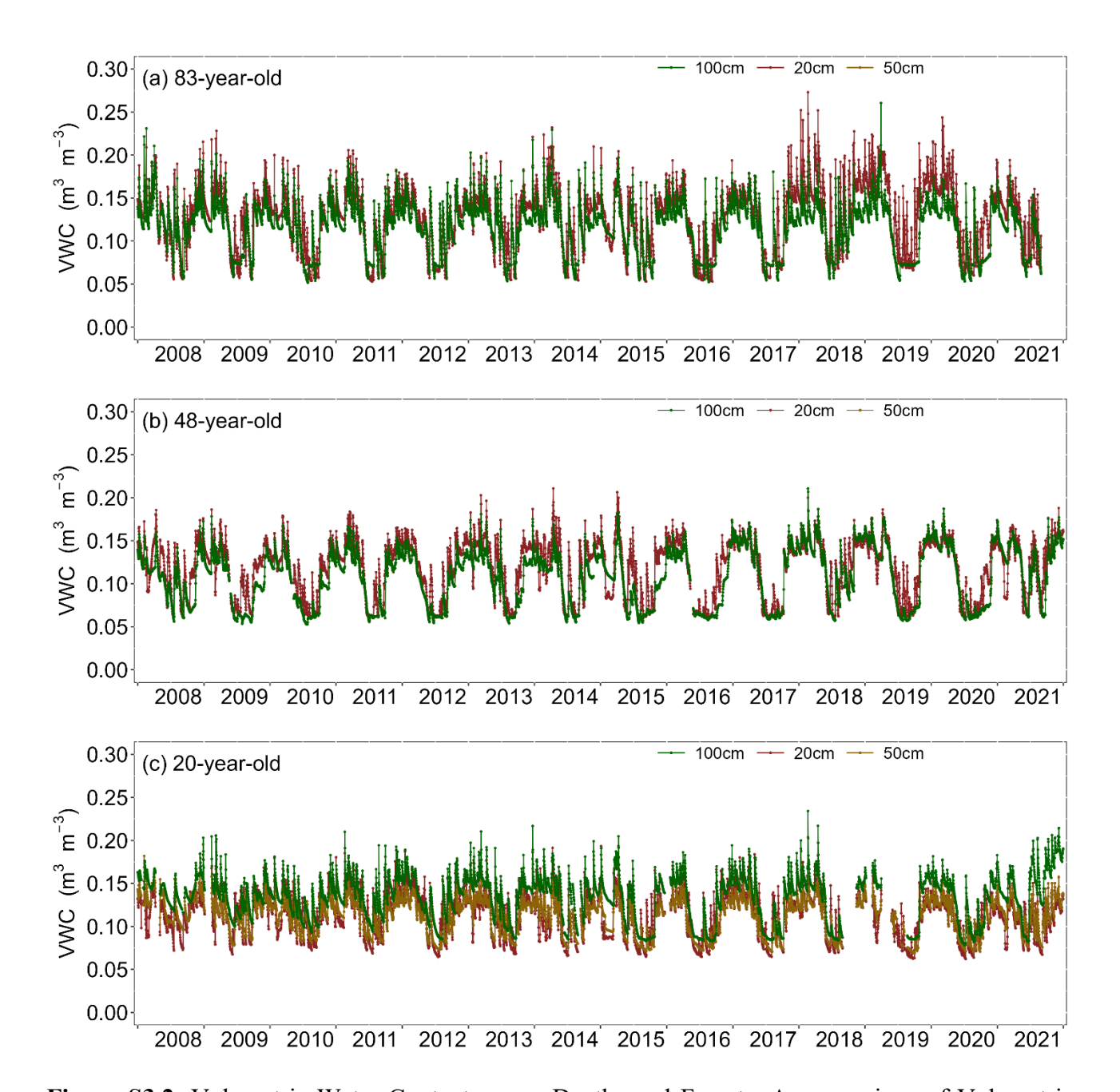


**Figure S3.2**: Volumetric Water Content across Depths and Forests. A comparison of Volumetric Water Content (VWC) at three soil depths (20 cm, 50 cm, and 100 cm) for the (a) 83-year-old coniferous forest, (b) 48-year-old coniferous forest, and (c) 20-year-old coniferous forest.

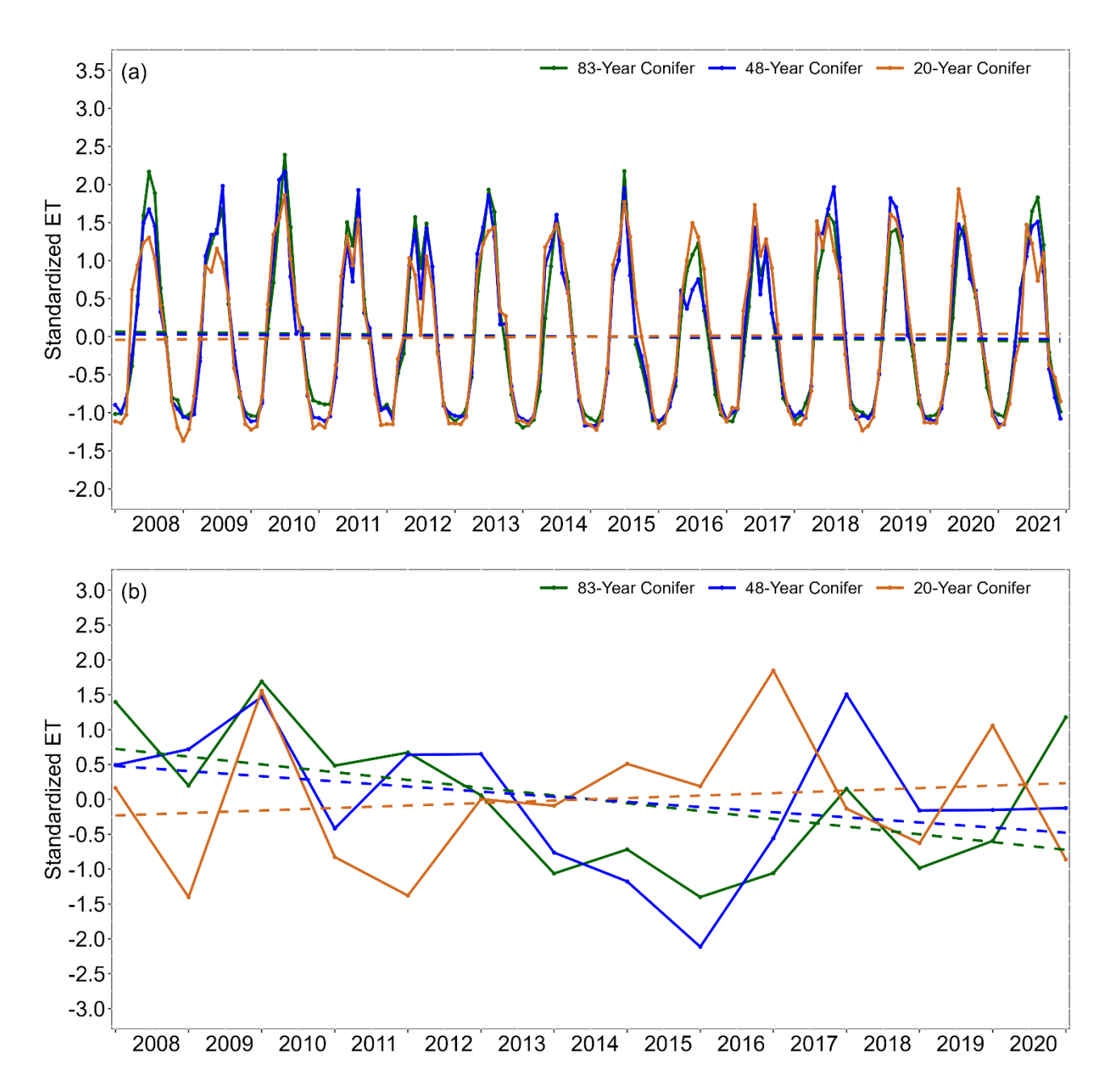


**Figure S3.3**: Trend in evapotranspiration over the years. (a) Trend of standardized monthly evapotranspiration (ET) across a age sequence of white pine coniferous forest for the 2008 to 2020 period; (b) Trend in standardized yearly evapotranspiration (ET) across a age sequence of white pine coniferous forest for the 2008 to 2020 period.

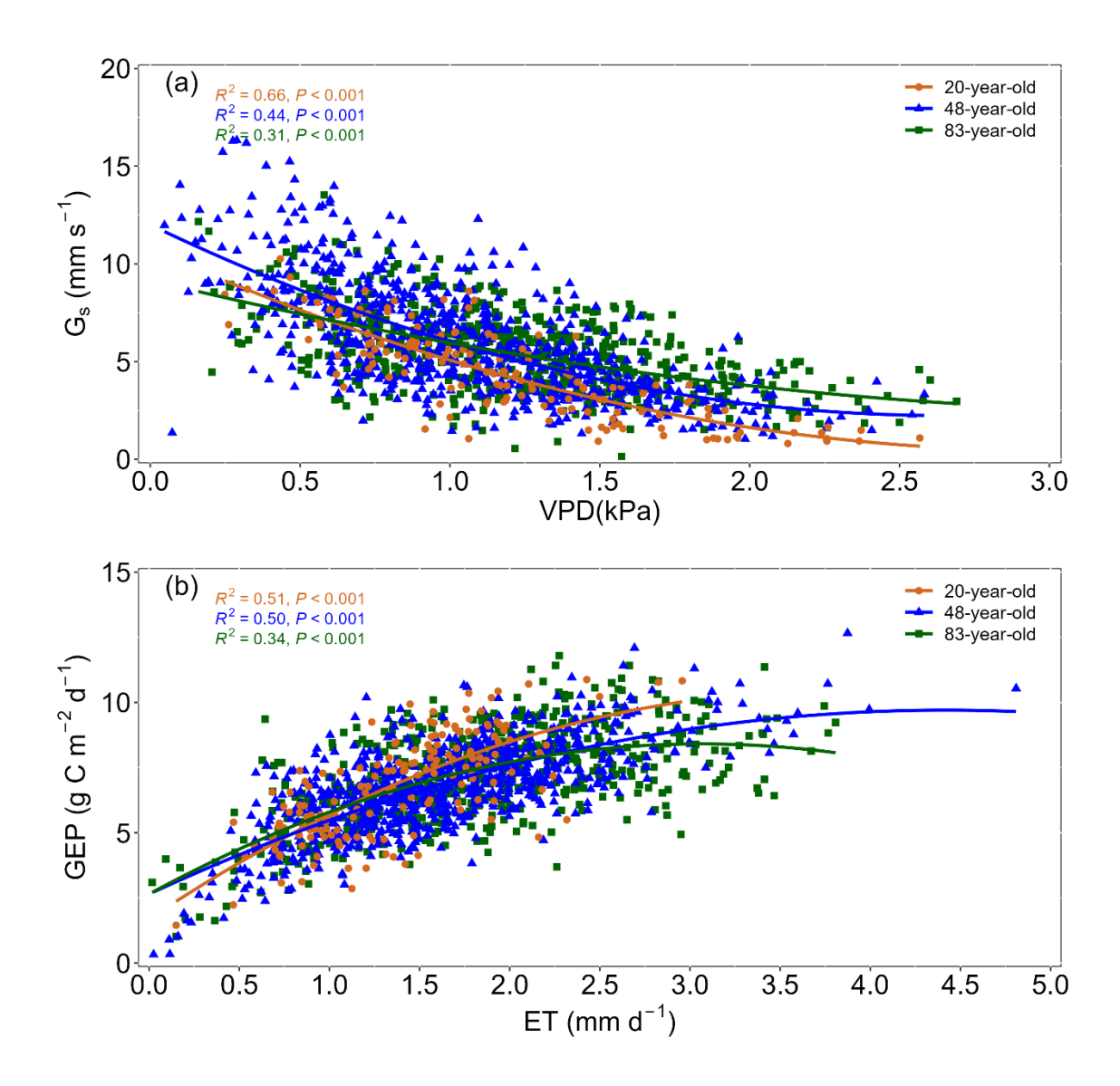


**Figure S3.4**: Physiological process on three white pine temperate forests of different age. (a) Relationship between daytime mean (9:00 to 16:00, PPFD > 200  $\mu$ mol m<sup>2</sup> s<sup>-1</sup>) values of bulk surface conductance Gs and VPD for rain-free and REW  $\leq$  0.4 periods using data from 2008 to 2021. (b) Daily mean gross ecosystem productivity (GEP) vs evapotranspiration (ET) for 2008 to 2021 period when REW  $\leq$  0.4.

## **CHAPTER 4:**

# EVALUATING HYSTERESIS PATTERNS IN SAP FLOW OF A RED PINE FOREST SUBJECTED TO DIFFERENT VARIABLE RETENTION HARVESTING TREATMENTS

## 4.1 Abstract

Forests significantly influence regional and global water cycles through transpiration, which is affected by meteorological variables, soil water availability, and stand and site characteristics. Variable Retention Harvesting (VRH) is a forest management practice designed to enhance forest growth, improve biodiversity, preserve ecosystem function, and provide economic revenue from harvested timber. Application of VRH treatment in forest ecosystems can potentially impact the response of forest transpiration to environmental controls. This study analyzed the impacts of four different VRH treatments on sap flow velocity (SV) in an 83-year-old red pine (*Pinus resinosa* Ait.) plantation forest in the Great Lakes region in Canada. These VRH treatments included 55% aggregated (55A), 55% dispersed (55D), 33% aggregated (33A), 33% dispersed (33D) basal area retentions, and an unharvested control (CN) plots, one hectare each. Analysis of counterclockwise hysteresis loops between SV and meteorological variables showed larger hysteresis loop areas between SV and photosynthetically active radiation (PAR) compared to vapor pressure deficit (VPD) and air temperature (Tair), particularly in the summer due to clear sky and warm temperatures. Overall, the results showed that PAR was the primary control on half hourly and daily SV across VRH treatments, followed by Tair at daily timescale and VPD at half hourly timescales. The larger hysteresis loop areas and higher SV values were observed in the CN and 55D treatments, followed by 55A, 33D, and 33A plots. This finding suggested that dispersed retention of 55% basal area (55D) is the optimal forest management practice that can be utilized to enhance transpiration and forest growth. These findings will help forest managers and other stakeholders to adopt the best forest management practices to enhance forest growth, water use efficiency, and resilience to climate change.

## 4.2 Introduction

Forests cover more than 31% of the Earth's surface and have a crucial role in the global water and energy cycles (Bonan, 2008). Transpiration, which is the primary way for plants to release water through stomata into the atmosphere, influences the local climate and precipitation patterns (Bonan, 2015; Ellison et al., 2017). It also significantly affects biogeochemical cycles and other forest characteristics (Bonan, 2008; Jasechko et al., 2013; Schlesinger & Jasechko, 2014; Wang & Dickinson, 2012). Therefore, accurate understanding of forest transpiration is essential for determining the forest water budget (David et al., 2004; Ma et al., 2017) and water resources management. It is also important to evaluate the impacts of climate change on forest ecosystem and develop sustainable and climate tailored forest management practices that can help to provide nature based climate solutions by enhancing forest carbon uptake (Boggs et al., 2015; Ma et al., 2017)

One of the most widely used methods to quantify transpiration from forests is the sap flow thermal dissipation method developed by Granier in 1985. With this method sap flow velocity is measured, then is converted to transpiration at the tree level, and can be then upscaled to stand level using forest basal area (Wilson et al., 2001). Quantification of sap flow is also beneficial to understand the effect of forest structural changes such as thinning or natural die off on water balance. It also helps to understand and identify the physiological regulations or major controls of transpiration, which is essential to gain insight into the role of transpiration in forest hydrology and water budgets (Boggs et al., 2015). Previous studies in the literature have indicated that meteorological factors, such as

photosynthetic active radiation (PAR), air temperature (Tair) and vapor pressure deficit (VPD) are the primary controls of sap flow or transpiration in individual trees (Bovard et al., 2005; Deng et al., 2021; Ma et al., 2017; Wever et al., 2002), especially in energy-limited environments. Conversely, studies in water-limited environments have highlighted the importance of soil moisture on the response of sap flow to environmental variables (Brinkmann et al., 2016; Hassler et al., 2018; Zhao et al., 2017). However, there is a need to conduct more in-depth studies of forest transpiration and its governing factors, particularly in temperature regions which are increasingly experiencing water stresses due to climate change and extreme weather events (Arain et al., 2022) to better understand and manage water resources in these regions.

Most forests in the eastern North American temperate region are either planted or naturally regenerated under some form of management (Bonan, 2008). In these forests, tree composition, age, density as well as application of specific management practices can significantly impact the sap flow and its response to environmental factors, thereby affecting the overall water balance (Bodo & Arain, 2022). For example, harvesting or thinning of closely packed forest canopies may reduce competition for light, water and nutrients and may promote enhanced growth in the remaining trees (Park et al., 2018). This practice also leads to an increase in the transpiration of remaining trees, particularly in cases where there is an increase in radiation, temperature, vapor pressure deficit, wind speed and soil water content (Bladon et al., 2006; Boggs et al., 2015; del Campo et al., 2022; Park et al., 2018). Bodo and Arain (2022) and Hussain et al. (2024) have observed distinctive sap flow and forest growth patterns in red pine trees subjected to various Variable Retention Harvesting (VRH) treatments. This silvicultural practice has potential to be widely used because it aims to retain different proportions and arrangements of canopy trees across a harvested area, mimicking the impact of natural disturbances on stand structure to enhance the forest growth and resilience to environmental stresses

(Bodo & Arain, 2022; Hussain et al., 2024; Zugic et al., 2021). However, there is a need to conduct more in-depth studies at fine temporal resolutions to fully understand the impact of different VRH regimes on sap flow in plantation or managed forests. Such studies will help to accurately estimate transpiration at different spatial and temporal scales and to develop sustainable and climate adapted forest management practices.

Understanding the impact of environmental controls on sap flow can be achieved by studying hysteresis processes. Hysteresis is a natural phenomenon observed across several plant species across different ecosystems (Su et al., 2022; Wang et al., 2019; Wan et al., 2024; Ewers et al., 2005; Zeppel et al., 2004; Gimenez et al., 2019). Hysteresis loops indicate that the relationship between environmental variables and sap flow is not a straightforward, direct relationship but rather one that involves time delays and disequilibrium (Zeppel et al., 2004). While previous studies have examined the impact of environmental controls on sap flow in plantation forests (Ma et al., 2017; Zhao et al., 2017), to our knowledge, there is no study in the literature that has evaluated the hysteresis responses of sap flow in trees under various plantation densities or forest management regimes such as VRH, across different temporal scales, including hourly and daily. Analyzing hysteresis of sap flow and hence transpiration can provide valuable insights into the complex interactions between forest ecosystems and the environment, which is crucial for understanding forest water dynamics and resilience in the face of climate change.

In this study, we measured sap flow in 2023 in an 83-year-old red pine (*Pinus resinosa* Ait.) plantation forest in the Great Lakes region in Canada, where variable retention harvesting (VRH) had been applied to assess their effectiveness in enhancing forest growth, water use and carbon uptake. The VRH experiment consisted of four treatments including a 55% dispersed retention (55D), a 55%

aggregate retention (55A), a 33% dispersed retention (33D), and a 33% aggregate retention (33A) of the basal area, and an unharvested control (CN) (Bodo & Arain, 2022; Zugic et al., 2021). The main goal of our study was to understand the seasonal dynamics of sap flow and its responses to environmental stresses within the context of VRH. The specific objectives of our study were to (1) examine hysteresis patterns in the sap flow velocity in response to major environmental factors such as PAR, Tair, VPD and soil water stress in each VRH treatment, (2) investigate seasonal variations in sap flow velocities among different treatments and (3) evaluate which VRH treatment may be most effective in sustaining forest evaporative demand under environmental stresses that are expected to become more severe and frequent in the future due to climate change. By accounting for time lags between sap flow velocity and environmental variables, we can more accurately estimate canopy transpiration across VRH treatments, minimizing errors in transpiration estimates.

#### 4.3 Methods

## 4.3.1 Study Site

This study was carried out in a temperate red pine (*Pinus resinosa* Ait.) plantation forest hereafter called TP31 due to the year of its establishment in 1931 at the St. Williams Conservation Reserve (SWCR) in Southern Ontario, Canada (Figure 4.1). The plantation covers an area of 21 hectares and was established by placing seedlings 2 meters apart in furrowed rows, with around 2500 trees per hectare. The plantation underwent thinning in the early 1960s, which reduced the stand density to about 1875 trees ha<sup>-1</sup>. In 2014, the Ontario Ministry of Natural Resources and Forestry (OMNRF) conducted a variable retention harvesting (VRH) experiment to evaluate the effectiveness of five different VRH treatments in promoting the natural succession and restoration of these plantations to native forest ecosystem, as well as in enhancing their resilience to climate change. The VRH

treatments were applied to 1-hectare plots with four replicates, each with different harvesting densities and patterns and un-harvested control as described earlier in Bodo and Arain (2022); Hussain et al., 2024; Zugic et al., 2021) and shown in Figure 1 and summarized in Table 4.1.

The topography of the site is predominantly flat, with an elevation of 184 meters. The soil is well-drained and sandy, and the climate is temperate (cool continental), with warm, humid summers and cold winters. The 29-year (1991-2020) average annual temperature is 8.4°C, and the average annual precipitation is 965 mm, with about 13% of it falling as snow, as reported by the Environment and Climate Change Canada weather station in Delhi, Ontario. This station is located approximately 20 km northwest of the study sites (Environment and Climate Change Canada (ECCC), 2023).

Red pine is a widely planted evergreen tree species in eastern North America, particularly near the Great Lakes and St. Lawrence River. It can grow as tall as 37 meters with straight logs which are commonly used as electrical poles in the region (Moore, 2002). Red pine cannot tolerate shade and typically grows as even-aged stands (Gilmore & Palik, 2023). The species is useful in restoring abandoned agricultural land as it is part of the original native plant community in the region (Palik and Kastendick, 2023).

Using traditional methods, around 20% of the trees at each plot were measured yearly for their DBH and height. The DBH of red pine trees ranged from 11.7 to 90.4 cm as of 2023, and their heights varied from 8.9 to 33.8 m as of 2014. The trees had a mean height of 21.6 m  $\pm$  5 m and an average DBH of  $30.9 \pm 8.3$  cm.

# 4.3.2 Sap Flow Measurements

Sap flow sensors were installed in at least four trees within each VRH treatment and the control plot. Trees were selected based on their overall health, such as full crown and undamaged bark, their proximity (less than 30 m away) to the data logger and power supply. The sensors were self-manufactured, Granier-style thermal-dissipation (TDP) sensors, following the guidelines given in Bodo & Arain (2021), Matheny et al. (2014), Pappas et al., (2018), and Peters et al., (2018). Each sensor consisted of two hollow needles, each 20 mm long, with a fine-wire, type T thermocouple at the midpoint (10 mm) of each needle. One of the needles was wrapped with insulated, constant wire, which provided constant heating when connected to the self-made circuit board and supplied 12 V power. The heated and non-heated needles were coated with thermal grease and inserted into a hollow metal tube on the north side of the tree at breast height (1.3 m above the ground), with a spacing of 10 cm (Bodo and Arain, 2022; Su et al., 2022). They were installed on the north side of the trees to avoid radiation loading and reduce errors in sap flow (Moon et al., 2015; Peters et al., 2018). In addition, spherical foam was placed around the probes and then tree trunks were wrapped with aluminum foil to reduce the effects of solar radiation and exposure to precipitation.

The raw measurements were made in millivolts (mV) and saved every 15 minutes using CR10X and CR23X dataloggers (Campbell Scientific Inc.). The data was collected continuously from January 1, 2023, to December 31, 2023, and then averaged into hourly intervals. However, some gaps occurred in the data during the growing season due to sensor failure and power interruptions. A time series of raw measurements was computed as the mean values measured in all the trees in each VHR treatment, resulting in a representative time series per treatment (Table 4.1).

Based on the temperature difference between the two probes, a dimensionless flow index (K) was calculated following Granier (1985, 1987) as follows:

$$K = \frac{\Delta V_{max} - \Delta V}{\Delta V} \tag{7}$$

where V represents the measured voltage (mV) and  $\Delta V$  (mV) is the measured voltage difference between the two probes. K values were calculated by determining pre-dawn zero-flow conditions calculated every 24 hours. Using the dimensionless variable K, sap flow velocity, SV (cm h<sup>-1</sup>) was calculated as:

$$SV = 0.0119 x K^{1.231} x 3600 (8)$$

Transpiration (T) for each individual tree was calculated as:

$$T_i = \rho_w x \, SV_i \, x \, (\frac{A_{si}}{A_{wi}}) \tag{9}$$

Where i denotes the individual sample tree,  $\rho_w$  is the density of water (kg m<sup>-3</sup>), BA is the stand basal area (m<sup>2</sup>) and  $\frac{A_{si}}{A_{wi}}$  is the ratio of sapwood area to tree wood area measured at DBH. Sapwood area (Asi) was calculated according to the equation described by Bodo and Arain (2021) as follows:

$$A_s(m^2) = 0.189 \, x \, DBH_i^{2.35} \tag{10}$$

where As is the sapwood area (m<sup>2</sup>) of tree i and 0.189 and 2.35 are site-specific parameters derived through tree cores taken from trees at this site by Bodo & Arain (2022).

Finally, stand-level transpiration per unit ground area (T, mm h<sup>-1</sup>) was calculated as

Ph.D. Thesis – E. Arango Ruda McMaster – School of Earth, Environment & Society

$$T = \frac{\sum_{i=1}^{n} T_i}{n} \times BA \tag{11}$$

Where n denotes the number of trees sampled in each plot and BA is the stand basal area (m<sup>2</sup>).

# 4.3.3 Meteorological Measurements

The micrometeorological measurements were made in a similar age white pine (*Pinus strobus*) plantation forest (CA-TP39, also known as CA-TP4 in the AmeriFlux network) adjacent (northside) to this red pine forest. This tower has been equipped with closed-path eddy-covariance system and weather station, which have enabled continuous measurements of half-hourly energy, water and carbon fluxes and meteorological variables including four components of radiation, photosynthetically active radiation, air temperature, humidity, wind speed and direction, soil temperature, and soil moisture at several depths (2, 5, 10, 20, 50 and 100 cm) since 2003 (Arain, 2018; Arain et al., 2022).

Precipitation data was collected using an accumulation rain gauge (Geonor Inc. model T200B) and a tipping-bucket rain gauge (Texas Inst. model TE525) in an open area in the south of red pine site. To ensure data accuracy, the precipitation measurements were cross validated with data obtained from the weather station in Delhi, Ontario, operated by Environment and Climate Change Canada (ECCC) (2023). All meteorological and soil data were averaged at half-hour intervals.

Based on the soil moisture measurement taken at TP39 site, the relative extractable water (REW) was calculated to classify the soil moisture stress. REW was calculated following the method described by Arain et al. (2022), Black (1979) and Bréda et al. (1995), as:

$$REW = \frac{\theta - \theta_{wp}}{\theta_{fc} - \theta_{wp}} \tag{14}$$

Where  $\theta$  is the measured soil water content in  $m^3$   $m^{-3}$  for the 0-30 cm soil layer,  $\theta_{wp}$  is the soil volumetric soil water content at wilting plant point (0.01  $m^3$   $m^{-3}$ ), and  $\theta_{fc}$  is the volumetric soil water content at field capacity (0.16  $m^3$   $m^{-3}$ ). The expression  $\theta_{fc}$  -  $\theta_{wp}$  is the difference between the soil water reserve at field capacity and the permanent wilting point. A dry period or drought was considered when REW was  $\leq$  0.4 (Granier et al., 2007; Vilhar, 2016).

# 4.3.4 Statistical Analysis

The statistical analysis of data consisted of two steps. First, the relationship between sap flow velocity (SV) and environmental (e.g. PAR, Tair, VPD) and soil water status (REW) was explored in different VRH treatments at hourly and daily timescales using multiple linear regression (MLR) and principal component analysis (PCA). Before conducting this analysis, the multicollinearity among predictor variables was assessed through variance inflation factor (VIF) in different treatments (Lumley, 2020). Once the optimal model was selected, the multivariate regression analysis was conducted using standardized (z-scored) variables for PAR, Tair, VPD and REW. Standardization allowed for a quantitative comparison of the regression coefficients (Clogg et al., 1995). Furthermore, the relative significance of each variable was identified using the "relaimpo" package in R (Groempings, 2021). Second, the seasonal hysteresis patterns of sap flow velocity were analyzed for each VRH treatment for given environmental conditions such as high/low values of PAR, Tair, VPD and REW.

#### 4.4 Results

### 4.4.1 Variations in Environmental Conditions

The daily and seasonal dynamics of environmental variables are depicted in Figure 4.2 and Table 4.2. Daily PAR values steadily increased from January to July, reaching values up to 700 µmol m<sup>-2</sup> d<sup>-1</sup>, and then began to decline rapidly. PAR decreased to 186 μmol m<sup>-2</sup> mth<sup>-1</sup> in September and October and then stayed low through winter (Fig. 4.2a, Table 4.2). Low daily PAR values were observed during cloudy conditions as well, typically corresponding to rain episodes (Fig. 4.2a, d). Similarly, Tair showed higher values during the growing season, with the highest monthly value of 21.94 °C in July and 19.92 °C in August (Table 4.2, Fig. 4.2b). Notable daily peaks were observed on April 14 (26 °C), May 31 (28.2 °C), June 2 (30.6 °C) and September 5 (20.3 °C). Similarly, daily VPD exhibited peak values (> 1 kPa) on April 14 (2.8 kPa), May 29 (2.9 kPa), and June 2 (3.2 kPa), which is consistent with high Tair values. June was the month exhibiting the higher average VPD of 0.94 kPa (Table 4.2). Overall, VPD values consistently decreased from July to December (Fig. 4.2c). Although, some peaks in daily VPD were observed in October. Higher values of REW ranging from 1 to 1.2 were observed at the beginning of the water year, which spans from November to April, while REW values below 0.5 were noted during the summer months. REW was influenced by precipitation events, particularly heavy rainfalls. For example, REW increased from 0.42 to 1.16 for one of the largest rainfall events of 33 mm on June 12. REW increased rapidly with each successive rainfall and decreased slowly during subsequent rain-free days (Fig. 4.2d). Overall, REW started to decrease the onset of the growing season (April) and reached its lowest values in October, increasing again in the fall due to decrease atmospheric demand and the shedding of leaves from the trees.

# 4.4.2 Dynamic of Sap Flow Velocity

Sap flow velocity (i.e. SV) displayed distinctive variation between seasons, months, and VRH treatments (Fig. 4.3, Table S4.1). At the diurnal scale, SV typically rose rapidly in the morning (around 6:00 a.m.), reached its highest point between 1:00 and 2:00 p.m., remained stable for about an hour, and then decreased to the lowest value around 9:00 p.m. During the summer, the CN and 55D treatments showed SV values of up to ~7 cm h<sup>-1</sup> (Fig. 4.3a, e), while peak SV values of 5 cm h<sup>-1</sup>, 4.3 cm h<sup>-1</sup>, and 4 cm h<sup>-1</sup> were observed for 55A, 33D, and 33A treatments, respectively (Fig. 4.3c, b, d). Overall, the CN and 55D treatments exhibited the higher SV values over the growing season with an average 1.9 cm h<sup>-1</sup> each (Table S4.1).

# 4.4.3 Hysteresis between Sap Flow and Meteorological Variables in VRH Treatments

The hourly mean SV showed a diurnal pattern similar to that that of Tair (Fig. 4.4f-j) and VPD (Fig. 4.4k-o). However, Tair and VPD cycles lagged behind PAR typically by about 2 hours. This lag resulted in distinct counterclockwise hysteresis loops in the relationship between SV and meteorological variables across all VHR treatments (Fig. 4.4). As the environmental variable (e.g. PAR, Tair, VPD) increased in the morning, SV also increased and peaked at an optimal value of the environmental variable. In the afternoon, sap flow velocity declined with decreasing PAR (Tair, VPD). However, at the same PAR (Tair, VPD), SV was higher in the afternoon than in the morning. Interestingly, in some months, particularly during June and July, the relationship between SV and VPD/Tair followed a clockwise hysteresis loop (Fig. 4.5). This means that SV had higher values in the morning compared to the afternoon for the same environmental variable values.

The strength of the hysteresis curves was greatly influenced by seasonal changes and specific environmental conditions. The hysteresis loops of SV with PAR were larger in summer, followed by spring and fall, due to roughly 2-hour delay in SV following PAR (Fig 4a-e). In contrast, the hysteresis area was smaller for SV with Tair/VPD across seasons (Fig. 4.4, Fig. 4.5). Furthermore, the hysteresis area was more pronounced on days with clear sky conditions and high temperatures, seemingly unaffected by the soil water conditions (Fig. S4.2).

## 4.4.4 Relationship between sap flow velocity and environmental conditions

High sap flow velocity was associated with clear-sky and high Tair (25 to  $30^{\circ}$ C) and VPD (0.8 – 1.2 kPa) conditions (Fig. S4.1a, d, g). Although very high VPD (~2.5 kPa) and Tair (~35 °C) limited SV (not shown), low soil moisture conditions (REW <0.4) did not seem significantly limit SV (not shown). On the contrary, cloudy and low VPD conditions decreased SV (Fig. S4.1c, f, i). SV across VRH treatments exhibited similar patterns in response to environmental variables, but CN and 55D exhibited the highest values. These patterns align with the primary factors influencing SV at daily time scale (Table 4.3, Fig. 4.6). The MLR revealed that PAR (lmg=0.36) was the primary factor influencing SV, followed by Tair (lmg=0.24) and VPD (lmg=0.46) at daily and half hourly timescale, respectively (lmg values correspond to the average values per treatment). However, there was no strong relationship between SV and REW (Table 4.3, Fig. 4.6). Interestingly, in the CN and 55D treatment, VPD played a more significant role in explaining the variability of SV than Tair. The meteorological factors analyzed in this study showed varying degrees of correlation with each other, but they did not exceed the accepted values for multicollinearity (not shown). For instance, higher solar radiation often coincided with higher Tair and VPD levels (Fig. S4.1). The combined effect of these meteorological factors could predict sap flow changes with a high degree of accuracy (R<sup>2</sup> >

0.5), emphasizing the importance of considering their interaction (Table 4.3, Table S4.2). Finally, the principal component analysis showed that VPD, PAR and Tair can explain 73.8% of the variation in SV over the growing seasons (Fig. 4.6a).

### 4.5 Discussion

## 4.5.1 Response of Sap Flow Velocity to Environmental Variables

The response of sap flow to environmental controls such as Tair, VPD and soil moisture is influenced by tree species and density (Bachofen et al., 2023), shedding light of the profound impacts of forest management practices on tree transpiration and the water cycle. Results from the MLR analysis showed that PAR was a major control on SV, followed by Tair at daily and VPD at hourly timescale which agrees with an earlier study performed at this site by Bodo and Arain (2022). These results are also consistent with other studies in the literature that have shown that reduced solar radiation due to cloud coverage is among the main factors that reduce sap flow in many regions (Bovard et al., 2005; Gimenez et al., 2019; Kunert et al., 2017; Moradi et al., 2016). Previous studies conducted across various climate zones and plant species have also reported the dominant role of PAR and VPD in regulating transpiration (Bovard et al., 2005; Ma et al., 2017; Zheng & Wang, 2014), where soil water availability plays a less evident role (Ma et al., 2017). Indeed, Novick et al., (2016) demonstrated that atmospheric demand causes a reduction in evapotranspiration to a greater extent than soil moisture availability by reducing stomatal conductance.

Ma et al. (2017) highlighted threshold controls for VPD on SV for black locust species in Loess Plateau, China. Similarly, we identified that the threshold controls for VPD on SV were between 1.5 kPa and 2 kPa and were consistent across all VHR treatments. SV for 33D, 55A, and 33A treatment

increased almost linearly with VPD up to around 1.5 kPa before reaching a plateau corresponding to a value of 5.1 cm h<sup>-1</sup>, 4.6 cm h<sup>-1</sup>, and 3.0 cm h<sup>-1</sup>, respectively, and subsequently decreasing at higher values of VPD (Fig. 4.6d). Contrary, the plateau values were higher for the CN (9.3 cm h<sup>-1</sup>) and 55D (8.38 cm h<sup>-1</sup>) treatments when VPD levels ranged between 1.8 – 2 kPa (Fig. 4.6d). These patterns have been observed in multiple studies that describe the relationship between evapotranspiration and VPD. It is attributed to a decline in stomatal conductance due to stomatal closure to reduce excess water loss (Franks et al., 1997; Grossiord et al., 2020).

Previous studies have indicated a strong correlation between soil water content and SV across several tree species (Gazal et al., 2006; Horna et al., 2011; Oren & Pataki, 2001), as thinning practices increasing soil moisture due to reduce competition and enhance transpiration of remaining trees (del Campo et al., 2022). However, our study did not find a significant relationship between SV and soil moisture (Table 4.3). This suggests that transpiration rates reflect driving meteorological forces such as PAR, Tair and VPD rather than fluctuation in soil water supply (Kunert et al., 2017). There are potential reasons for this weak relationship. First, the studied region exhibits lower soil moisture variation than meteorological variables analyzed due to well drained sandy soils. Second, there was a lack of direct soil moisture measurements in each VRH plot due to resources constrain, however soil characteristics at both white pine and red pines sites were very similar. Third, the site is in an energy-limited region rather than a water-limited one, making SV more susceptible to variations in meteorological controls (Hassler et al., 2018). Fourth, the weak relationship may be inherent to the tree species, as red pine is tolerant to drier conditions (Gilmore and Palik, 2005), and is affiliated to a certain functional type and hydraulic traits to conserve water (Bachofen et al., 2023).

# 4.5.2 Hysteresis Patterns of Sap Flow

Hysteresis is a phenomenon in plants that reflects how they manage evaporative demand in relation to environmental controls and soil water availability (Ma et al., 2017). In our study, we observed diurnal hysteresis patterns in SV of red pine trees in response to environmental factors, as reported in other studies (Ewers et al., 2005; Looker et al., 2018; Wang et al., 2019; Matheny et al., 2014). A greater phase difference (asynchrony) between SV and the environmental variable, resulted in a more pronounced hysteresis pattern, as seen in the relationship of SV to PAR (Fig. 4.4a-e). Additionally, the magnitude of the hysteresis was closely linked to the seasonal changes in the meteorological conditions typical of the temperate region. For instance, the area within the hysteresis loop was smaller in spring (April) and fall (October to November) compared to that of summer months (Fig. 4.4, Fig. 4.5). Further, changes in meteorological conditions, such as excessively high or too low VPD in association with heatwaves and cloudy conditions, respectively, directed the hysteresis magnitude (Fig. S4.3).

The hysteresis between SV and environmental variables acts as a self-protection mechanism for plants, helping them avoid dehydration by regulating stomatal control (Wang et al., 2019), enabling red pine to avoid overlaps of peak SV and peak environmental conditions (PAR, VPD, and Tair) (Chen et al., 2011). This mechanism helps to prevent excessive water extraction from the tree trunks, which could damage the xylem vessels by causing embolism and collapse of the hydraulic conductive tissue (Chen et al., 2011; Lu et al., 2011; Zeppel et al., 2004). Therefore, it is a conservative water use strategy of red pine in response to environmental drivers (Ma et al., 2017).

This study introduces a new perspective by examining the hysteresis patterns between SV and environmental variable across VRH treatments. The larger hysteresis loops observed in the CN and

55D treatments suggest that a more uniform canopy cover with higher retention levels enhances the ability of red pine trees to withstand climate extremes (Bodo and Arain, 2022). This resilience is attributed to differences in microclimate, light distribution, and water availability resulting from these specific planting treatments (Li et al., 2020). Therefore, higher tree density combined with uniformly spaced residual trees intensifies the lag between environmental changes and sap flow responses (Hong et al., 2019).

The hysteresis loops observed in this study often occurred in counterclockwise direction, particularly between SV and PAR (Fig. 4.4, Fig. 4.5). The delayed increase in sap flow suggests an efficient water transport system capable of meeting photosynthetic demands even as PAR increases (Ma et al., 2017; Wang et al., 2019). This pattern illustrates the adaptive response of red pine to varying light conditions (Gilmore and Palik, 2005). Counterclockwise hysteresis loops were also observed between SV and both VPD and Tair. Similarly, Wang et al. (2019) reported counterclockwise loops for sap flow and VPD/Tair in the humid, low-energy environment of the Scottish Highlands for Scots pine forest. The authors attributed this to frequent summer rainfall, which regularly replenishes soil moisture, limiting water deficit, and consistently meeting transpiration demands.

In certain months, particularly in June, SV exhibited clockwise hysteresis loops with VPD/Tair (Fig. 4.5m, n). This pattern indicates that SV peaks earlier in the day compared to the meteorological drivers, and further increases in VPD or Tair do not result in additional water loss through plant transpiration, as stomata close in response to these changes (Zhang et al., 2014). Thus, the clockwise hysteresis implies a conservation mechanism in plants to prevent continuous water loss under high evaporative demand which is typical of summer months (Ma et al., 2017; Wang et al., 2019).

A noticeable difference in the occurrence of clockwise and counterclockwise loops in SV has been reported in the literature. Clockwise loops are more frequently documented (Matheny et al., 2014; Tie et al., 2017), whereas counterclockwise loops are less common, except in response to radiation (Gimenez et al., 2019; Li et al., 2015). Studies indicate that clockwise SV hysteresis is prevalent in tropical forest of Costa Rica (O'Brien et al., 2004), tropical secondary forests in Panama (Bretfeld et al., 2018), temperate forests of Australia (Zeppel et al., 2004), trees in eastern Amazon (da Costa et al., 2018), the boreal forest in Canada (Pappas et al., 2018), and temperate forest of North America (Matheny et al., 2014).

## 4.5.3 Effects of VRH on Sap Flow of Red Pines

Recent studies have highlighted that forest structure, particularly the differences in basal area, significantly affects variation in transpiration (Hassler et al., 2018). For instance, Bachofen et al. (2023) demonstrated that the structure of the stand is more important than climate in explaining the sensitivity of SV to VPD. Moreover, thinning practices that inherently changes the structure of the canopy, can increase transpiration by enhancing soil water availability - due to reduced water consumption and interception by the canopy- as well as by increasing light availability and airflow within the canopy (Gebhardt et al., 2014; Song et al., 2020; Wang et al., 2019). Our results support this argument, indicating that retaining 55% of the basal area after thinning is more beneficial for promoting transpiration and hence forest growth and carbon uptake (Table S4.1). This is because higher tree density and uniformly spaced residual trees potentially provide better light distributions and soil moisture availability. These results are in line with previous studies that reported the highest daily gross primary productivity (GPP) values (Hussain et al., 2024) and increased water use (Bodo & Arain, 2022) in the 55D treatment. Additionally, using tree ring measurements, Zugic et al., (2021)

found that higher retention levels, after accounting for retained tree biomass, resulted in greater growth and carbon sequestration. These findings suggest that thinning in a uniformly dispersed pattern, retaining more than half of the initial basal area (moderate thinning), is a viable forest management practice to enhance tree level water-use, growth and carbon uptake. This information is valuable for forest managers and policymakers in developing forest management strategies tailored to mitigate the impacts of climate change.

### 4.6 Conclusions

In this study, we analyzed the response of sap flow to environmental controls across temporal scales including half-hourly, daily, and monthly in VRH treatments and control plots in the Great Lakes region in southern Ontario, Canada. Multiple linear regression analysis indicated that PAR and VPD were the dominant factor explaining the variability of sap flow at hourly time scale, while PAR followed by Tair where the dominant controls at daily timescale. We observed hysteresis patterns between sap flow and environmental variables, with higher magnitude of the hysteresis in summer months and in the CN and 55D treatments. Contrary to most studies, we identified counterclockwise hysteresis loops where sap flow lagged behind meteorological changes, particularly showing a phase shift with respect to PAR. Our findings indicate that retaining more than half of the initial basal area in uniform dispersal form (e.g. 55D treatment) resulted in higher sap flow compared to lower retention levels or an aggregate spatial distribution of residual canopy trees. Therefore, retention of more than half of the canopy or basal area is a viable forest management or thinning practice to enhance tree level water-use, growth and carbon uptake. Our study provides valuable insights for researchers, forest managers, and decision makers in developing forest management practices aimed at enhancing growth and transpiration among remaining trees following VRH, thereby contributing

to climate mitigation and adaptation goals.

# 4.7 Acknowledgements

This study was funded by Natural Sciences and Engineering Research Council (NSERC) of Canada Discovery and Alliance Mission grants, Global Water Futures Program Observatory (GWFO) program, and the US National Science Foundation (NSF) - Social Science and Humanities Research Council (SSHRC) of Canada funded Global Centre for Climate Change Impacts on Transboundary Waters grant. In-kind support from the Ontario Ministry of Natural Resources and Forestry (OMNRF), Ontario Ministry of Environment, Conservation and Parks and the St. Williams Conservation Reserve Community Council (SWCRCC) is also acknowledged. We thank Bill Parker, Ken Elliott and Steve Williams from OMNRF for establishing the VRH experiment in this red pine stand. Finally, we acknowledge support from Zoran Nesic at the University of British Columbia (Dr. T. A. Black's group) in assistance with eddy covariance flux and sap flow measurements. We would like to express our gratitude for the support provided during fieldwork activities by the members of the Hydro-meteorology lab at McMaster University. Special thanks to Alana Bodo, Farbod Tabaei, Jason Brodeur, Lejla Latifovic, and Noah Stegman, and for their assistance in the fieldwork, data quality control and archiving.

### 4.8 References

- Arain, A. (2018). AmeriFlux BASE CA-TP4 Ontario Turkey Point 1939 Plantation White Pine, Ver. 4-5, AmeriFlux AMP, (Dataset).
- Arain, A., Xu, B., Brodeur, J. J., Khomik, M., Peichl, M., Beamesderfer, E., Restrepo-Couple, N., & Thorne, R. (2022). Heat and drought impact on carbon exchange in an age-sequence of temperate pine forests. Ecological Processes, 11(1). https://doi.org/10.1186/s13717-021-00349-7
- Bachofen, C., Poyatos, R., Flo, V., Martínez-Vilalta, J., Mencuccini, M., Granda, V., & Grossiord, C. (2023). Stand structure of Central European forests matters more than climate for transpiration sensitivity to VPD. Journal of Applied Ecology, 60(5), 886–897. https://doi.org/10.1111/1365-2664.14383
- Black, T. A. (1979). Evapotranspiration From Douglas Fir Stands Exposed to Soil Water Deficits. Water Resources Research, 15(1), 164–170. https://doi.org/10.1029/WR015i001p00164
- Bladon, K. D., Silins, U., Landhäusser, S. M., & Lieffers, V. J. (2006). Differential transpiration by three boreal tree species in response to increased evaporative demand after variable retention harvesting. Agricultural and Forest Meteorology, 138(1–4), 104–119. https://doi.org/10.1016/j.agrformet.2006.03.015
- Bodo, A. V., & Arain, M. A. (2021). Radial variations in xylem sap flux in a temperate red pine plantation forest. Ecological Processes, 10(1), 0–9. https://doi.org/10.1186/s13717-021-00295-4
- Bodo, A. V., & Arain, M. A. (2022). Effects of variable retention harvesting on canopy transpiration in a red pine plantation forest. Ecological Processes, 11(1). https://doi.org/10.1186/S13717-022-00366-0
- Boggs, J., Sun, G., Domec, J. C., McNulty, S., & Treasure, E. (2015). Clearcutting upland forest alters transpiration of residual trees in the riparian buffer zone. Hydrological Processes, 29(24), 4979–4992. https://doi.org/10.1002/hyp.10474
- Bonan, G. B. (2008). Forests and Climate Change: Forcings, Feedbacks, and the Climate Benefits of Forests. Science, 320(5882), 1444–1449. Ht
- tps://doi.org/10.1126/science.1155121
- Bonan, G. B. (2015). Ecological Climatology: Concepts and Applications (3rd ed.). Cambridge University Press. https://doi.org/10.1017/CBO9781107339200
- Bovard, B. D., Curtis, P. S., Vogel, C. S., Su, H. B., & Schmid, H. P. (2005). Environmental controls on sap flow in a northern hardwood forest. Tree Physiology, 25, 31–38.

- Bréda, N., Granier, A., & Aussenac, G. (1995). Effects of thinning on soil and tree water relations, transpiration and growth in an oak forest (Quercus petraea (Matt.) Liebl.). Tree Physiology, 15(5), 295–306. https://doi.org/10.1093/treephys/15.5.295
- Bretfeld, M., Ewers, B. E., & Hall, J. S. (2018). Plant water use responses along secondary forest succession during the 2015–2016 El Niño drought in Panama. New Phytologist, 219(3), 885–899. https://doi.org/10.1111/nph.15071
- Brinkmann, N., Eugster, W., Zweifel, R., Buchmann, N., & Kahmen, A. (2016). Temperate tree species show identical response in tree water deficit but different sensitivities in sap flow to summer soil drying. Tree Physiology, 36(12), 1508–1519. https://doi.org/10.1093/treephys/tpw062
- Chen, L., Zhang, Z., Li, Z., Tang, J., Caldwell, P., & Zhang, W. (2011). Biophysical control of whole tree transpiration under an urban environment in Northern China. Journal of Hydrology, 402(3–4), 388–400. https://doi.org/10.1016/j.jhydrol.2011.03.034
- Clogg, C. C., Petkova, E., & Haritou, A. (1995). Statistical Methods for Comparing Regression Coefficients Between Models. American Journal of Sociology, 100(5), 1261–1293. https://www.jstor.org/stable/2782277
- da Costa, A. C. L., Rowland, L., Oliveira, R. S., Oliveira, A. A. R., Binks, O. J., Salmon, Y., Vasconcelos, S. S., Junior, J. A. S., Ferreira, L. V., Poyatos, R., Mencuccini, M., & Meir, P. (2018). Stand dynamics modulate water cycling and mortality risk in droughted tropical forest. Global Change Biology, 24(1), 249–258. https://doi.org/10.1111/gcb.13851
- David, T. S., Ferreira, M. I., Cohen, S., Pereira, J. S., & David, J. S. (2004). Constraints on transpiration from an evergreen oak tree in southern Portugal. Agricultural and Forest Meteorology, 122(3–4), 193–205. https://doi.org/10.1016/j.agrformet.2003.09.014
- del Campo, A. D., Otsuki, K., Serengil, Y., Blanco, J. A., Yousefpour, R., & Wei, X. (2022). A global synthesis on the effects of thinning on hydrological processes: Implications for forest management. In Forest Ecology and Management (Vol. 519). Elsevier B.V. https://doi.org/10.1016/j.foreco.2022.120324
- Deng, Y., Wu, S., Ke, J., & Zhu, A. (2021). Effects of meteorological factors and groundwater depths on plant sap flow velocities in karst critical zone. Science of the Total Environment, 781. https://doi.org/10.1016/j.scitotenv.2021.146764
- Ellison, D., Morris, C. E., Locatelli, B., Sheil, D., Cohen, J., Murdiyarso, D., Gutierrez, V., Noordwijk, M. van, Creed, I. F., Pokorny, J., Gaveau, D., Spracklen, D. V., Tobella, A. B., Ilstedt, U., Teuling, A. J., Gebrehiwot, S. G., Sands, D. C., Muys, B., Verbist, B., ... Sullivan, C. A. (2017). Trees, forests and water: Cool insights for a hot world. Global Environmental Change, 43, 51–61. https://doi.org/10.1016/j.gloenvcha.2017.01.002
- Environment and Climate Change Canada (ECCC). (2023, January). Climate Data Online.

- Https://Climate.Weather.Gc.ca. Accessed 16 January.
- Ewers, B. E., Gower, S. T., Bond-Lamberty, B., & Wang, C. K. (2005). Effects of stand age and tree species on canopy transpiration and average stomatal conductance of boreal forests. Plant, Cell and Environment, 28(5), 660–678. https://doi.org/10.1111/j.1365-3040.2005.01312.x
- Franks, P. J., Cowan, I. R., & Farquhar, G. D. (1997). The apparent feedforward response of stomata to air vapour pressure deficit: Information revealed by different experimental procedures with two rainforest trees. Plant, Cell and Environment, 20(1), 142–145. https://doi.org/10.1046/j.1365-3040.1997.d01-14.x
- Gazal, R. M., Scott, R. L., Goodrich, D. C., & Williams, D. G. (2006). Controls on transpiration in a semiarid riparian cottonwood forest. Agricultural and Forest Meteorology, 137(1–2), 56–67. https://doi.org/10.1016/j.agrformet.2006.03.002
- Gebhardt, T., Häberle, K. H., Matyssek, R., Schulz, C., & Ammer, C. (2014). The more, the better? Water relations of Norway spruce stands after progressive thinning. Agricultural and Forest Meteorology, 197, 235–243. https://doi.org/10.1016/j.agrformet.2014.05.013
- Gilmore, D. W., & Palik, B. J. (2005). NCSM-A Revised Managers Handbook for Red Pine in the North Central Region. www.ncrs.fs.fed.us
- Gimenez, B. O., Jardine, K. J., Higuchi, N., Negrón-Juárez, R. I., Sampaio-Filho, I. de J., Cobello, L. O., Fontes, C. G., Dawson, T. E., Varadharajan, C., Christianson, D. S., Spanner, G. C., Araújo, A. C., Warren, J. M., Newman, B. D., Holm, J. A., Koven, C. D., McDowell, N. G., & Chambers, J. Q. (2019). Species-specific shifts in diurnal sap velocity dynamics and hysteretic behavior of ecophysiological variables during the 2015–2016 el niño event in the amazon forest. Frontiers in Plant Science, 10. https://doi.org/10.3389/fpls.2019.00830
- Granier, A. (1985). Une nouvelle méthode pour la mesure du flux de sève brute dans le tronc des arbres. Ann. Sci. For., 42(2), 81–88. https://doi.org/10.1051/forest:19850204
- Granier, A. (1987). Evaluation of transpiration in a Douglas-fir stand by means of sap flow measurements. Tree Physiology, 3(4), 309–320. https://doi.org/10.1093/treephys/3.4.309
- Granier, A., Reichstein, M., Bréda, N., Janssens, I. A., Falge, E., Ciais, P., Grünwald, T., Aubinet, M., Berbigier, P., Bernhofer, C., Buchmann, N., Facini, O., Grassi, G., Heinesch, B., Ilvesniemi, H., Keronen, P., Knohl, A., Köstner, B., Lagergren, F., ... Wang, Q. (2007). Evidence for soil water control on carbon and water dynamics in European forests during the extremely dry year: 2003. Agricultural and Forest Meteorology, 143(1–2), 123–145. https://doi.org/10.1016/j.agrformet.2006.12.004
- Groempings, U. (2021). The Relative Importance of Regressors in Linear Models. https://prof.bht-berlin.de/groemping/relaimpo/,
- Grossiord, C., Buckley, T. N., Cernusak, L. A., Novick, K. A., Poulter, B., Siegwolf, R. T. W.,

- Sperry, J. S., & Mcdowell, N. G. (2020). Tansley review Plant responses to rising vapor pressure deficit. 1550–1566. https://doi.org/10.1111/nph.16485
- Hassler, S. K., Weiler, M., & Blume, T. (2018). Tree-, stand- and site-specific controls on landscape-scale patterns of transpiration. Hydrology and Earth System Sciences, 22(1), 13–30. https://doi.org/10.5194/hess-22-13-2018
- Hong, L., Guo, J., Liu, Z., Wang, Y., Ma, J., Wang, X., & Zhang, Z. (2019). Time-lag effect between sap flow and environmental factors of Larix principis-rupprechtii Mayr. Forests, 10(11). https://doi.org/10.3390/f10110971
- Horna, V., Schuldt, B., Brix, S., & Leuschner, C. (2011). Environment and tree size controlling stem sap flux in a perhumid tropical forest of Central Sulawesi, Indonesia. Annals of Forest Science, 68(5), 1027–1038. https://doi.org/10.1007/s13595-011-0110-2
- Hussain, N., Arain, M. A., Wang, S., Parker, W. C., & Elliott, K. A. (2024). Evaluating the effectiveness of different variable retention harvesting treatments on forest carbon uptake using remote sensing. Remote Sensing Applications: Society and Environment, 33. https://doi.org/10.1016/j.rsase.2023.101124
- Jasechko, S., Sharp, Z. D., Gibson, J. J., Birks, S. J., Yi, Y., & Fawcett, P. J. (2013). Terrestrial water fluxes dominated by transpiration. Nature, 496(7445), 347–350. https://doi.org/10.1038/nature11983
- Li, C., Barclay, H., Roitberg, B., & Lalonde, R. (2020). Forest Productivity Enhancement and Compensatory Growth: A Review and Synthesis. In Frontiers in Plant Science (Vol. 11). Frontiers Media S.A. https://doi.org/10.3389/fpls.2020.575211
- Li, W., Yu, T. F., Li, X. Y., & Zhao, C. Y. (2015). Sap flow characteristics and their response to environmental variables in a desert riparian forest along lower Heihe River Basin, Northwest China. Environmental Monitoring and Assessment, 188(10). https://doi.org/10.1007/s10661-016-5570-2
- Looker, N., Martin, J., Hoylman, Z., Jencso, K., & Hu, J. (2018). Diurnal and seasonal coupling of conifer sap flow and vapour pressure deficit across topoclimatic gradients in a subalpine catchment. Ecohydrology, 11(7). https://doi.org/10.1002/eco.1994
- Lumley, T. (2020). Thomas Lumley Based on Fortran Code by Alan Miller.
- Lu, N., Chen, S., Wilske, B., Sun, G., & Chen, J. (2011). Evapotranspiration and soil water relationships in a range of disturbed and undisturbed ecosystems in the semi-arid Inner Mongolia, China. Journal of Plant Ecology, 4(2), 49–60. https://doi.org/10.1093/jpe/rtq035
- Ma, C., Luo, Y., Shao, M., Li, X., Sun, L., & Jia, X. (2017). Environmental controls on sap flow in black locust forest in Loess Plateau, China. Scientific Reports, 7(1). https://doi.org/10.1038/s41598-017-13532-8

- Matheny, A. M., Bohrer, G., Vogel, C. S., Morin, T. H., He, L., Frasson, R. P. D. M., Mirfenderesgi, G., Schäfer, K. V. R., Gough, C. M., Ivanov, V. Y., & Curtis, P. S. (2014). Species-specific transpiration responses to intermediate disturbance in a northern hardwood forest. Journal of Geophysical Research: Biogeosciences, 119(12), 2292–2311. https://doi.org/10.1002/2014JG002804
- Moon, M., Kim, T., Park, J., Cho, S., Ryu, D., & Kim, H. S. (2015). Variation in sap flux density and its effect on stand transpiration estimates of Korean pine stands. Journal of Forest Research, 20(1), 85–93. https://doi.org/10.1007/s10310-014-0463-0
- Moore, L. M. (2002). RED PINE Plant Fact Sheet. http://www.na.fs.fed.us/spfo/for\_images/misci
- Moradi, I., Arkin, P., Ferraro, R., Eriksson, P., & Fetzer, E. (2016). Diurnal variation of tropospheric relative humidity in tropical regions. Atmospheric Chemistry and Physics, 16(11), 6913–6929. https://doi.org/10.5194/acp-16-6913-2016
- Novick, K. A., Ficklin, D. L., Stoy, P. C., Williams, C. A., Bohrer, G., Oishi, A. C., Papuga, S. A., Blanken, P. D., Noormets, A., Sulman, B. N., Scott, R. L., Wang, L., & Phillips, R. P. (2016). The increasing importance of atmospheric demand for ecosystem water and carbon fluxes. In Nature Climate Change (Vol. 6, Issue 11, pp. 1023–1027). https://doi.org/10.1038/nclimate3114
- O'Brien, J. J., Oberbauer, S. F., & Clark, D. B. (2004). Whole tree xylem sap flow responses to multiple environmental variables in a wet tropical forest. Plant, Cell and Environment, 27(5), 551–567. https://doi.org/10.1111/j.1365-3040.2003.01160.x
- Oren, R., & Pataki, D. E. (2001). Transpiration in response to variation in microclimate and soil moisture in southeastern deciduous forests. Oecologia, 127(4), 549–559. https://doi.org/10.1007/s004420000622
- Palik, B. J., & Kastendick, D. N. (2023). Restoration of woody plant communities in red pine plantations on abandoned agricultural land in northern Minnesota, USA. Forest Ecology and Management, 541. https://doi.org/10.1016/j.foreco.2023.121095
- Pappas, C., Matheny, A. M., Baltzer, J. L., Barr, A. G., Black, T. A., Bohrer, G., Detto, M., Maillet, J., Roy, A., Sonnentag, O., & Stephens, J. (2018). Boreal tree hydrodynamics: Asynchronous, diverging, yet complementary. Tree Physiology, 38(7), 953–964. https://doi.org/10.1093/treephys/tpy043
- Park, J., Kim, T., Moon, M., Cho, S., Ryu, D., & Seok Kim, H. (2018). Effects of thinning intensities on tree water use, growth, and resultant water use efficiency of 50-year-old Pinus koraiensis forest over four years. Forest Ecology and Management, 408, 121–128. https://doi.org/10.1016/j.foreco.2017.09.031
- Peters, R. L., Fonti, P., Frank, D. C., Poyatos, R., Pappas, C., Kahmen, A., Carraro, V., Prendin, A. L., Schneider, L., Baltzer, J. L., Baron-Gafford, G. A., Dietrich, L., Heinrich, I., Minor, R.

- L., Sonnentag, O., Matheny, A. M., Wightman, M. G., & Steppe, K. (2018). Quantification of uncertainties in conifer sap flow measured with the thermal dissipation method. New Phytologist, 219(4), 1283–1299. https://doi.org/10.1111/nph.15241
- Schlesinger, W. H., & Jasechko, S. (2014). Transpiration in the global water cycle. Agricultural and Forest Meteorology, 189–190, 115–117. https://doi.org/10.1016/J.AGRFORMET.2014.01.011
- Song, L., Zhu, J., Zheng, X., Wang, K., Lü, L., Zhang, X., & Hao, G. (2020). Transpiration and canopy conductance dynamics of Pinus sylvestris var. mongolica in its natural range and in an introduced region in the sandy plains of Northern China. Agricultural and Forest Meteorology, 281. https://doi.org/10.1016/j.agrformet.2019.107830
- Su, Y., Wang, X., Sun, Y., & Wu, H. (2022). Sap Flow Velocity in Fraxinus pennsylvanica in Response to Water Stress and Microclimatic Variables. Frontiers in Plant Science, 13. https://doi.org/10.3389/fpls.2022.884526
- Tie, Q., Hu, H., Tian, F., Guan, H., & Lin, H. (2017). Environmental and physiological controls on sap flow in a subhumid mountainous catchment in North China. Agricultural and Forest Meteorology, 240–241, 46–57. https://doi.org/10.1016/j.agrformet.2017.03.018
- Vilhar, U. (2016). Comparison of drought stress indices in beech forests: A modelling study. IForest, 9(4), 635–642. https://doi.org/10.3832/ifor1630-008
- Wang, H., Tetzlaff, D., Dick, J. J., & Soulsby, C. (2017). Assessing the environmental controls on Scots pine transpiration and the implications for water partitioning in a boreal headwater catchment. Agricultural and Forest Meteorology, 240–241, 58–66. https://doi.org/10.1016/j.agrformet.2017.04.002
- Wang, H., Tetzlaff, D., & Soulsby, C. (2019). Hysteretic response of sap flow in Scots pine (Pinus sylvestris) to meteorological forcing in a humid low-energy headwater catchment. Ecohydrology, 12(6). https://doi.org/10.1002/eco.2125
- Wang, K., & Dickinson, R. E. (2012). A review of global terrestrial evapotranspiration: Observation, modeling, climatology, and climatic variability. In Reviews of Geophysics (Vol. 50, Issue 2). Blackwell Publishing Ltd. https://doi.org/10.1029/2011RG000373
- Wang, Y., Wei, X., del Campo, A. D., Winkler, R., Wu, J., Li, Q., & Liu, W. (2019). Juvenile thinning can effectively mitigate the effects of drought on tree growth and water consumption in a young Pinus contorta stand in the interior of British Columbia, Canada. Forest Ecology and Management, 454, 117667. https://doi.org/10.1016/J.FORECO.2019.117667
- Wan, Y., Peng, L., Anwaier, A., Shi, H., Li, D., Ma, Y., & Shi, Q. (2024). Effects of meteorological factors and groundwater depths on sap flow density of Populus euphratica in a desert oasis, Taklamakan Desert, China. Frontiers in Plant Science, 15. https://doi.org/10.3389/fpls.2024.1330426

- Wilson, K. B., Hanson, P. J., Mulholland, P. J., Baldocchi, D. D., & Wullschleger, S. D. (2001). A comparison of methods for determining forest evapotranspiration and its components: sapflow, soil water budget, eddy covariance and catchment water balance. In Agricultural and Forest Meteorology (Vol. 106).
- Zeppel, M. J. B., Murray, B. R., Barton, C., & Eamus, D. (2004). Seasonal responses of xylem sap velocity to VPD and solar radiation during drought in a stand of native trees in temperate Australia. Functional Plant Biology, 31(5), 461–470. https://doi.org/10.1071/FP03220
- Zhang, Q., Manzoni, S., Katul, G., Porporato, A., & Yang, D. (2014). The hysteretic evapotranspiration Vapor pressure deficit relation. Journal of Geophysical Research: Biogeosciences, 119(2), 125–140. https://doi.org/10.1002/2013JG002484
- Zhao, C. Y., Si, J. H., Feng, Q., Yu, T. F., & Li, P. Du. (2017). Comparative study of daytime and nighttime sap flow of Populus euphratica. Plant Growth Regulation, 82(2), 353–362. https://doi.org/10.1007/s10725-017-0263-6
- Zheng, C., & Wang, Q. (2014). Water-use response to climate factors at whole tree and branch scale for a dominant desert species in central Asia: Haloxylon ammodendron. Ecohydrology, 7(1), 56–63. https://doi.org/10.1002/eco.1321
- Zugic, J. I., Pisaric, M. F. J., McKenzie, S. M., Parker, W. C., Elliott, K. A., & Arain, M. A. (2021). The Impact of Variable Retention Harvesting on Growth and Carbon Sequestration of a Red Pine (Pinus resinosa Ait.) Plantation Forest in Southern Ontario, Canada. Frontiers in Forests and Global Change, 4(December), 1–13. https://doi.org/10.3389/ffgc.2021.725890

**Table 4.1:** Details of Variable Retention Harvesting (VRH) treatments collected in the red-pine plantation in 2014.

Plot abbreviatio n	previatio retained Pattern of harve		Stand Density (trees plot -1)	Averag e DBH (m)	Average As - (m <sup>2</sup> )	Number of average sensors
33A	33	Aggregate	178	0.30	0.06	7
33D	33	Dispersed	118	0.37	0.09	8
55A	55	Aggregate	213	0.32	0.07	12
55D	55	Dispersed	235	0.32	0.06	3
CN		Control - unharvested	432	0.29	0.05	13

Note: Biometric measurements were conducted in 2014. DBH stands for diameter at breast (1.3m) height (1.3 m). As is sapwood area.

**Table 4.2:** Mean annual values of meteorological variables (air temperature, Tair; vapor pressure deficit, VPD; photosynthetic active radiation, PAR), soil moisture in the 0-20 cm soil layer,  $\theta_{0-20}$  (m<sup>3</sup> m<sup>-3</sup>), relative extractable water for 0-20 cm soil layer, REW<sub>0-20</sub>, and annual total precipitation, P.

Month	Ta (°C)	VPD (kPa)	PAR (µmol m <sup>-2</sup> mth <sup>-1</sup> )	$\theta_{0-20} \ (m^3 \ m^{-3})$	REW	P
January	0.08	0.11	83	0.17	1.10	71
February	-0.12	0.21	188	0.17	1.07	56
March	1.42	0.22	259	0.18	1.16	80
April	8.84	0.51	367	0.16	0.99	111
May	14.05	0.89	513	0.11	0.70	25
June	19.11	0.94	470	0.09	0.53	50
July	21.94	0.76	465	0.09	0.55	125
August	19.92	0.67	403	0.09	0.55	82
September	18.15	0.61	353	0.09	0.52	34
October	12.35	0.45	186	0.09	0.55	66
November	4.88	0.32	104	0.13	0.81	66
December	3.81	0.19	69	0.17	1.04	86
Mean ± Std*	$10.37 \pm 7.91$	$\boldsymbol{0.49 \pm 0.27}$	$288.26 \pm 153.78$	$0.13 \pm 0.04$	$0.80 \pm 0.25$	$71 \pm 28$

<sup>\*</sup> Values for P are annual total  $\pm$  Standard Deviation, Std.

**Table 4.3:** Multivariate regression analysis of standardized daily sap flow velocity (SV) across variable retention harvesting (VRH) treatments and control plot (33A, 33D, 55A, 55D, CN) regressed against standardized explanatory variables, including vapor pressure deficit (VPD), air temperature (Tair), photosynthetic active radiation (PAR), relative extractable water (REW). Significance levels are indicated as follows: [0-0.001] = '\*\*\*'; (0.01-0.01] = '\*\*'; (0.01-0.05] = '\*'; (0.05-0.1] = '.'; (0.1-1] = '.'

Treatment	Regressor	Estimate	Std. Error	t Value	Pr(> t )	Significance	lmg	$\mathbb{R}^2$
	Intercept	-0.011	0.038	-0.301	0.76374			
	PARdn	0.492	0.061	8.059	1.24E-14	***	0.354	
33A	Tair	0.389	0.069	5.623	3.85E-08	***	0.301	0.49
	VPD	-0.209	0.073	-2.844	0.00472	**	0.171	
	REW	-0.119	0.059	-2.017	0.04447	*	0.173	
	Intercept	-0.014	0.02813	-0.491	0.623754			
	PARdn	0.587	0.04522	12.977	< 2e-16	***	0.391	
33D	Tair	0.292	0.05125	5.705	2.49E-08	***	0.238	0.72
	VPD	-0.058	0.05435	-1.072	0.284403		0.211	
	REW	-0.150	0.04362	-3.432	0.000671	***	0.161	
	Intercept	-0.014	0.028	-0.498	0.61853			_
	PARdn	0.617	0.046	13.486	< 2e-16	***	0.3850	
55A	Tair	0.385	0.052	7.412	9.52E-13	***	0.2660	0.71
	VPD	-0.198	0.055	-3.594	0.000372	***	0.1819	
	REW	-0.153	0.044	-3.472	0.000582	***	0.1672	
	Intercept	0.083	0.029	2.827	0.004997	**		
	PARdn	0.377	0.048	7.797	9.34E-14	***	0.2830	
55D	Tair	0.265	0.055	4.859	1.86E-06	***	0.2607	0.73
	VPD	0.212	0.066	3.215	0.001442	**	0.2721	
	REW	-0.164	0.045	-3.605	0.000363	***	0.1842	
CN	Intercept	0.0492	0.0320	1.537	1.25E-01			
	PARdn	0.4748	0.0522	9.091	< 2e-16	***	0.375	
	Tair	0.1442	0.060	2.403	0.016811	*	0.204	0.66
	VPD	0.2366	0.0680	3.478	0.000574	***	0.293	
	REW	-0.0946	0.0498	-1.900	0.058252	•	0.128	

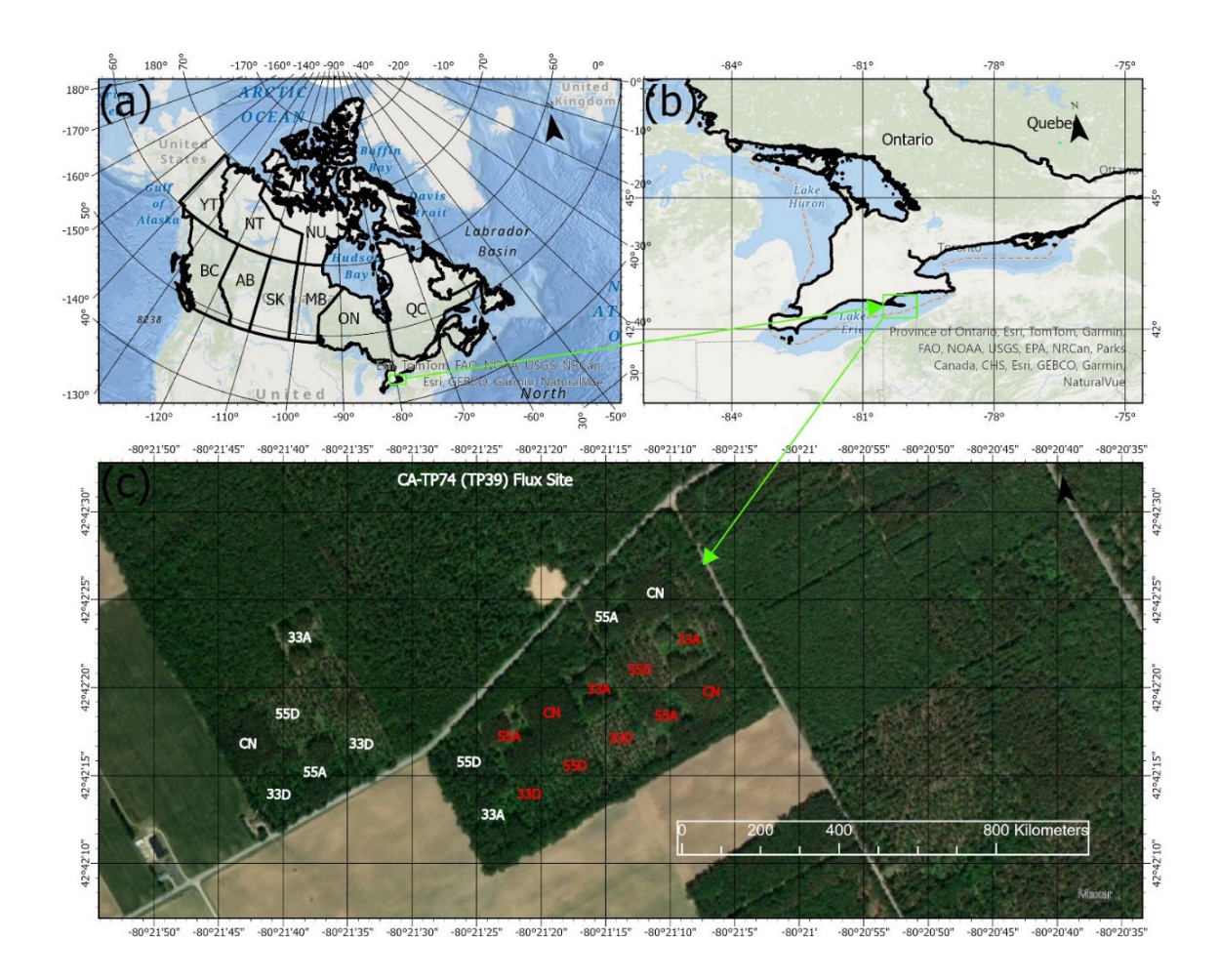


**Figure 4.1**: (a) Location map of provinces of Canada, (b) Ontario map, and (c) aerial view of the location of the Variable Retention Harvesting (VRH) treatments, one hectare each. Plots where sap flow measurements were conducted are marked with red text. Eddy covariance flux tower in the adjacent white pine plantation (1939 known as CA-TP4 in Ameriflux) is also shown.

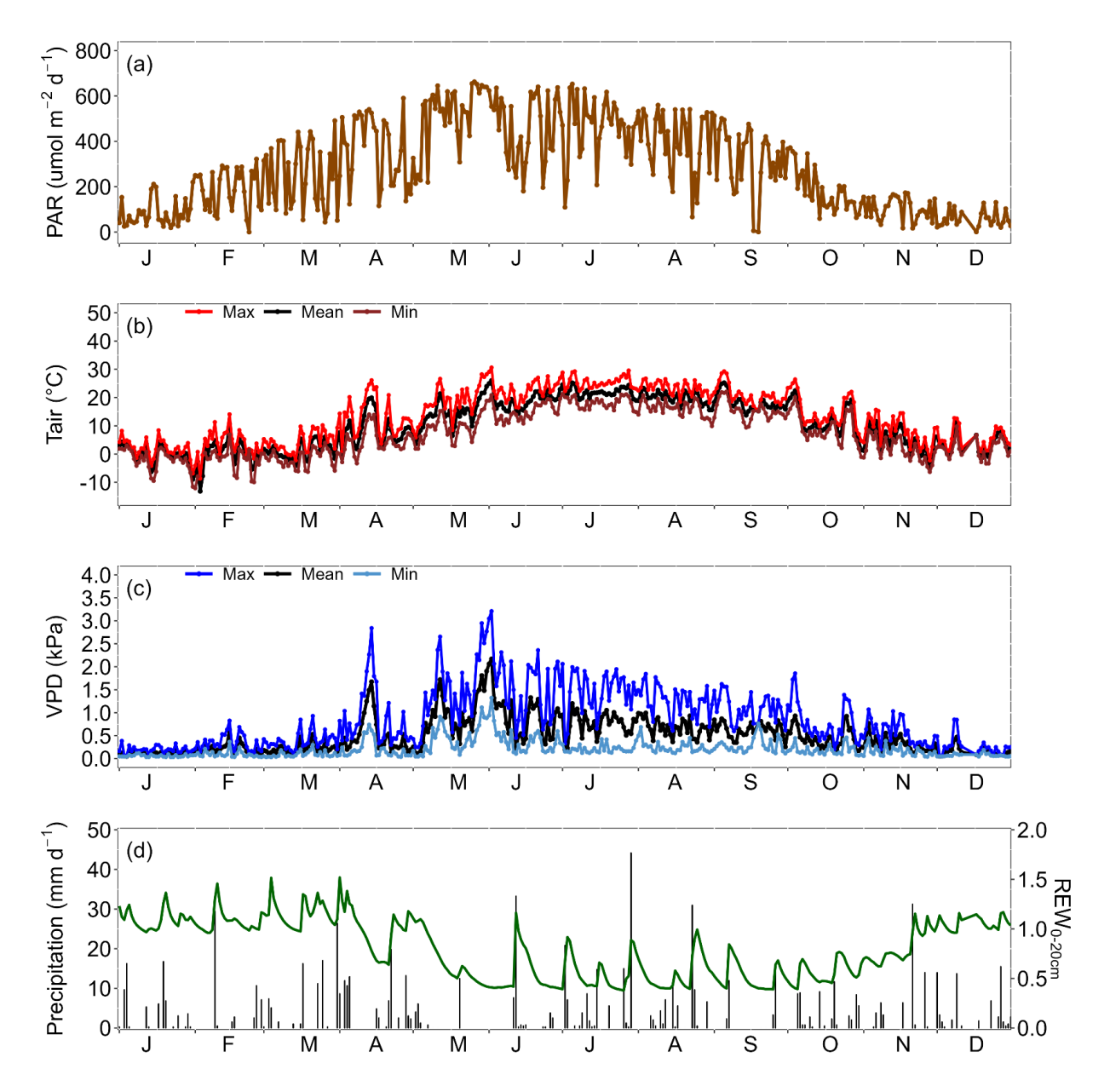


**Figure 4.2**: Meteorological and soil moisture conditions. Daily averages of photosynthetic active radiation (PAR), air temperature (Tair), vapor pressure deficit (VPD), relative extractable water (REW) and daily total values of precipitation (P).

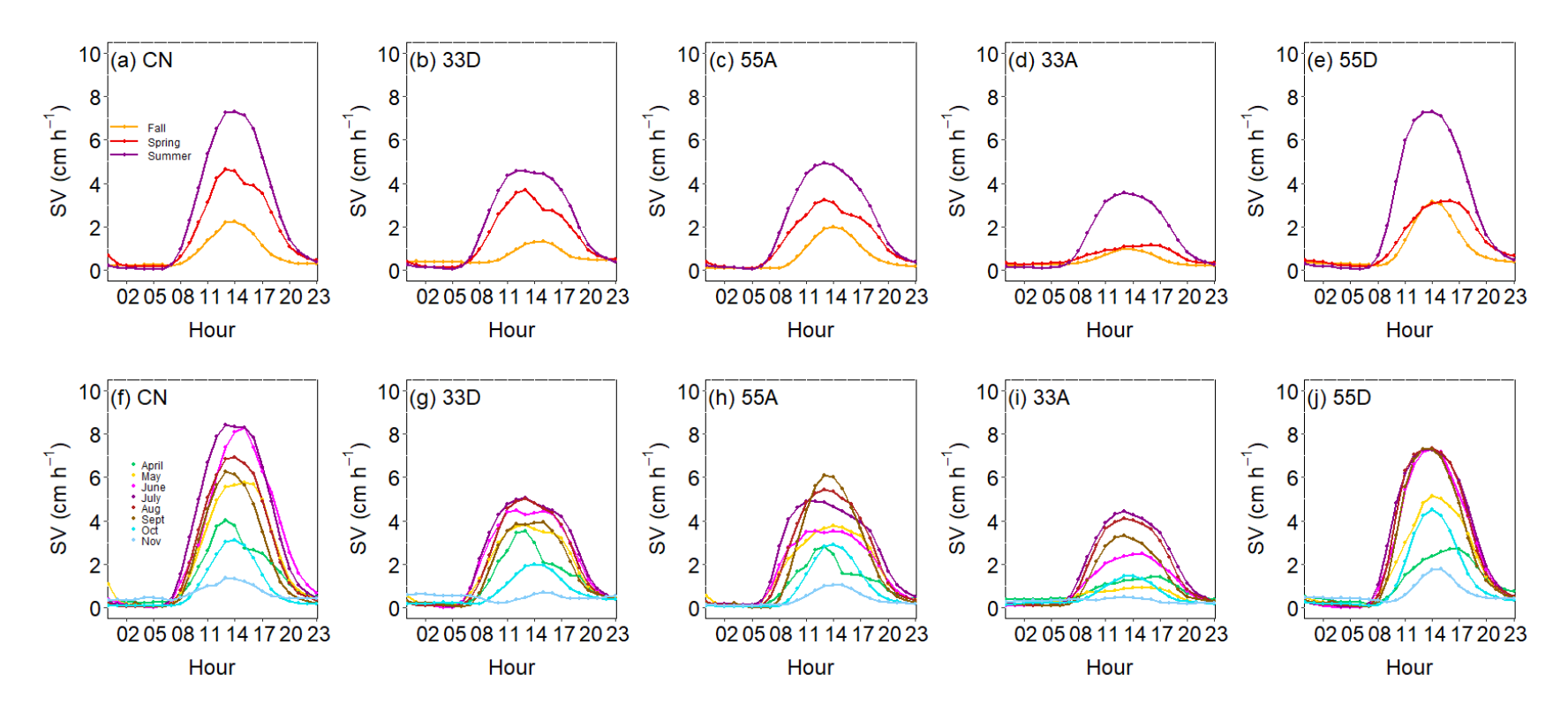


**Figure 4.3**: Diurnal patterns of sap flow velocity for different VRH treatments. (a-e) Mean diurnal pattern of sap flow velocity (SV) for all treatments for spring, summer, and fall of 2023; (f-j) Mean diurnal pattern of sap flow velocity (SV) per month per VRH treatment for the growing season (April-November) of 2023.

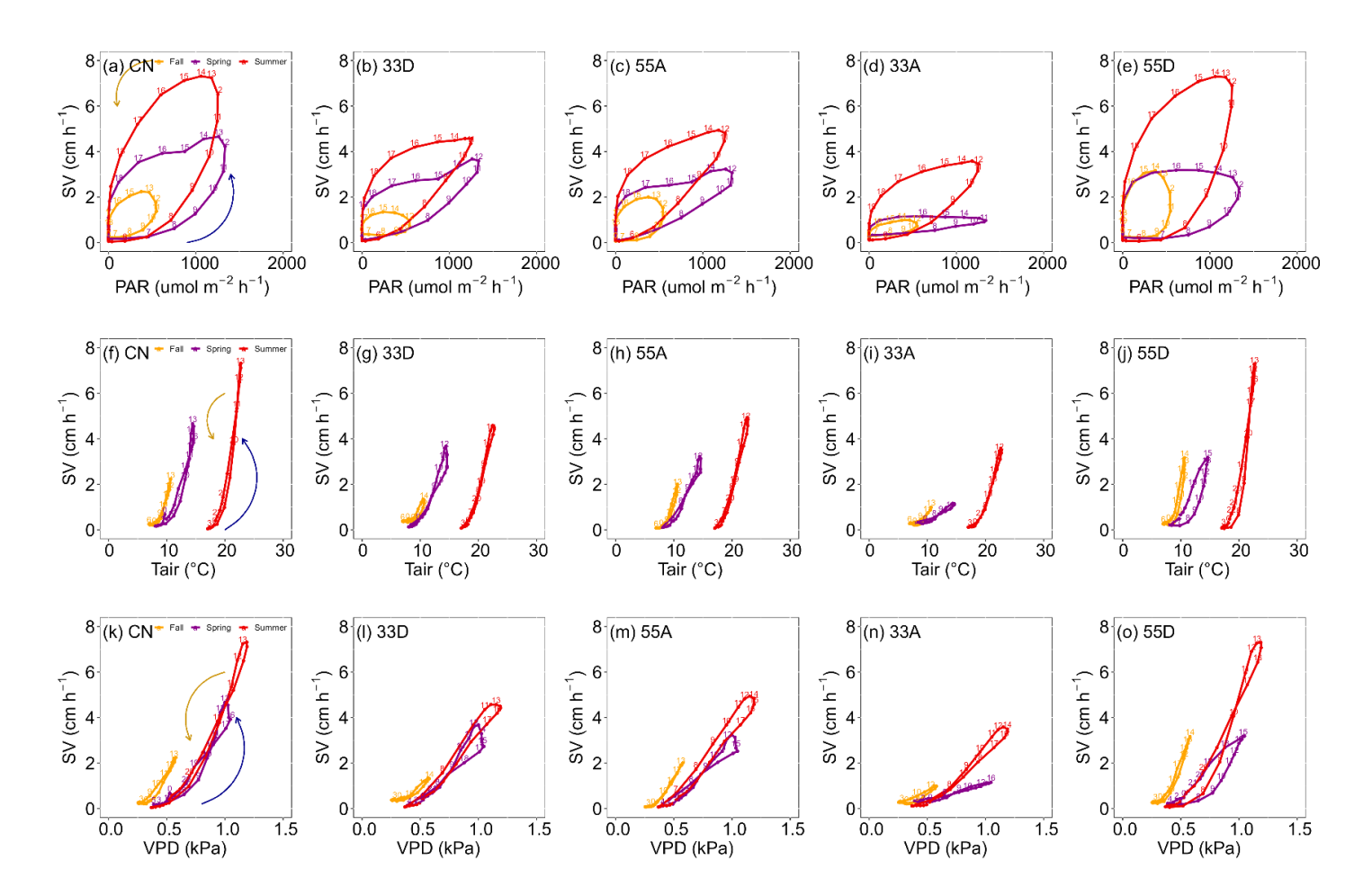


**Figure 4.4**: Hysteresis responses of sap flow velocity (SV) to environmental controls in each VRH treatment and control plot to (a-e) photosynthetic active radiation (PAR); (f-j) air temperature (Tair); and (k-o) vapor pressure deficit (VPD). Data points are hourly values averaged per season including fall (yellow lines), spring (magenta lines), and summer (red lines). The solid blue arrows indicate the direction of the response in the morning and the yellow one indicates the direction of response in the afternoon. The area enclosed by the SV trajectories indicates the strength of the hysteresis loop.

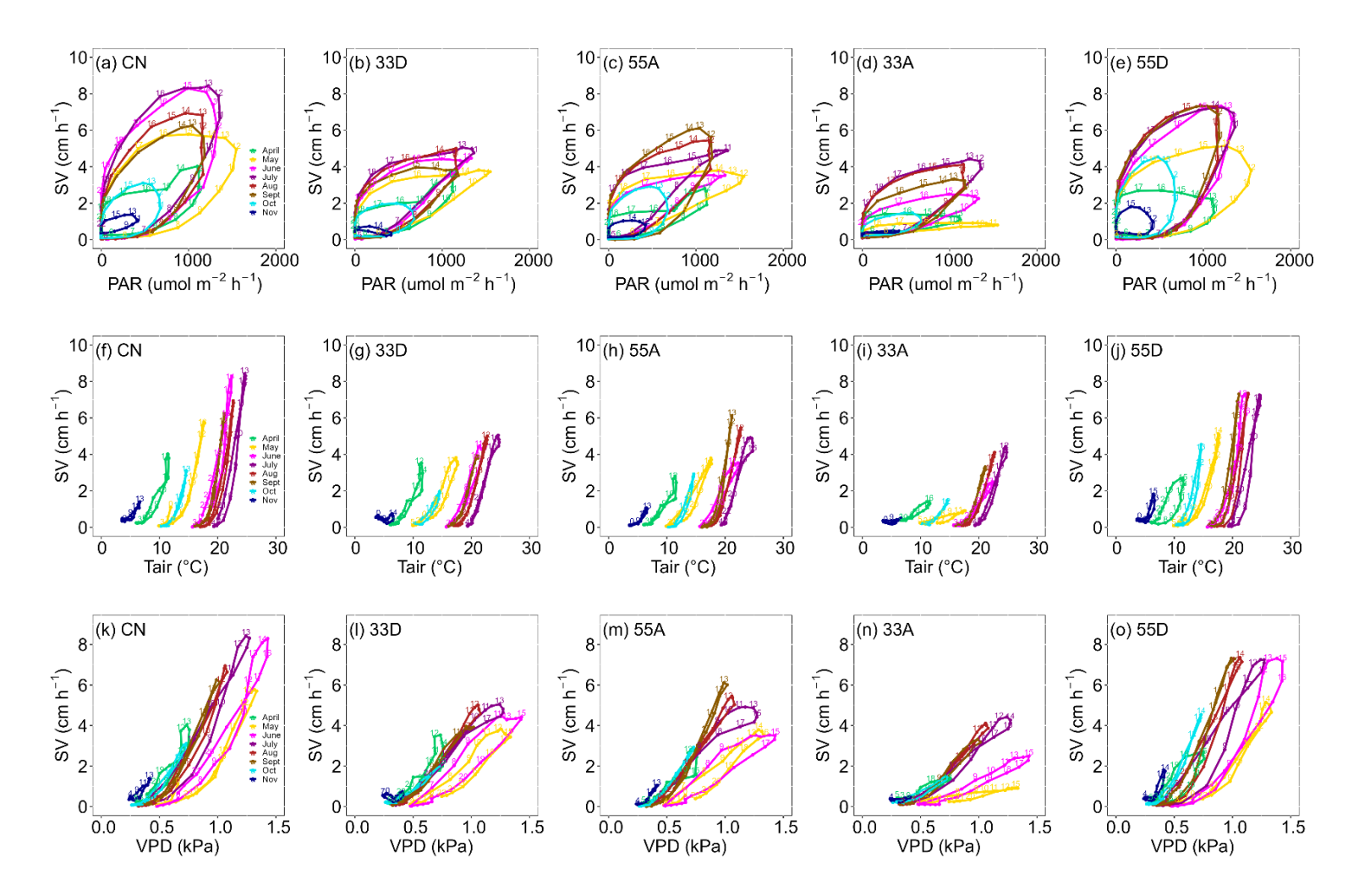


**Figure 4.5**: Hysteresis response of sap flow velocity to environmental controls over the growing season from April to November. (a-e) photosynthetic active radiation (PAR); (f-j) air temperature (Tair); and (k-o) vapor pressure deficit (VPD). Data points are hourly values averaged per season. The solid blue arrows indicate the direction of the response in the morning and the yellow one indicates the direction of response in the afternoon. The area enclosed by the SV trajectories indicates the strength of the hysteresis loop.

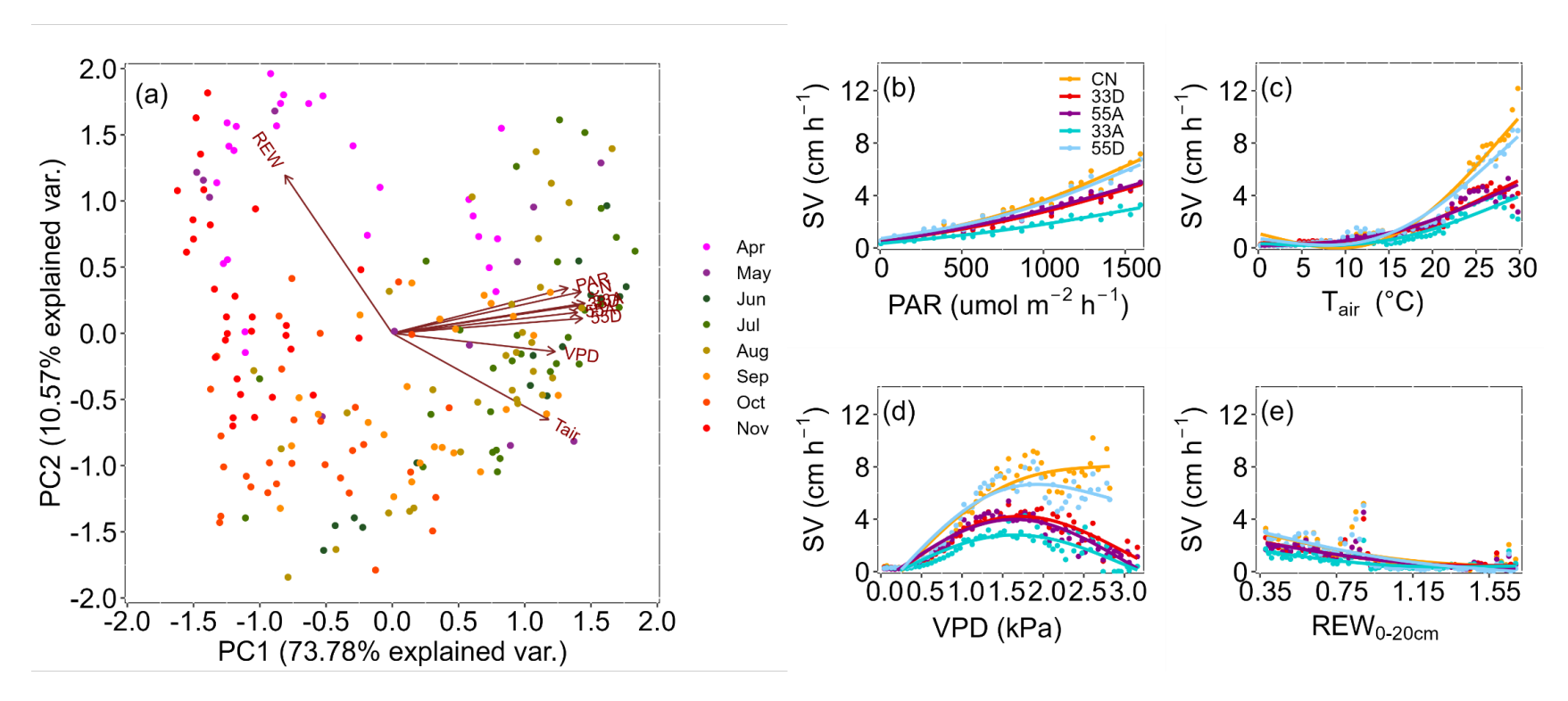


**Figure 4.6**: Response of sap flow velocity (SV) to meteorological variables and soil water stress. (a) Principal Component Analysis (PCA) applied to daily SV values in 2023. The first two principal components, PC1 and PC2, accounted for 79.3% and 8.1% of the total variance, respectively. Correlations between bin-average SV values and (b) photosynthetic active radiation, PAR (bin of 60 umol m-2 h-1); (c) air temperature, Tair (bin of 0.5 °C); (d) vapor pressure deficit. VPD (bin of 0.05 kPa); and (e) relative extractable water, REW (bin of 0.02) for each Variable Retention Harvesting (VRH) treatments (i.e. 33A, 33D, 55A, 55D) and the control plot, CN.

**Table S4.1:** Monthly total transpiration (T, mm mth<sup>-1</sup>) and precipitation (P, mm mth<sup>-1</sup>), monthly ratios of transpiration to precipitation (T/P) and mean sap flow velocity (SV, cm h<sup>-1</sup>) for different Variable Retention Harvesting (VRH) treatments and control plot.

Month		April	May	June	July	August	September	October	November	Total
P (mm)		111	25	50	125	82	34	66	66	$559 \pm 11.8$
	T	17.5	12.3	23.9	43.0	38.5	23.9	13.2	7.5	179.7 ±
33A	T/P	0.2	0.5	0.5	0.3	0.5	0.7	0.2	0.1	0.3
	SV	0.77	0.52	1.05	1.82	1.63	1.17	0.56	0.33	$1.0 \pm 0.5$
	T	30.1	42.7	49.1	57.1	50.6	33.6	18.8	12.3	$294.4 \pm 14.9$
33D	T/P	0.3	1.7	1.0	0.5	0.6	1.0	0.3	0.2	0.5
	SV	1.23	1.69	2.02	2.26	2.00	1.54	0.74	0.50	$1.5 \pm 0.6$
	T	23.3	40.8	39.0	56.4	52.2	40.1	20.8	9.0	$281.6 \pm 15.2$
55A	T/P	0.2	1.6	0.8	0.5	0.6	1.2	0.3	0.1	0.5
	SV	1.00	1.69	1.69	2.33	2.16	1.91	0.86	0.38	$1.5 \pm 0.6$
	T	27.6	15.3	28.1	69.1	66.3	50.0	32.0	16.0	$304.4 \pm 19.9$
55D	T/P	0.2	0.6	0.6	0.6	0.8	1.5	0.5	0.2	0.5
	SV	1.18	1.69	2.31	2.87	2.76	2.39	1.33	0.69	$1.9 \pm 0.7$
CN	T	32.2	34.8	30.3	74.5	56.1	38.5	20.9	14.7	$301.8 \pm 18.0$
	T/P	0.3	1.4	0.6	0.6	0.7	1.1	0.3	0.2	0.5
	SV	1.43	2.05	2.61	3.21	2.41	1.91	0.90	0.65	$1.9 \pm 0.8$

**Table S4.2:** Multivariate regression analysis of standardized hourly sap flow velocity (SV) across five variable retention harvesting (VRH) treatments (33A, 33D, 55A, 55D, CN) regressed against standardized explanatory variables, including vapor pressure deficit (VPD), air temperature (Tair), photosynthetic active radiation (PAR), relative extractable water (REW). Significance levels are indicated as follows: [0-0.001] = '\*\*\*'; (0.001-0.01] = '\*\*'; (0.01-0.05] = '\*'; (0.05-0.1] = '.'; (0.1-1] = '.'

Treatment	Regressor	Estimate	Std. Error	t Value	<b>Pr(&gt; t )</b>	Significanc e	lmg	$\mathbb{R}^2$
	Intercept	-0.001	0.008	-0.076	0.939			
	PARdn	0.337	0.010	32.845	< 2e-16	***	0.391	
33A	Tair	0.114	0.015	7.764	9.23E- 15	***	0.179	0.42
	VPD	0.299	0.013	22.363	< 2e-16	***	0.360	
	REW	-0.015	0.012	-1.203	0.229		0.070	
	Intercept	-0.001	0.006920 8	-0.109	0.9133			
	PARdn	0.437	0.008513 4	6.498	8.62E- 11	***	0.431	
33D	Tair	0.079	0.012160 1	6.498	8.62E- 11	***	0.151	0.59
	VPD	0.367	0.011109 5	33.028	< 2e-16	***	0.358	
	REW	-0.021	0.010090 9	-2.055	0.0399	*	0.060	
	Intercept	0.000	0.007	0.003	0.997			
_	PARdn	0.435	0.009	49.826	<2e-16	***	0.4309	
55A	Tair	0.129	0.012	10.367	<2e-16	***	0.1672	0.58
	VPD	0.321	0.011	28.195	<2e-16	***	0.3390	
	REW	-0.011	0.010	-1.049	0.294		0.0629	
	Intercept	0.094	0.007	12.900	< 2e-16	***		
_	PARdn	0.265	0.009	28.091	< 2e-16	***	0.2742	
55D	Tair	0.001	0.013	0.051	0.9591		0.1603	0.61
47	VPD	0.673	0.013	50.227	< 2e-16	***	0.4962	
	REW	-0.029	0.011	-2.733	0.00629	**	0.0694	
	Intercept	0.0614	0.0070	8.813	< 2e-16	***		
CN	PARdn	0.3182	0.0089	35.926	< 2e-16	***	0.3243	
	Tair	-0.0513	0.0124	-4.137	3.56E- 05	***	0.1338	0.62
	VPD	0.6604	0.0123	53.513	< 2e-16	***	0.4942	
	REW	-0.0041	0.0102	-0.402	0.688		0.0477	

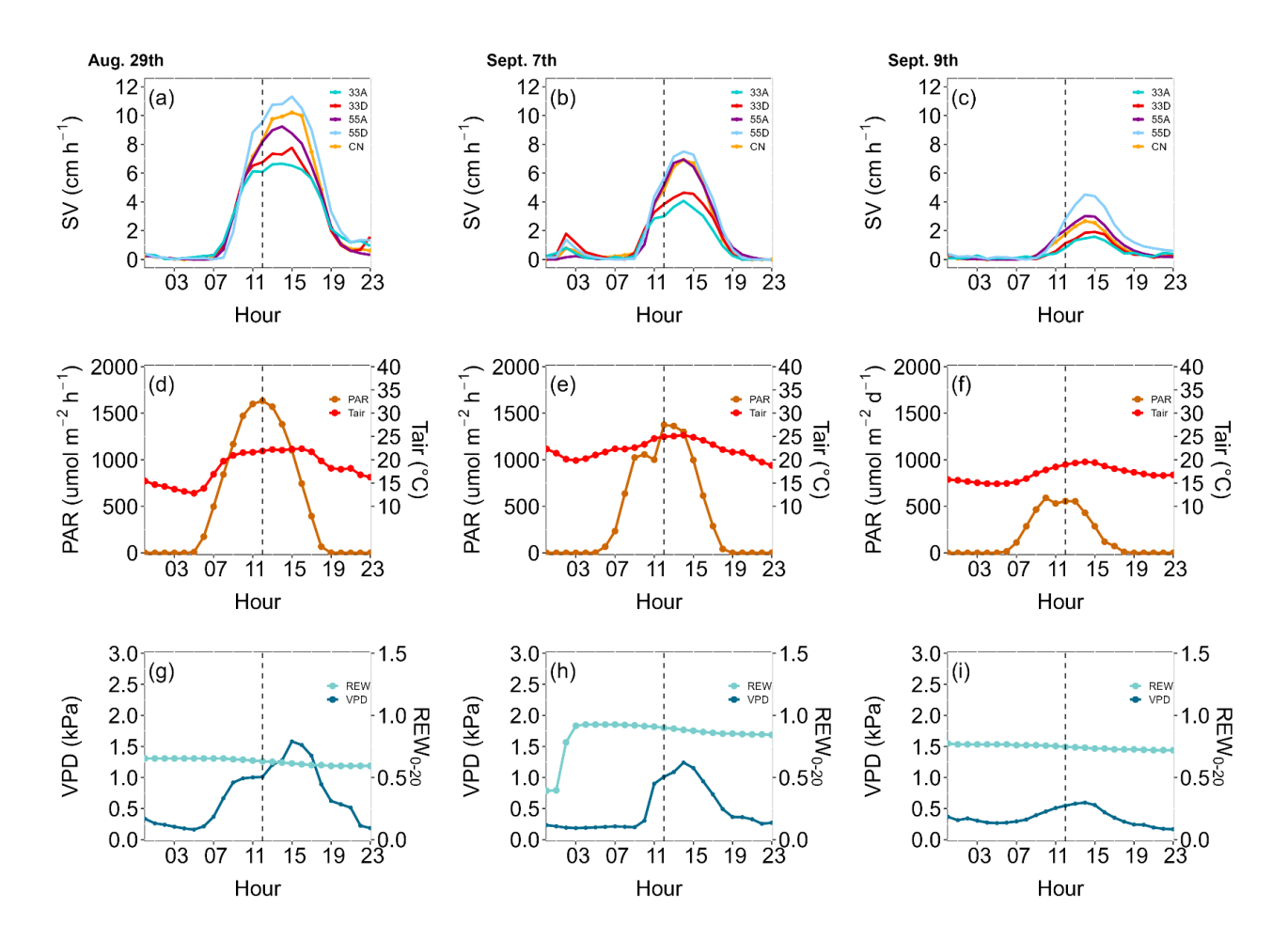


**Figure S4.1**: Diurnal cycles half-hourly values of sap flow velocity (SV) and environmental variables. (a-c) SV, (d-f) photosynthetic active radiation (PAR) and air temperature (Tair) and (g-i) vapor pressure deficit (VPD) and relative extractable water (REW) on August 29th, September 7th and September 9th in 2023. Dashed vertical lines indicate noon time.

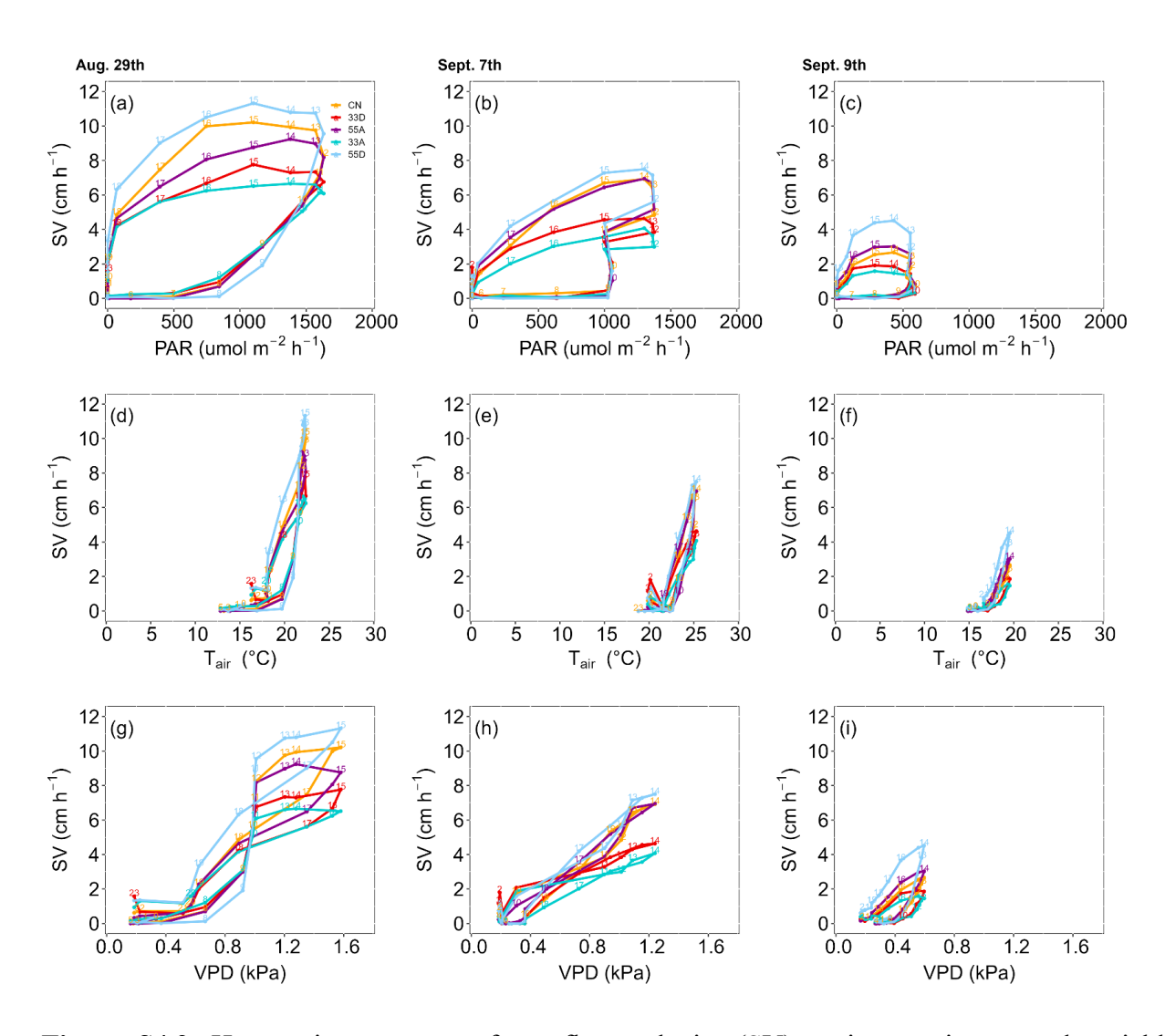


**Figure S4.2**: Hysteresis responses of sap flow velocity (SV) against environmental variables including (a-c) photosynthetic active radiation (PAR), (d-f) air temperature (Tair) and (g-i) vapor pressure deficit (VPD) on August 29th, September 7th and September 9th in 2023.

#### **CHAPTER 5:**

### **SUMMARY AND CONCLUSIONS**

# 5.1. Summary of the Results

This doctoral dissertation provides an in-depth analysis of water flux dynamics in managed temperate forests of different ages and species in Southern Ontario, Canada. It focuses on their responses to dry and hot conditions by using measured eddy covariance, sap flow, meteorological and biometric data. The comprehensive research setup and diverse range of forest stands used in this study offer valuable in-situ data to inform forest and water resource managers about the most suitable forest management practices that can be adopted to enhance forest growth and carbon sequestration and secure water yields, biodiversity, and sustainability under changing climate.

The results in Chapter 2 revealed an increase in ET and a decrease in WUE in response to compound weather events, including drought and heatwaves in a managed deciduous forest. Low WUE was mainly due to the negative impact of extreme weather on the photosynthetic capacity of the forest. However, despite drought conditions, the forest maintained a positive water balance over the years, emphasizing the importance of these temperate forests in sustaining water yield. In addition, ET was mainly controlled by PAR and Tair at daily timescale as the photosynthetic capacity of the forest is strongly linked to the climate seasonality and light availability. This forest exhibited strong clockwise hysteresis patterns with Tair and VPD due to the lagged response of Tair/VPD following changes in PAR. The study underscores the resilience of ET and WUE in this oak-dominated forest in the face of climate change and extreme weather events, highlighting the need for policies that ensure the hydrological integrity of these vital ecosystems.

The results in Chapter 3 showed higher WUE in younger conifer stands due to lower ET and higher GEP, indicating that younger forests with homogeneous canopies are more efficient in carbon uptake per unit of water loss. The findings also showed reduced ET and increased WUE during late summer drought conditions. The analysis of ET sensitivity to drought suggested that older forests are more resilient and less sensitive to dry conditions, likely due to the higher diversity of understory trees resulting from partial thinning activities. In contrast to deciduous forests, Tair was the primary driver of ET and WUE in the three coniferous forests at monthly timescale, reflecting the sensitivity of these stands to increasing temperatures. This long-term flux observation study enhances our understanding of water exchanges in different-aged temperate plantation forests in Eastern North America and contributes to a better understanding of their responses to extreme weather events.

The results of Chapter 4 revealed a strong hysteresis response of sap flow to PAR, with a smaller hysteresis with Tair and VPD. This suggests a self-protection mechanism in trees, allowing them to avoid dehydration by regulating stomatal control. The study further showed that PAR and Tair were the major drivers of daily SV across all VRH treatments, whereas at hourly timescale PAR and VPD was more closely associated with SV. Tree-level transpiration was the highest in the CN and 55D treatments, followed by 55A, 33D, and 33A. The results suggest that dispersed retention harvesting (55D plot or 55% basal area retention) creates favorable environmental conditions for forest growth by reducing competition for water among trees, as shown by enhanced transpiration, thus maximizing their growth and carbon uptake. Overall, this dissertation's findings provide valuable insights for developing forest management practices that enhance forest growth, water use efficiency, and resilience to climate change.

# 5.2. Significance and relevance of the study results

During the eighteenth and nineteenth centuries, much of North America's natural forests were cleared for non-forest uses such as agriculture (Bonan, 2008; Millar & Stephenson, 2015). In the twentieth century, as agricultural lands were abandoned in favor of industrialization and due to the migration of the population to urban areas, these abandoned or marginal lands became the focus of afforestation and reforestation efforts (Millar & Stephenson, 2015). Forests were planted in many parts of Canada and the United States, and these plantation stands were subsequently managed and harvested primarily for timber supply. Plantation forests differ from naturally regenerated forests in several key aspects, including lower species diversity, variations in stand structure, and uniform tree ages, which may result in more vulnerable and less resilient forests (Thompson et al., 2009). The temperate forests studied in this dissertation are part of these reforestation efforts and provide a unique opportunity to study forest-atmosphere interactions in these managed forests in North America. In recent years, the importance of these plantation and managed forests has been further enhanced because of their potential role in sequestering atmospheric carbon dioxide to provide nature-based climate solutions to mitigate climate change and contribute to net zero carbon emission goals (Drever et al., 2021).

This study also addresses a significant gap in our understanding of water flux dynamics in managed forests. By analyzing ET, the research enhanced our knowledge of the water use of managed forests and their impact on the water cycle and yield, which is vital for water resource management and security. For instance, the study showed lower annual ET in deciduous forests compared to conifer plantations, providing valuable information for reforestation strategies to enhance water yield.

The WUE findings are relevant for analyzing global trends in coupling carbon and water processes and their responses to climate change and management practices. The observation of higher WUE in deciduous forests compared to similarly aged conifer plantation forests contrasts with previous research findings as typically needle leaf forest seem to have higher WUE (Tang et al., 2014; Zhang et al., 2023). However, the higher WUE in younger white pine plantations, due to their high productivity relative to ET, underscores the importance of considering forest age in timber and carbon and water management strategies.

Moreover, this research offers insights into how extreme weather events, driven by climate change, impact these forests' water dynamics. The study highlights how ET in deciduous forests increases due to concurrent and consecutive events such as hot and dry conditions and how ET in different age conifer stands is affected by late summer droughts, with older forests showing higher resilience and lower sensitivity to drought. Consecutive years of unusual weather conditions, such as droughts, were found to reduce WUE in pine forests, emphasizing the need for adaptive management strategies.

Understanding how environmental controls affect the variability in ET and WUE is crucial for predicting how forests will respond to environmental changes. For example, increasing temperatures can enhance transpiration rates, potentially leading to greater water stress. Changes in light conditions, such as increased cloud cover, could decrease transpiration rates, while higher VPD can also lead to water stress. This information is valuable for developing accurate prediction models to understand how forests will respond to future climate scenarios.

Lastly, this work contributes to quantifying transpiration in widely planted red pine forests, highlighting the role of environmental variables in the hysteresis patterns of transpiration in plantation forests. This information is critical for developing effective forest management practices that optimize water use and enhance forest resilience in the face of climate change.

### 5.3. Suggestions for Future Research

This study utilized the eddy covariance technique to estimate ecosystem ET in managed forests, complemented by sap flow methods to approximate transpiration. Future research should aim for precise partitioning of evapotranspiration into its components, particularly in deciduous forests with high tree species diversity. Understanding the components of total forest evapotranspiration is crucial for interpreting the influence of climate change on the water budget of plantation forests.

While this study focused on canopy evapotranspiration, future research should also investigate understory evapotranspiration, especially in older plantation forests with dense understory populations. Implementing an additional eddy covariance system in the forest understory (if there is enough turbulence) could provide valuable insights into the role of understory development on water fluxes and water use efficiency. In addition, concurrent below and above canopy eddy covariance measurements can be useful to partitioning ET more accurately.

Regular vegetation inventories would significantly enhance future research by providing detailed information about stand growth (diameter at breast height, DBH), structure, species composition, mortality rates, and leaf area index for each stand. These factors greatly influence water use, productivity, and carbon sequestration sensitivity to climate variables (Anderegg et al., 2018; Bachofen et al., 2023). In this regard, the use of drones and UAVs can be highly beneficial, reducing the need for lengthy and frequent field campaigns, minimizing personnel requirements, and providing more accurate measurements.

Long-term observations offer a unique opportunity to apply advanced techniques, such as time-series analysis, including wavelet analysis. Maintaining these observations is crucial for analyzing seasonal and interannual variability in energy, water, and carbon fluxes, as well as assessing the impacts of climate change on forest ecosystems. Additionally, this data is valuable for validating comprehensive terrestrial biosphere models, such as CLASSIC, CLM, ELM, JULES, and ORCHIDEE, and for integrating remote sensing data to develop higher spatial resolution datasets, representative of forest ecosystems around the world.

These future research directions will provide essential data and knowledge to help decision-makers develop best practices for managing plantation forests in the Great Lakes region as well as North America, contributing to improved forest management strategies, water use efficiency, and resilience to climate change.

### 5.4. References

- Anderegg, W. R. L., Konings, A. G., Trugman, A. T., Yu, K., Bowling, D. R., Gabbitas, R., Karp, D. S., Pacala, S., Sperry, J. S., Sulman, B. N., & Zenes, N. (2018). Hydraulic diversity of forests regulates ecosystem resilience during drought. *Nature*, *561*(7724), 538–541. https://doi.org/10.1038/s41586-018-0539-7
- Bachofen, C., Poyatos, R., Flo, V., Martínez-Vilalta, J., Mencuccini, M., Granda, V., & Grossiord, C. (2023). Stand structure of Central European forests matters more than climate for transpiration sensitivity to VPD. *Journal of Applied Ecology*, 60(5), 886–897. https://doi.org/10.1111/1365-2664.14383
- Bonan, G. B. (2008). Forests and Climate Change: Forcings, Feedbacks, and the Climate Benefits of Forests. *Science*, 320(5882), 1444–1449. https://doi.org/10.1126/science.1155121
- Drever, C. R., Cook-Patton, S. C., Akhter, F., Badiou, P. H., Chmura, G. L., Davidson, S. J., Desjardins, R. L., Dyk, A., Fargione, J. E., Fellows, M., Filewod, B., Hessing-Lewis, M., Jayasundara, S., Keeton, W. S., Kroeger, T., Lark, T. J., Le, E., Leavitt, S. M., Leclerc, M.-E., ... Kurz, W. A. (2021). Natural climate solutions for Canada. Sci. Adv, 7. https://doi.org/10.1126/sciadv.abd6034
- Millar, C. I., & Stephenson, N. L. (2015). Temperate forest health in an era of emerging megadisturbance. https://www.science.org
- Tang, X., Li, H., Desai, A. R., Nagy, Z., Luo, J., Kolb, T. E., Olioso, A., Xu, X., Yao, L., Kutsch, W., Pilegaard, K., Köstner, B., & Ammann, C. (2014). How is water-use efficiency of terrestrial ecosystems distributed and changing on Earth? *Scientific Reports*, 4, 1–11. https://doi.org/10.1038/srep07483
- Thompson, I., Mackey, B., McNulty, S., Mosseler, A., & Secretariat of the convention on the biological diversity. (2009). Forest resilience, biodiversity, and climate change: a synthesis of the biodiversity, resilience, stabiblity relationship in forest ecosystems.
- Zhang, Z., Zhang, L., Xu, H., Creed, I. F., Blanco, J. A., Wei, X., Sun, G., Asbjornsen, H., & Bishop, K. (2023). Forest water-use efficiency: Effects of climate change and management on the coupling of carbon and water processes. In *Forest Ecology and Management* (Vol. 534). Elsevier B.V. https://doi.org/10.1016/j.foreco.2023.120853